國 立 交 通 大 學

電信工程學系

博 士 論 文

蜂巢式 OFDMA 系統之效能改進技術

Performance Improvement Techniques for Cellular OFDMA Systems

研究生：傅宜康

指導教授：沈文和 教授

中 華 民 國 九十六 年 九 月

蜂巢式 OFDMA 系統之效能改進技術

Performances Improvement Techniques for Cellular OFDMA Systems

研究生：傅宜康　　Student: I-Kang Fu

指導教授：沈文和 博士　　Advisor: Dr. Wern-Ho Sheen

國立交通大學

電信工程學系

博士論文

A Dissertation
Submitted to Institute of Communication Engineering
College of Electrical and Computer Engineering
National Chiao Tung University
in Partial Fulfillment of the Requirements
for the Degree of Doctor of Philosophy
in
Communication Engineering
Hsinchu, Taiwan

2007 年 9 月

To my family – S. L. Fu, S. C. Chang, I. L. Fu, L. Y. Lee, Z. L. Kuo

Special thanks to my advisor – Prof. W. H. Sheen
and my friends in IEEE 802.16 Working Group.

Abstract

OFDMA (Orthogonal Frequency Division Multiple Access) is one of the key multiple access techniques to enable broadband wireless transmission for next generation mobile cellular systems. In order to improve and investigate the performance of cellular OFDMA systems, this dissertation proposes several advanced techniques and part of the designs have been adopt by the international standard organization. The downlink capacity of cellular OFDMA systems is first investigated through the proposed mathematical analysis. The proposed analysis is general and incorporates the effects of propagation environment, cell size, frequency reuse factors, reuse partitioning (fractional frequency reuse), antenna setups and etc. The numerical results show that the downlink capacity of cellular OFDMA system can be significantly improved by reuse partitioning and intra-cell frequency reuse. Then, an improved FBSS (Fast Base Station Switching) handover technique is proposed to improve the packet loss rate for the handover users. Simulation results show that the proposed technique can significantly reduce the packet loss rate for the users during FBSS at a slight expense on system capacity. In addition, a recent advance in multi-hop relay technology is introduced and investigated, and the benefit on user throughput enhancement and coverage extension by relay deployment are justified by simulation results. But it also shows that the capacity may not be improved by deploying relay stations with respect to the cellular OFDMA system with no relay. In order to improve the capacity of multi-hop cellular OFDMA systems, advanced frequency planning (reuse) techniques and path selection techniques are investigated and proposed. Compare to existing techniques, the proposed frequency planning (reuse) technique can lead to 60.87% ~ 137.75% capacity improvements under the guaranteed coverage. In addition, simulation results also show that further 16.87% ~ 26.31% capacity improvement can be achieved by advanced path selection based on proposed SINR prediction technique.

摘　要

OFDMA (Orthogonal Frequency Divisional Multiple Access)被視為是下一代行動通訊系統之核心技術，其重要性在可於高速資料傳輸時有效解決符際干擾(Inter Symbol Interference, ISI)的問題。以 OFDMA 為核心之蜂巢式無線接取網路將會是下一代無線寬頻通訊系統之核心。為了提升及探討蜂巢式 OFDMA 系統之效能，本論文提出了多種技術以探討或提升系統之效能。首先，本文提出了一套新型之數學分析方法以探討蜂巢式 OFDMA 系統之下鏈系統容量，且該分析方法可廣泛納入細胞涵蓋範圍、頻率重用係數、頻率分段重用(reuse partitioning)、天線組態等效應，藉由分析數值結果顯示透過頻率分段重用技術搭配細胞內之頻率重複使用可顯著的提升系統容量。本論文並進一步提出一套改良型之快速基地台切換(Fast Base Station Switching, FBSS)技術，其設計在於結合頻率分段重用技術以預留部分干擾較輕微之通道以提升換手中的使用者之訊號品質。模擬結果顯示所提出之技術可可大幅減低(93.6%)使用者在換手過程中所遭受之封包遺失率，且僅些微的損耗(5.82%)部份系統容量。此外，本論文介紹並探討了一種可應用於蜂巢式 OFDMA 系統之 Multi-hop Relay 技術標準：IEEE 802.16j，並透過電腦模擬探討採用 Multi-hop Relay 技術對於系統整體效能之影響。模擬結果顯示於系統加入中繼站(Relay Station)可有效提升使用者傳輸速率及系統涵蓋範圍，但結果亦顯示系統容量有可能因為資料轉傳所額外消耗的資源而惡化。為了有效提升 Multi-hop 蜂巢式 OFDMA 系統之容量，本論文進一步提出了新型之頻率規劃及重複使用技術以及以 SINR 預測為基礎之新型路徑選擇技術。相較於現有之頻率規劃方法，本文所提出之方法可大幅(60.87%~137.75%)提升系統容量且不影響系統有效之涵蓋範圍，而模擬結果亦顯示所提出之路徑選擇方法可進一步提升 16.87%~26.31%之系統容量。

Table of Contents

List of Figures

List of Tables

Chapter 1

Introduction

Advances in mobile communication technologies in last decade have dramatically changed human's lives. From mobile telephony to mobile Internet, people are able to access information anytime and anywhere. Today, people can make reservation for their dinner by mobile phone when they are driving on high way, or they can receive/reply some urgent emails by wireless Internet when they are traveling on the train in a foreign country. Such a convenience further triggers more people's expectation on more fruitful applications by wireless communication. Therefore, higher transmission rate, ubiquitous network connectivity, lower access fee, seamless service and etc. are the common desires on next generation mobile communication systems by the people around the world [1].

One of the most popular technologies used by mobile communication systems is the radio transmission technology, i.e. transmitting the information signal through radio waves. Thanks the advances in semi-conductor technologies, the cost on manufacturing the devices for radio transmission and signal processing is much lower than before and it makes the mobile communication products be very popular around the world in a very short time. However, the radio frequency spectrum is a very scarce resource and always controlled by the government in each country. The privilege to provide mobile communication services via a specific frequency bandwidth (i.e. licensed-band) is very expensive, for example, some companies spend more than ten billion Taiwan dollars to acquire the privilege to perform the services via 3G/3.5G systems. Therefore, there will be many technical challenges to serve more users with

higher transmission rate by such a scarce radio bandwidth.

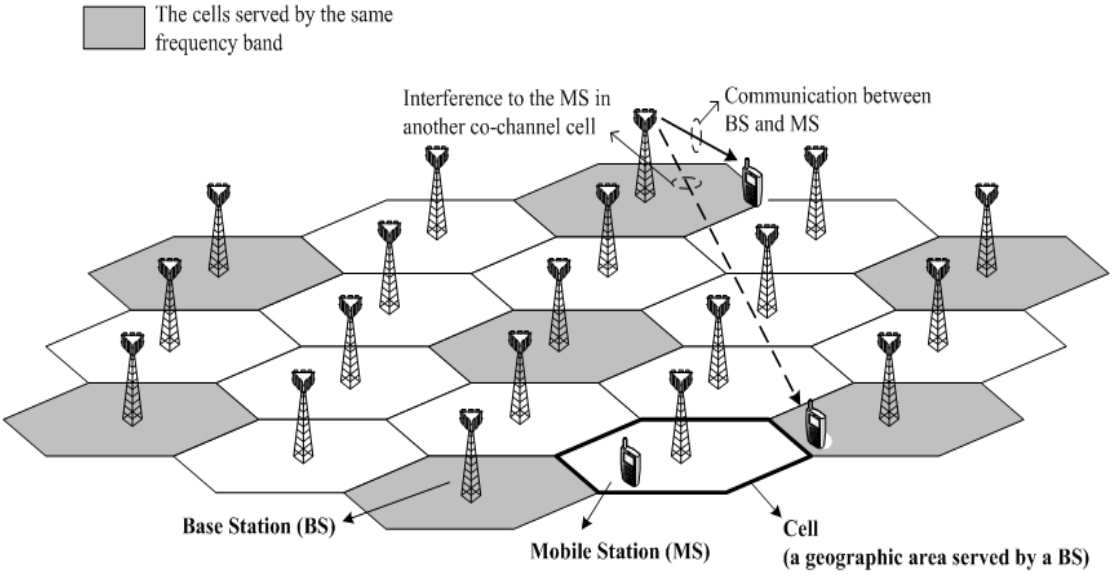

Figure 1. Cellular Structure

A. Cellular Structure

The most general resolution to the aforementioned problem is reusing the same frequency bandwidth in different geographic area, which is called frequency reuse [2]. In order to manage the interference when the same bandwidth is reused to transmit different signals, the cellular structure as shown in Figure 1 is used as a tool to determine the area served by each frequency band. Note that a cell is defined as the coverage served by a base station (BS). By separating the cells which use the same frequency (called co-channel cells) far enough, the interference will degrade to a very low level when received by the mobile station (MS) or BS in the co-channel cells, so that the received signal quality in each cell can be higher than an acceptable level for normal communication. In the modern mobile communication systems which operate in licensed-bands, the cellular structure is the fundamental architecture when

deploying its radio access network.

B. OFDMA (Orthogonal Frequency Division Multiple Access)

In addition, next-generation mobile communication is envisaged to support multimedia services over a wide variety of operation environments: indoors, outdoors, low-mobility, high-mobility, etc. Data rate up to several tens Mbps is essential in order to support a multitude of services with guaranteed QoS. Meanwhile, very high spectrum efficiency, at least one order in magnitude higher than the 3G systems, is needed to best utilize the very scarce radio spectrum in the future. One key challenge in designing such a system is to overcome inter-symbol interference (ISI) incurred by high-data-rate transmission. Furthermore, technology advancements in multiple access techniques, intelligent antenna systems, coding/decoding, etc. have to be exploited fully so as to achieve the targeted spectrum efficiency [3].

OFDM (orthogonal frequency division multiplexing) is an effective modulation/multiplexing scheme to combat ISI in a high-data-rate environment, where frequency band is divided into sub-carriers and over which data are transmitted in parallel. Through the use of cyclic-prefix, ISI can be avoided completely in a multi-path channel as long as the cyclic-prefix is larger than the maximum delay spread [4].

OFDM can also be used as an effective multiple access scheme [5]. In particular, OFDMA (orthogonal frequency division multiple access), a form of combining OFDM and FDMA (frequency division multiple access), has been widely regarded as one of the most promising multiple access schemes for the next generation systems [2,6]. OFDMA has been adopted in the 3GPP-LTE (long term evolution) down-link [7 and IEEE 802.16e [8] specifications.

In this dissertation, the system combines with cellular structure and OFDMA (i.e. cellular OFDMA system) will be first investigated in Chapter 2 and Chapter 3. In Chapter 2, the design tradeoffs on the cellular structure for cellular OFDMA systems will be investigated by a proposed mathematical analysis. In Chapter 3, a popular handover mechanism called fast base station switching (FBSS) is introduced and an improved version is also proposed.

C. Multi-hop Relay

When the system operators try to upgrade their cellular OFDMA networks to support a much higher transmission rate, there will be a transmit power problem. For example, ten times in transmission rate will result in more than ten times in transmit power in order to meet the required signal to interference plus noise ratio (SINR) [9]. Since the transmit power cannot be increased unlimitedly due to the hardware cost or battery life of a MS, the coverage holes may exist between adjacent BSs.

Traditional solution to this problem is to deploy additional BSs or repeaters to serve the coverage holes. Unfortunately, the cost of BS is very high and the wire-line backhaul may not be available everywhere. Repeater, on the other hand, has the problem of amplifying interference and has no intelligence of signal control and processing. Recently, relay station (RS) that receives and forwards signals from source to destination through radio has been developed as a more cost-effective solution. Since RSs do not need a wire-line backhaul, the deployment cost of RSs will be much lower than that of BSs. Meanwhile, RS can decode the signal from the source and forward it to the destination. Intelligent resource scheduling and cooperative transmission can be applied to obtain better system performance [10].

In Chapter 4, an overview of modern advances on multi-hop relay network and the first multi-hop relay specification “IEEE 802.16j” is given. The benefit of multi-hop

relay with respect to the cellular OFDMA systems with no relay is studied in this chapter with simulation. In Chapter 5, a new frequency planning technique with a novel measurement and report mechanism for multi-hop cellular OFDMA systems (i.e. the cellular OFDMA systems with multi-hop relay technology) are proposed. A novel path selection based on SINR prediction is proposed in Chapter 6 and, finally, the conclusion is provided in Chapter 7.

Chapter 2

Capacity Improvement Techniques for Cellular OFDMA Systems

OFDMA (orthogonal frequency division multiple access) is widely regarded as a key multiple access technology for broadband mobile radio systems, and has been adopted in the 3GPP-LTE (long term evolution) down-link and IEEE 802.16e specifications. This chapter analyzes the down-link capacity of multi-cell OFDMA systems under a randomized multiple access interference, a result of applying random sub-carrier allocation among cells/sectors. A mathematical analysis is proposed in Section 2.1 to efficiently evaluate the system capacity which is obtained through mainly time-consuming computer simulations previously. The analysis is general enough to take into account the effects of propagation environment, cell size, frequency reuse factor, reuse partitioning (fractional frequency reuse), antenna set-ups, etc. In Section 2.2, an OFDMA system resembling that specified in IEEE 802.16e is analyzed to illustrate how the analysis can be used to optimize the design of a system to achieve the highest capacity.

2.1 Downlink Capacity Analysis of Cellular OFDMA Systems

The capacity of OFDMA systems has recently been investigated in the literatures. In [11] and [12], the up- and down-link capacity of multi-cell OFDMA systems was investigated through computer simulations. The system capacity was compared for various propagation models and resource allocation methods. In [13], both uplink and

downlink were simulated, and their results indicated that the system suffers a severe degradation from using a large cell radius and/or having high loading in the interfering cells. In [14], the downlink capacity of multi-cell OFDMA was compared with CDMA (code division multiple access) through simulations. Numerical results show that OFDMA can achieve higher capacity when operating in the Rayleigh fading channel.

Instead of resorting time-consuming computer simulations, this chapter aims to provide an efficient mathematical analysis on the downlink capacity of multi-cell OFDMA systems with randomized multiple access interference (MAI), a result of applying random sub-carrier allocation among cells/sectors which has been adopted in IEEE 802.16e [8]. Efficient capacity evaluation is indispensable for optimal system design that gives the best tradeoff among different system parameters. The analysis is general enough to include the effects of reuse partitioning (fractional frequency reuse), different antenna set-ups and multiple modulation and code schemes (MCS).

2.1.1 Cellular OFDMA System Model

Figure 2(a) depicts the considered multi-cell architecture. The reference base station (BS) is denoted as BS_0, and the interfering BSs are denoted as BS_q, q = 1, 2 … Q, where Q is the number of the interfering BSs. Cell radius R is the same for every BS, and the distance between adjacent interfering BSs is given by $D = \sqrt{3K} \cdot R$, where K is the reuse factor (cluster size) [15]. K is a key system parameter that balances link performance and system capacity. Different K values are investigated in Section IV.

OFDMA is a combination of OFDM and FDMA, where frequency band is divided into orthogonal sub-carriers, and these sub-carries are grouped (allocated) together to

consist of a channel to serve users. In real systems, sub-carriers in channels are not overlapping in a cell/sector so as to avoid intra-cell/sector interference [7,8]. As a

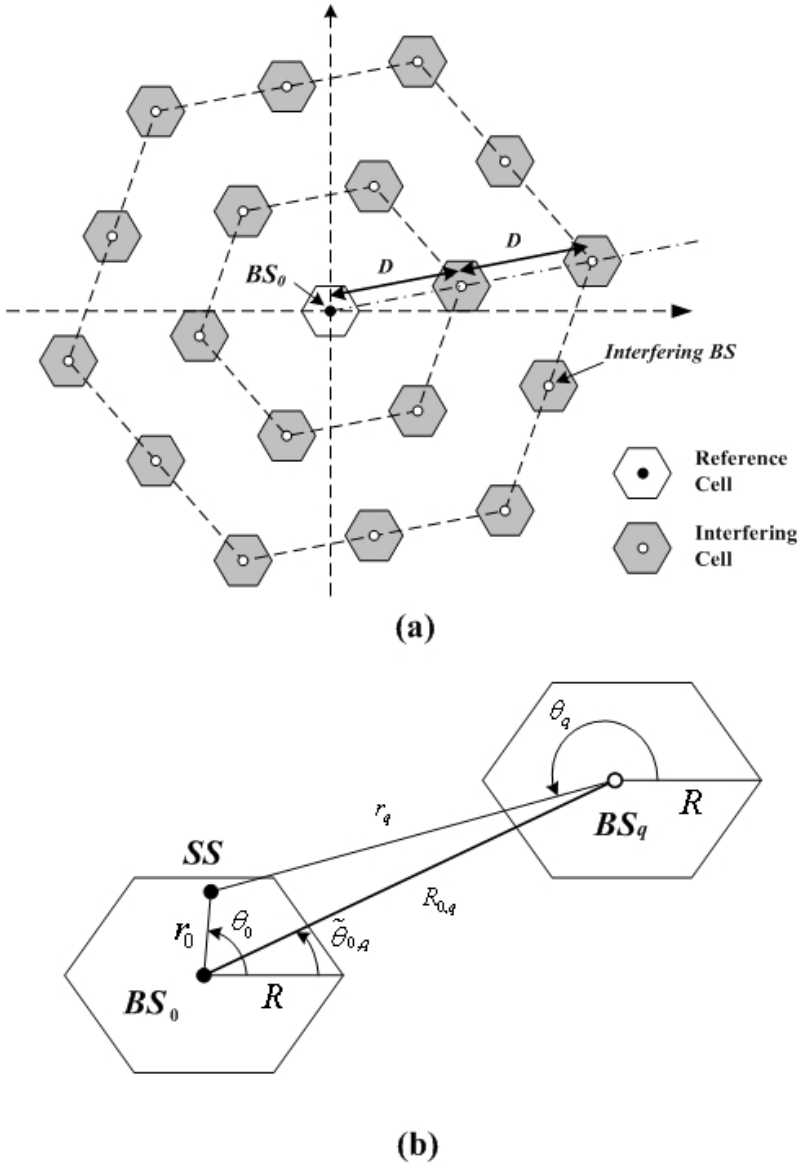

Figure 2. (a) Geometry of interfering cells ($Q = 18$) (b) Geometry of the reference cell and the interfering cell q

consequence, the co-channel inter-cell/sector interference becomes the main limiting factor to the system capacity in a multi-cell deployment, given a channel bandwidth.

A. Diversity Sub-carrier Allocation and Permutation

Two types of sub-carriers allocation to a channel are popular in real OFDMA systems [7,8]. One is diversity allocation, where sub-carriers in a channel are distributed over the entire frequency band, and the other is adjacent allocation, where sub-carriers are adjacent to each other. Diversity allocation is designed to obtain frequency diversity at link level, and adjacent allocation is meant to exploit multi-user diversity through frequency-selective scheduling for low-mobility users at system level [16]. In this work, we are only concerned with diversity allocation.

In diversity allocation, the way of allocating sub-carriers into a channel is often *permuted* randomly among cells/sectors so as to randomize the inter-cell/sector MAI. It eliminates the most severe interfering scenario in a multi-cell environment like in a narrow-band system and makes the worst-case network planning not necessary. For example, in the IEEE 802.16e OFDMA downlink, sub-carrier allocation is done with a pseudo-randomly sub-carrier mapping process, called sub-carrier permutation [8]. The basic idea is explained with Figure 3 as follows. Firstly, the available sub-carriers are divided into N_S sub-bands, with each of them consisting of N_C adjacent sub-carriers. Then each of the sub-carriers in a sub-band is allocated to one of N_C channels (called sub-channel in IEEE 802.16e) in a non-overlapping way. Thus, each of the channels consists exactly of N_S sub-carriers. For users in the same cell/sector, they use different channels so that there is no intra-cell/sector interference. Secondly, the way of allocating sub-carriers into sub-channels is *permuted* pseudo-randomly in different cells/sectors in order to randomize the inter-cell/sector interference. The sub-carrier allocations for different cells are illustrated in Figure 3. In the IEEE 802.16 OFDMA system, the sub-carrier permutation of a cell/sector is fixed and determined by the cell/sector ID [8]. To facilitate analysis, nevertheless, sub-carrier allocation will be assumed fully random from one cell/sector to another in the

following. With this arrangement, we say that the inter-cell/sector MAI has been randomized completely, and, therefore, each sub-carrier/channel experiences the same statistical characteristics of MAI [17,18].

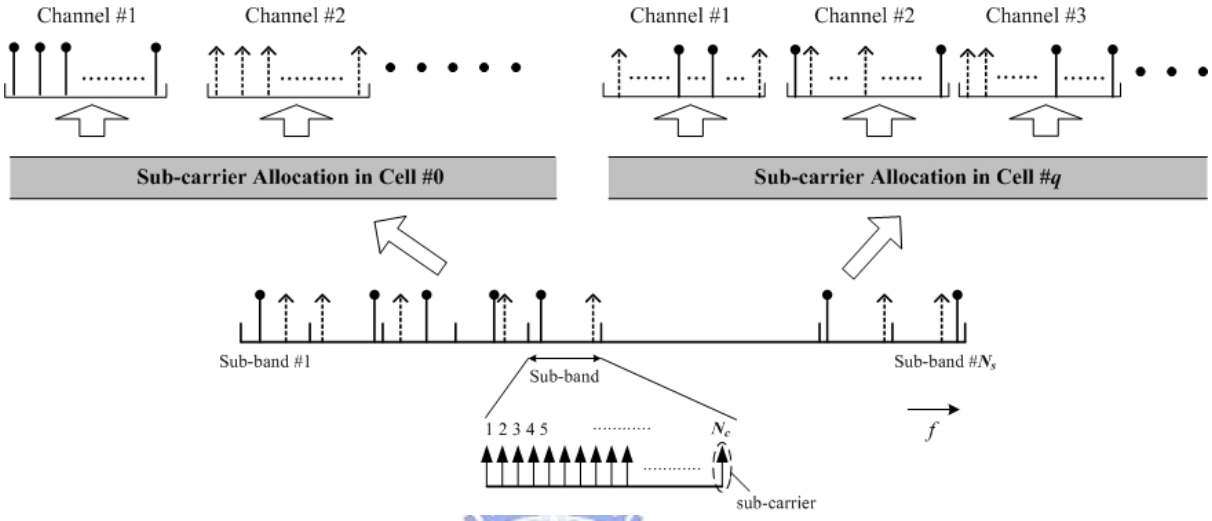

Figure 3. Example sub-carrier allocation and permutation in OFDMA systems

B. Reuse Partitioning (Fractional Frequency Reuse)

Reuse partitioning is a cell structure, where a regular cell is divided (ideally) into two or more concentric cell-regions, each with a different frequency reuse factor (K) [19]. By allowing the inner cell-regions to use a smaller reuse factor leads to a higher system capacity, as compared to the regular cell structure where the same reuse factor is used for the entire cell.

Figure 4 illustrates the concept of reuse partitioning with a TDD frame structure. In Figure 4(a), a regular cell is divided into Z cell-regions with the z-th region denoted by $\{\omega_{z-1}R < r_0 \le \omega_z R,\ 0 < \theta_0 \le 2\pi\}$, where $\omega_{z-1} \le \omega_z$, $\omega_0 = 0$, $\omega_Z = 1$, and $1 \le z \le Z$. Then, the TDD frame is partitioned into Z resource-zones, and within a resource-zone, the radio resource is further divided into K_z resource-regions as

shown in Figure 4(b), where K_z is the reuse factor for *z*-th cell-region. Finally, each of the resource-region is allotted to BSs according to the designated reuse factor and cell regions.

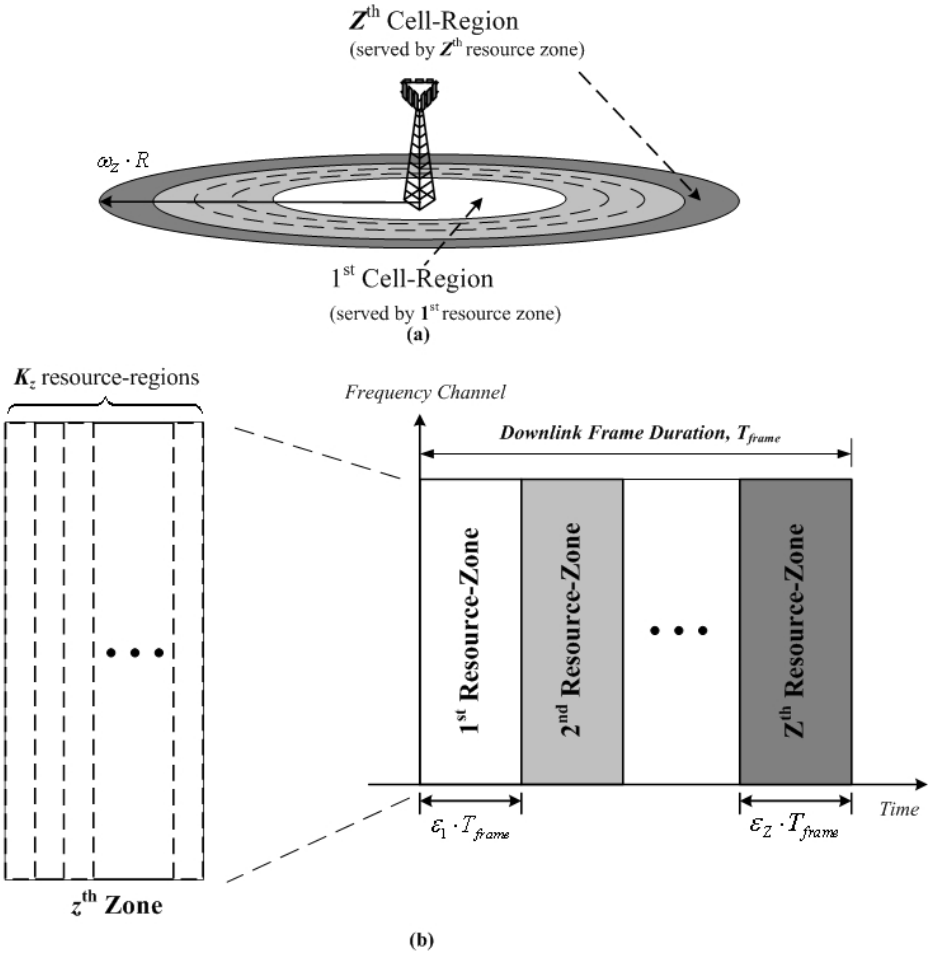

Figure 4 The concept of reuse partitioning: (a) divide the cell into Z concentric regions and (b) serve each region by corresponding frame zone with different K_z

C. Antenna Setups

Different antenna configurations have been used to increase system capacity and/or link quality of a cellular system. Two antenna configurations are to be considered, including 3-sector antenna and switched-beam smart antenna. For the 3-sector

antenna, the antenna pattern of each sector is the one specified in [20]

$$G_{j,dB}(\theta) = 14 - \min\left[12\left(\frac{18\cdot(\theta-\varphi_j)^2}{7\pi}\right), 20\right] \quad dBi, \quad j = 1,2,3, \tag{2.1}$$

where $-\pi < \theta - \varphi_j \le \pi$, φ_j is the steering direction of the antenna for *j*-th sector, which are 0, $2\pi/3$ and $4\pi/3$, respectively.

For the switched-beam smart antenna, the linear equally spaced (LES) array with omni-directional antenna elements is employed to form a number of fixed beams to cover different area of a cell, and users are served by the beam with the highest gain [21]. The *j*-th beam pattern is given by [22]

$$G_j(\theta) = \left|\frac{\sin\left(\frac{\beta W d}{2}(\cos\varphi_j - \cos\theta)\right)}{\sin\left(\frac{\beta d}{2}(\cos\varphi_j - \cos\theta)\right)}\right|^2, \tag{2.2}$$

where φ_j is the steering direction of *j*-th beam, d is the distance between antenna elements, W is the number of antenna elements, $\beta = 2\pi/\lambda$ is the phase propagation factor, and λ is the wavelength. In the following, the "sector" and "beam" will be used interchangeably.

Two extreme cases of channel reuse among sectors (beams) of a cell are to be considered. One is that different sectors use different set of channels, i.e., channels are not reused among sectors (no-reuse), and the other is that all the channels are reused in all sectors (full-reuse). Because of the non-perfect antenna pattern, there will be intra-cell interference when channels in the full-reuse case.

For easy presentation, the considered cell architecture will be described by the vector $(\{K_1, K_2 \cdots K_Z\}, J, 1/J)$ or $(\{K_1, K_2 \cdots K_Z\}, J, 1)$, where K_z is again the reuse factor for the *z*-th cell-region, the second element *J* is the number of sectors (beams) in a cell, and the third element is the fraction of channels in a cell used by a

sector. In other words, "$1/J$" denotes the no-reuse case, and "1" denotes the full-reuse case.

2.1.2 Capacity Analysis of Cellular OFDMA Systems

The downlink capacity of the power-controlled multi-cell OFDMA system is analyzed in this section. In the power-controlled system, the BS's transmit power toward a particular user is controlled to just meet the link performance requirement of a modulation and code scheme (MCS), and hence reducing the interference to the co-channel users. More than one MCS-class is considered in the analysis.

Three common assumptions are made to facilitate the analysis. First, users are distributed uniformly over each cell-region of the cell/sector. Second, user is served by the sector (beam) with highest received power. And, third, user is ideally power controlled to just meet the required SINR.

Consider a user located at (r_0, θ_0) in Figure 2(b), served by the *z*-th cell-region in the *j*-th sector (beam) of BS_0 and using the *u*-th MCS-class in a specific channel. For convenience, each user is assumed to use one channel only. Since all channels look the same to a user in the diversity sub-carrier allocation, there is no need to differentiate which channel is used by a user.

In the power-controlled systems, the received SINR of the user is controlled to meet to the target value ρ_u,

$$\rho_u = \frac{p_{j,u,z}(r_0,\theta_0)\cdot G_{0,j}(\theta_0)\cdot L_0(r_0)}{I_z(r_0,\theta_0)+N}, \tag{2.3}$$

where $p_{j,u,z}(r_0,\theta_0)$ is the downlink transmit power for the user, $G_{0,j}(\theta_0)$ is the antenna gain toward the direction θ_0, $L_0(r_0)$ is the propagation loss, and $I_z(r_0,\theta)$ and N are the power of MAI and thermal noise, respectively. Note that $G_{0,j}(\theta_0)$

might be different for different j in the case of switched-beam smart antenna, and that is the reason why we need to differentiate the beam where the user is located in. The propagation loss $L_0(r_0)$ is modeled as

$$L_0(r_0) = A \cdot r_0^{-l} \cdot \chi_0, \tag{2.4}$$

where A is a constant determined by the path-loss model, l is the path-loss exponent, and χ_0 is a log-normal random variable with zero mean and variance σ_{dB}^2 in dB. The effect of small-scale multi-path fading is included in determining the link performance ρ_u, and thus is not explicitly treated here. From Equation (2.3), the required transmit power for the user is given by

$$p_{j,z,u}(r_0,\theta_0) = \frac{\rho_u \cdot \left(I_z(r_0,\theta_0) + N\right)}{A \cdot r_0^{-l} \cdot \chi_0 \cdot G_{0,j}\left(\theta_0\right)}. \tag{2.5}$$

The analysis consists of three steps. Firstly, we obtain the average transmit power $p_{j,z,u} = E\left[p_{j,z,u}(r_0,\theta_0)\right]$ for a particular MCS-class user who is located uniformly over the z-th cell-region of the j-th sector (beam), where $E[\cdot]$ denotes the operation of taking average. Secondly, the total transmission rates of the u-th MCS-class users in z-th cell-region of the j-th sector is calculated by

$$M_{j,z,u} \cdot \frac{\varepsilon_z}{K_z} \cdot \frac{m_u c_u N_S}{T_{OFDM}} \text{ bps}, \tag{2.6}$$

where $M_{j,z,u}$ is the total number of user in z-th cell-region of the j-th sector using the u-th MCS-class, m_u and c_u are the bit number carried by the signal constellation and the coding rate, respectively, ε_z is the ratio of the percentage of frame duration for serving the users in z-th cell-region as depicted in Figure 4(b), and T_{OFDM} is the OFDM symbol duration. Finally, the (average) system capacity is evaluated as

$$C = \sum_{j=1}^{J}\sum_{z=1}^{Z}\sum_{u=1}^{U} \widehat{M}_{j,z,u} \cdot \frac{\varepsilon_z}{K_z} \cdot \frac{m_u c_u N_S}{T_{OFDM}} \quad \text{bps/cell} \tag{2.7}$$

where U is the number of MCS-classes, and

$$\left[\widehat{M}_{j,z,1},\cdots,\widehat{M}_{j,z,U}\right] = \arg \max_{\left[M_{j,z,1},\cdots,M_{j,z,U}\right]} \left\{ \sum_{u=1}^{U} M_{j,z,u} \cdot \frac{\varepsilon_z m_u c_u N_S}{K_z T_{OFDM}} \right\}$$

$$\text{subject to} \quad \begin{cases} \sum_{u=1}^{U} \widehat{M}_{j,z,u} \cdot E\left[p_{j,z,u}\right] \le P_{T,j} \\ \sum_{u=1}^{U} \widehat{M}_{j,z,u} \le N_{C,j} \end{cases}, \quad 1 \le j \le J. \quad , \tag{2.8}$$

where $P_{T,j}$ and $N_{C,j}$ are the transmit power and number of channels allotted to the j-th sector, respectively. The first constraint in Equation (2.8) is due to the maximum transmit power $P_{T,j}$, and the second is due to the maximum number of channels $N_{C,j}$.

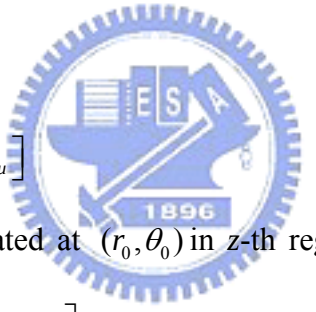

2.1.2.1 Evaluation of $E\left[p_{j,z,u}\right]$

Again, consider a user located at (r_0,θ_0) in z-th region of the j-th sector of BS_0, using the u-th MCS-class. $E\left[p_{j,z,u}\right]$, by definition, is given by

$$E\left[p_{j,z,u}\right] = \underset{\boldsymbol{\chi}}{E}\left[\underset{r_0,\theta_0}{E}\left[\rho_u \cdot \frac{I_z(r_0,\theta_0)+N}{A \cdot r_0^{-l} \cdot \chi_0 \cdot G_{0,j}(\theta_0)}\right]\right]$$

$$= \underset{\boldsymbol{\chi}}{E}\left[\rho_u \cdot \int_{\omega_{z-1}\cdot R}^{\omega_z \cdot R}\int_0^{2\pi}\left[\begin{array}{l}\left(\sum_{q_z=1}^{Q}\sum_{v=1}^{J} P_{T,v}^{(q_z)} \cdot G_{q_z,v}(\theta_{q_z}) \cdot A \cdot r_{q_z}^{-l} \cdot \chi_{q_z} + \sum_{v=1,v\neq j}^{J} P_{0,v} \cdot G_{0,v}(\theta_0) \cdot A \cdot r_0^{-l} \cdot \chi_0 + N\right) \\ \cdot\left(N_C \cdot G_{0,j}(\theta_0) \cdot A \cdot r_0^{-l} \cdot \chi_0\right)^{-1} \cdot r_0 \cdot f_j(r_0,\theta_0) \cdot \lambda_j(\theta_0) \cdot dr_0 d\theta_0\end{array}\right]\right], \tag{2.9}$$

where $\boldsymbol{\chi}$ is the vector of $Q+1$ independent random variables $\left[\chi_0\ \chi_1\ \chi_2\ \cdots\ \chi_Q\right]$ that characterize the shadowing effect from the interfering cells, $P_{T,v}^{(q_z)}$ is the total transmit power of BS_{q_z} over its v-th sector, $G_{q_z,v}(\theta_{q_z})$ is the corresponding antenna gain over the direction θ_{q_z} (see Figure 2(b)), $\lambda_j(\theta_0)$ is an

indicator function to indicate that if the location is served by j-th sector, that is,

$$\lambda_j(\theta_0)=\begin{cases}1 & if\ j=\arg\left\{\max_v G_{0,v}(\theta_0)\right\}\\ 0 & if\ j\neq\arg\left\{\max_v G_{0,v}(\theta_0)\right\}\end{cases}. \tag{2.10}$$

$f_j(r_0,\theta_0)=\left(a_j\cdot\pi R^2\right)^{-1}$ is the density function of user location in a sector, where $a_j=1/2\pi\cdot\int_0^{2\pi}\lambda_j(\theta_0)d\theta_0$. r_{q_z}, θ_{q_z}, r_{q_z} and R_{0,q_z} are the geometrical parameters when reuse factor K_z is selected as indicated in Figure 2(b). In Equation (2.9), the term

$$\frac{1}{N_C}\sum_{v=1,v\neq j}^{J}P_{T,v}^{(0)}\cdot G_{0,v}(\theta_0)\cdot A\cdot r_0^{-l}\cdot\chi_0 \tag{2.11}$$

is the intra-cell interference in the intra-cell frequency reuse case which is equal to zero when no channel is reused in the same cell.

The first step of the derivation is to evaluate $E_{r_0,\theta_0}\left[p_{j,z,u}\right]$, which can be rewritten as

$$\begin{aligned}E_{r_0,\theta_0}\left[p_{j,z,u}\right]=&\frac{\rho_u}{N_C}\cdot\int_{\omega_{z-1}\cdot R}^{\omega_z\cdot R}\int_0^{2\pi}\frac{\sum_{q_z=1}^{Q}\sum_{v=1}^{J}P_{T,v}^{(q_z)}\cdot G_{q_z,v}(\theta_{q_z})\cdot A\cdot r_{q_z}^{-l}\cdot\chi_{q_z}}{G_{0,j}(\theta_0)\cdot A\cdot r_0^{-l}\cdot\chi_0}\cdot\frac{\lambda_j(\theta_0)}{a_j\cdot\pi\cdot R^2}\cdot r_0dr_0d\theta_0\\&+\frac{\rho_u}{N_C}\cdot\int_{\omega_{z-1}\cdot R}^{\omega_z\cdot R}\int_0^{2\pi}\frac{\sum_{v=1,v\neq j}^{J}P_{T,v}^{(0)}\cdot G_{0,v}(\theta_0)\cdot A\cdot r_0^{-l}\cdot\chi_0}{G_{0,j}(\theta_0)\cdot A\cdot r_0^{-l}\cdot\chi_0}\cdot\frac{\lambda_j(\theta_0)}{a_j\cdot\pi\cdot R^2}\cdot r_0dr_0d\theta_0\\&+\rho_u\cdot\int_{\omega_{z-1}\cdot R}^{\omega_z\cdot R}\int_0^{2\pi}\frac{N}{G_{0,j}(\theta_0)\cdot A\cdot r_0^{-l}\cdot\chi_0}\cdot\frac{\lambda_j(\theta_0)}{a_j\cdot\pi\cdot R^2}\cdot r_0dr_0d\theta_0\end{aligned} \tag{2.12}$$

The first term in Equation (2.12) can be further simplified as

$$\frac{\rho_u}{N_C}\cdot\int_{\omega_{z-1}\cdot R}^{\omega_z\cdot R}\int_0^{2\pi}\frac{\sum_{q_z=1}^{Q}\sum_{v=1}^{J}P_{q_z,v}\cdot G_{q_z,v}\left(\theta_{q_z}\right)\cdot A\cdot r_{q_z}^{\ -l}\cdot\chi_{q_z}}{G_{0,j}\left(\theta_0\right)\cdot A\cdot r_0^{\ -l}\cdot\chi_0}\cdot\frac{r_0}{a_j\cdot\pi\cdot R^2}\cdot\lambda_j\left(\theta_0\right)\cdot dr_0 d\theta_0$$

$$=\frac{\rho_u}{a_j\cdot N_C\cdot\pi\cdot R^2}\cdot\int_{\omega_{z-1}\cdot R}^{\omega_z\cdot R}\int_0^{2\pi}\frac{\sum_{q_z=1}^{Q}\sum_{v=1}^{J}P_{q_z,v}\cdot G_{q_z,v}\left(\theta_{q_z}\right)\cdot\chi_{q_z}\cdot r_0}{G_{0,j}\left(\theta_0\right)\cdot\chi_0}\cdot\left(\frac{\sqrt{r_0^{\ 2}+R_{0,q_z}^{\ \ 2}-2R_{0,q_z}r_0\cos\left(\theta_0-\tilde{\theta}_{0,q_z}\right)}}{r_0}\right)^{-l}\cdot\lambda_j\left(\theta_0\right)\cdot dr_0 d\theta_0 \quad , \tag{2.13}$$

$$=\frac{\rho_u}{a_j\cdot N_C\cdot\pi\cdot R^2}\cdot\sum_{q=1}^{Q}\frac{\chi_{q_z}}{\chi_0}\cdot\alpha_{j,z}\left(q_z\right)$$

where

$$\alpha_{j,z}\left(q_z\right)=\int_{\omega_{z-1}\cdot R}^{\omega_z\cdot R}\int_0^{2\pi}\frac{\sum_{v=1}^{J}P_{q_z,v}\cdot G_{q_z,v}\left(\theta_{q_z}\right)\cdot r_0}{G_{0,j}\left(\theta_0\right)}\cdot\left(\frac{\sqrt{r_0^{\ 2}+R_{0,q_z}^{\ \ 2}-2R_{0,q_z}r_0\cos\left(\theta_0-\tilde{\theta}_{0,q_z}\right)}}{r_0}\right)^{-l}\cdot\lambda_j\left(\theta_0\right)\cdot dr_0 d\theta_0 \tag{2.14}$$

and

$$\theta_{q_z}=\tan^{-1}\left(\frac{r_0\cdot\sin\left(\theta_0\right)-R_{0,q_z}\cdot\sin\left(\tilde{\theta}_{0,q_z}\right)}{r_0\cdot\cos\left(\theta_0\right)-R_{0,q_z}\cdot\cos\left(\tilde{\theta}_{0,q_z}\right)}\right). \tag{2.15}$$

In addition, the second term in Equation (2.12) is simplified as

$$\frac{\rho_u}{N_C}\cdot\int_{\omega_{z-1}\cdot R}^{\omega_z\cdot R}\int_0^{2\pi}\frac{\sum_{v=1,v\neq j}^{J}P_{0,v}\cdot G_{0,v}\left(\theta_0\right)\cdot A\cdot r_0^{\ -l}\cdot\chi_0}{G_{0,j}\left(\theta_0\right)\cdot A\cdot r_0^{\ -l}\cdot\chi_0}\cdot\frac{\lambda_j\left(\theta_0\right)}{a_j\cdot\pi\cdot R^2}\cdot r_0 dr_0 d\theta_0$$

$$=\frac{\rho_u}{a_j\cdot N_C}\cdot\int_0^{2\pi}\frac{\sum_{v=1,v\neq j}^{J}P_{0,v}\cdot G_{0,v}\left(\theta_0\right)}{G_{0,j}\left(\theta_0\right)}\cdot\lambda_j\left(\theta_0\right)\cdot\left(\int_{\omega_{z-1}\cdot R}^{\omega_z\cdot R}\frac{r_0}{\pi\cdot R^2}dr_0\right)d\theta_0 \quad , \tag{2.16}$$

$$=\frac{\rho_u\cdot\left(\omega_z^{\ 2}-\omega_{z-1}^{\ \ 2}\right)}{2\pi\cdot a_j\cdot N_C}\cdot\beta_j$$

where

$$\beta_j=\int_0^{2\pi}\frac{\sum_{v=1,v\neq j}^{J}P_{0,v}\cdot G_{0,v}\left(\theta_0\right)}{G_{0,j}\left(\theta_0\right)}\cdot\lambda_j\left(\theta_0\right)d\theta_0. \tag{2.17}$$

Finally, the last term in Equation (2.12) is simplified as

$$\begin{aligned}
&\rho_u \cdot \int_{\omega_{z-1}\cdot R}^{\omega_z \cdot R} \int_0^{2\pi} \frac{N}{G_{0,j}(\theta_0)\cdot A \cdot r_0^{-l} \cdot \chi_0} \cdot \frac{r_0}{a_j \cdot \pi \cdot R^2} \cdot \lambda_j(\theta_0) \cdot dr_0 d\theta_0 \\
&= \rho_u \cdot \frac{N}{a_j \cdot \pi \cdot R^2 \cdot A \cdot \chi_0} \int_{\omega_{z-1}\cdot R}^{\omega_z \cdot R} r_0^{l+1} dr_0 \int_0^{2\pi} \frac{\lambda_j(\theta_0)}{G_{0,j}(\theta_0)} d\theta_0 \\
&= \frac{\rho_u \cdot N}{a_j \cdot \pi \cdot R^2 \cdot A \cdot \chi_0} \cdot \frac{\left[(\omega_z \cdot R)^{l+2} - (\omega_{z-1} \cdot R)^{l+2}\right]}{(l+2)} \cdot \int_0^{2\pi} \frac{\lambda_j(\theta_0)}{G_{0,j}(\theta_0)} d\theta_0 \\
&= \frac{\rho_u \cdot N \cdot \left(\omega_z^{\,l+2} - \omega_{z-1}^{\,l+2}\right) \cdot R^l}{a_j \cdot \pi \cdot A \cdot (l+2)} \cdot \frac{\gamma_j}{\chi_0}
\end{aligned} \tag{2.18}$$

where

$$\gamma_j = \int_0^{2\pi} \frac{\lambda_j(\theta_0)}{G_{0,j}(\theta_0)}\, d\theta_0 . \tag{2.19}$$

Therefore, we have

$$\begin{aligned}
\underset{r_0,\theta_0}{E}\left[p_{j,z,u}\right] &= \frac{\rho_u}{a_j \cdot N_C \cdot \pi \cdot \chi_0} \cdot \left[\sum_{q_z=1}^{Q} \frac{\alpha_{j,z}(q_z)}{R^2} \cdot \chi_{q_z} + \frac{N \cdot N_C \cdot \gamma_j \cdot R^l}{A \cdot (l+2)} \cdot \left(\omega_z^{\,l+2} - \omega_{z-1}^{\,l+2}\right)\right] \\
&\quad + \frac{\rho_u \cdot \beta_j}{2\pi \cdot a_j \cdot N_C} \cdot \left(\omega_z^{\,2} - \omega_{z-1}^{\,2}\right) \\
&\approx \frac{\rho_u}{a_j \cdot N_C \cdot \pi \cdot \chi_0} \cdot \tilde{\chi} + \frac{\rho_u \cdot \beta_j}{2\pi \cdot a_j \cdot N_C} \cdot \left(\omega_z^{\,2} - \omega_{z-1}^{\,2}\right) \\
&= \frac{\rho_u}{a_j \cdot N_C \cdot \pi} \cdot \tilde{\tilde{\chi}} + \frac{\rho_u \cdot \beta_j}{2\pi \cdot a_j \cdot N_C} \cdot \left(\omega_z^{\,2} - \omega_{z-1}^{\,2}\right)
\end{aligned} \tag{2.20}$$

where

$$\tilde{\chi} \approx \sum_{q_z=1}^{Q} \frac{\alpha_{j,z}(q_z)}{R^2} \cdot \chi_{q_z} + \frac{N \cdot N_C \cdot \gamma_j \cdot R^l}{A \cdot (l+2)} \cdot \left(\omega_z^{\,l+2} - \omega_{z-1}^{\,l+2}\right) \tag{2.21}$$

and $\tilde{\tilde{\chi}} = \tilde{\chi} / \chi_0$. $\tilde{\chi}$ is a log-normally distributed random variable to approximate the summation of Q log-normal random variables plus a constant. The mean and variance of $\tilde{\chi}$ can be obtained in [23, 24]

$$E\left[\tilde{\chi}\right]=\sum_{q_z=1}^{Q}\exp\left[\ln\left(\frac{\alpha_{j,z}(q_z)}{R^2}\right)+\left(\frac{\ln(10)\cdot\sigma_{dB}}{10\sqrt{2}}\right)^2\right]+\frac{N\cdot N_C\cdot\gamma_j\cdot R^l}{A\cdot(l+2)}\cdot\left(\omega_z^{\,l+2}-\omega_{z-1}^{\,l+2}\right)$$
$$Var\left[\tilde{\chi}\right]=\sum_{q_z=1}^{Q}\exp\left[2\cdot\ln\left(\frac{\alpha_{j,z}(q_z)}{R^2}\right)+\left(\frac{\ln(10)\cdot\sigma_{dB}}{10}\right)^2\right]\cdot\left(\exp\left[\left(\frac{\ln(10)\cdot\sigma_{dB}}{10}\right)^2\right]-1\right) \quad (2.22)$$

Therefore, its variance and mean in dB are

$$\sigma_{\tilde{\chi}}^2=\left(\frac{10}{\ln(10)}\right)^2\cdot\ln\left(\frac{Var\left[\tilde{\chi}\right]}{\left(E\left[\tilde{\chi}\right]\right)^2}+1\right), \quad (2.23)$$

$$m_{\tilde{\chi}}=10\cdot\log_{10}\left(E\left[\tilde{\chi}\right]\right)-\frac{\ln(10)}{20}\sigma_{\tilde{\chi}}^2. \quad (2.24)$$

Since χ_0 has zero mean and variance σ_{dB}^2 in dB, the $\tilde{\tilde{\chi}}$ will be a log-normal random variable with mean equal to $m_{\tilde{\chi}}$ and variance equal to $\sigma_{\tilde{\chi}}^2+\sigma_{dB}^2$ in dB. Therefore, $E\left[p_{j,z,u}\right]$ can be approximated as

$$E\left[p_{j,z,u}\right]\approx\frac{\rho_u}{a_j\cdot N_C\cdot\pi}\cdot\exp\left[\frac{\ln(10)}{10}\cdot m_{\tilde{\chi}}+\left(\frac{\ln(10)}{10}\right)^2\cdot\frac{\left(\sigma_{\tilde{\chi}}^2+\sigma_{dB}^2\right)}{2}\right]+\frac{\rho_u}{2\pi\cdot a_j\cdot N_C}\cdot\beta_j. \quad (2.25)$$

Once $E\left[p_{j,z,u}\right]$ is known from Equation (2.25), the system capacity in Equation (2.8) can be evaluated.

2.2 Capacity Improvement Techniques for Cellular OFDMA Systems

In this section, an example OFDMA system resembling that of IEEE 802.16e is analyzed to illustrate how the proposed analysis can be used to optimize the design of the system. The OFDMA parameters are listed in Table 1. For the switched-beam smart antenna, 12 antenna elements are used to generate the same number of beams with the steering directions being equally distributed over $[0, 2\pi)$. For the full-reuse case, $N_{C,j} = 216$. Otherwise, channels are divided equally into each sector (beam) with $N_{C,j} = 72$ and $N_{C,j} = 18$ for the 3-sector and switched-beam smart antenna, respectively.

Maximum transmit power of base station is assumed to be 50 Watts, which is equally divided to each sector (beam). Furthermore, $A = 6.01 \times 10^{-13}$ and $l = 4.375$ in Equation (2.4), the same as those used in the IEEE 802.16 type-B path-loss model with 2 GHz carrier frequency [8] and $\sigma_{dB}^2 = 8$ dB. Three MCS-classes are considered for numerical results: QPSK, 16QAM and 64QAM with 1/2 code rate Convolutional Turbo Code (CTC). The required SINR for MCS classes of QPSK, 16QAM and 64QAM are 5dB, 10.5dB and 16dB, respectively, to ensure the BER (Bit Error Rate) lower than 10^{-6} [8].

The system capacity for different frequency reuse factors with only one MCS-class (MCS-class with QPSK) and no reuse partitioning are shown as in Figure 5. Fundamentally, the system capacity is limited by two dominant factors. One is the number of available channels in a sector (beam), the other is the intra- and/or

Table 1 OFDMA parameters used in numerical results

Parameter	**Value**
Total Bandwidth	10 MHz
FFT size	1024
OFDM symbol duration (including cyclic-prefix), T_{OFDM}	102.9 μs
Cyclic-prefix	11.4μs
Sub-carrier frequency spacing	10.94 kHz
Number of sub-channels, N_C	216
Number of sub-carriers in a sub-channel, N_S	4
Number of sub-carriers for data transmission	864
Number of sub-carriers for guard band	160 (1024-864)
Frame duration, T_{frame}	5ms

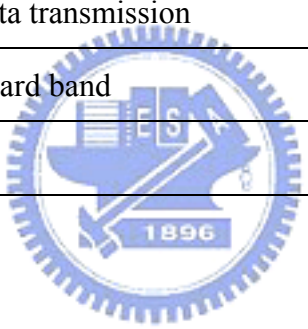

inter-cell interference. For a fixed antenna configuration, different reuse factors K and (channel) reuse patterns make a tradeoff between these two factors. Apparently, as seen in the figure, for the no-reuse case, the dominating limit factor is the number of available channels and therefore increasing K reduces the system capacity, although the inter-cell interference is reduced at the same time. For the full-reuse case, however, the intra-and/or inter-cell interference plays a more prominent role in determining the system capacity because the number of available channels has been increased by channel reuse. In this case, as is seen, $K = 3$ provides the best tradeoff between the available channels and intra- and/or inter-cell interference, and has the highest

capacity for both the 3-sector and switched-beam smart antennas. In addition, switched-beam smart antenna provides a significant gain over 3-sector antenna in full-reuse case because of more frequent channel reuse and larger antenna gain. Note that the performance of cell architecture $(\{1\},3,1)$ is worse than that of $(\{1\},3,1/3)$ because of too large intra- and/or inter-cell interference for using $K=1$. In the figure, it is also shown that simulation results match well with the numerical results; the difference is within 1.3% ~ 3.9%.

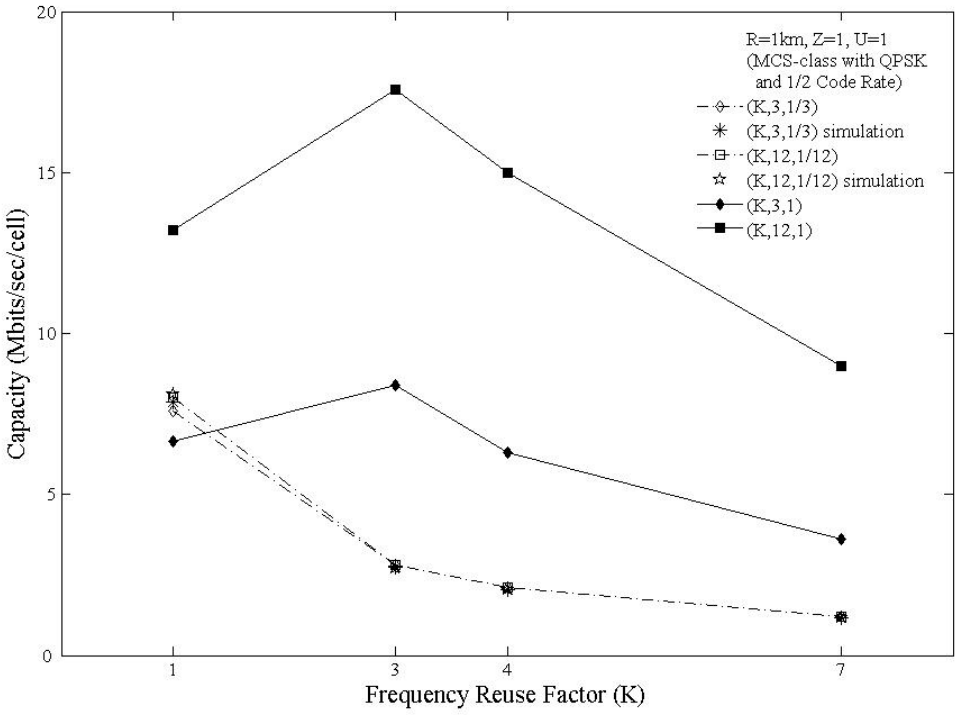

Figure 5. Downlink capacity of multi-cell OFDMA system with single MCS-class

Figure 6 shows the system capacity for different channel reuse patterns and antenna configurations with 3 MCS-classes. Recall that $K = 3$ provides the highest system capacity. Again, for multiple MCS-classes, employing full channel reuse improves the system capacity. The improvement is more significant for switched-beam smart antenna because of much less inter-cell interference.

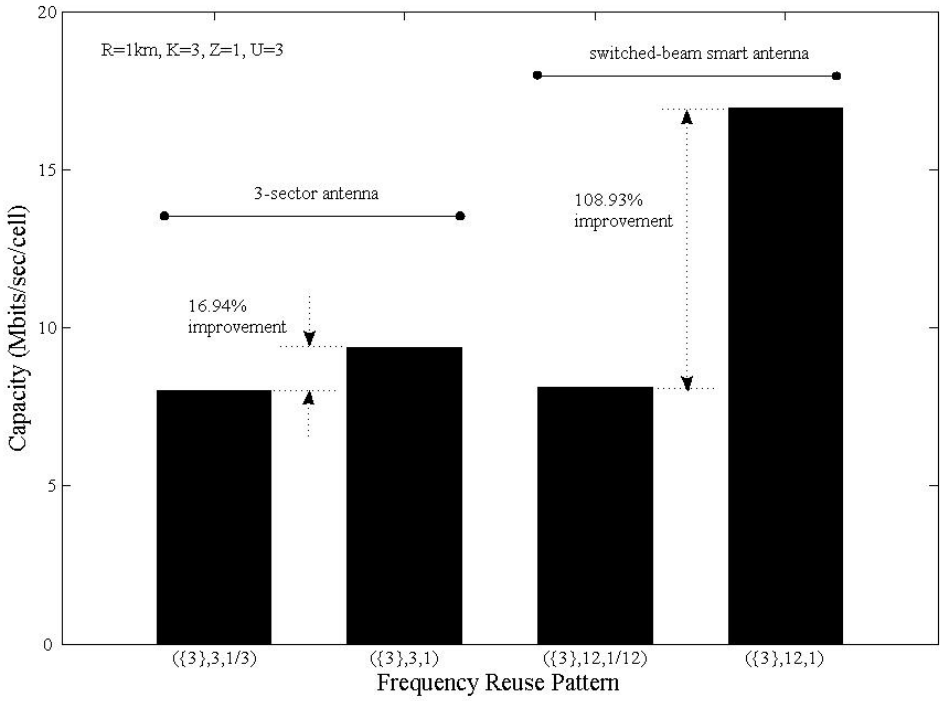

Figure 6. Downlink capacity of multi-cell OFDMA system with multiple MCS-classes

In Figure 7, the capacity improvement by using fractional frequency reuse is investigated. The results in the left side are reproduced from Figure 6 for comparison purpose. It shows that the capacity is substantially improved (97.1 - 300%) by applying reuse partitioning cell structure. Comparing the cases of $(\{3\},12,1)$ with $(\{1,3\},12,1)$, the improvement by reuse partitioning is very significant by intra-cell frequency reuse. It is because in the inner cell the MCS-class with 64QAM is almost employed exclusively throughout all the beams because low inter-cell interference.

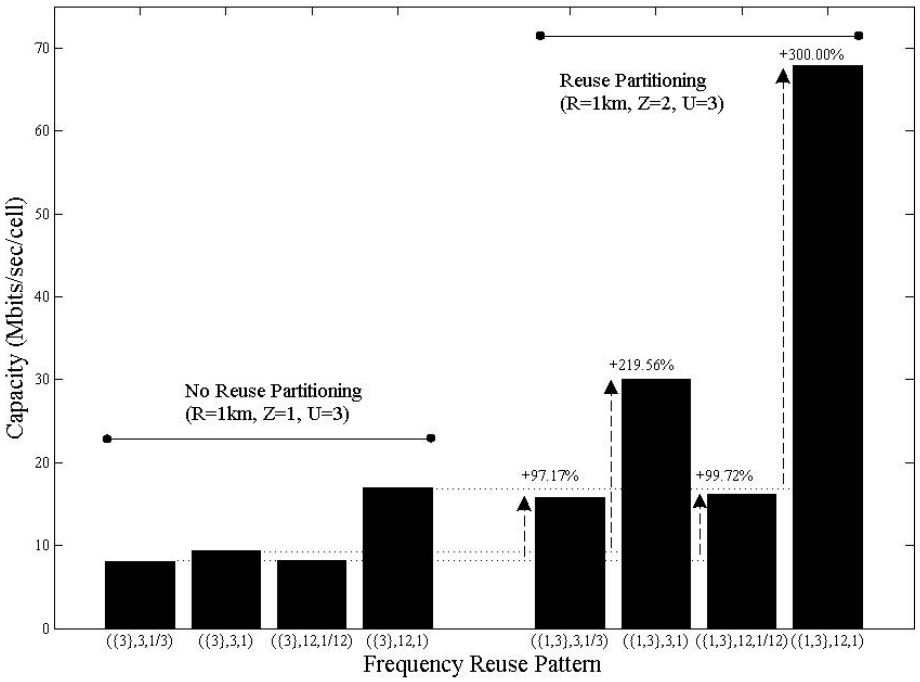

Figure 7. Downlink capacity of multi-cell OFDMA system with reuse partitioning

Chapter 3

An Improved Fast Base Station Switching Technique for Cellular OFDMA Systems

Fast base station switching (FBSS) is an important handover mechanism in the orthogonal frequency division multiple access (OFDMA) mobile cellular systems. By employing one radio connection and multiple network connections during handover, FBSS strikes a good balance between complexity and handover performance, as compared to hard handover and macro diversity handover. In Section 3.1, the FBSS defined in IEEE 802.16 standard is first overviewed. Then, an improved FBSS with reuse partitioning is proposed in Section 3.2 to improve the performance of the traditional FBSS in OFDMA mobile cellular systems.

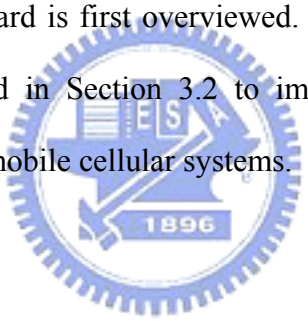

3.1 Fast Base Station Switching in IEEE 802.16 Network

There are three kinds of handover defined in IEEE 802.16e: hard handover, macro diversity handover (MDHO) and fast base station switching (FBSS). In hard handover, the system maintains only one connection in both the network and radio-link sections for the MS (mobile station), and therefore the network and radio-link connections to the target base station (BS) will be established only after breaking the existing ones. Hard handover is very simple, but services will be disrupted for a period of time needed for the establishment of the new connections. Contrary to hard handover, the system maintains multiple network and radio-link connections at the same time for the MS in MDHO. Therefore, both the network and radio-link connections to the target base stations can be established before breaking the existing ones. Since MDHO is

essentially a soft handover, the service disruption can be eliminated by having multiple network and radio-link connections simultaneously. MDHO needs more than one receiver in the MS and hence increases its complexity. In addition, two copies of radio resource are needed for handover users and that leads to lower system spectrum efficiency and higher downlink interference.

FBSS, on the other hand, takes advantage of the low service disruption time from MDHO and low MS complexity from hard handover [8,25]. At network section, FBSS establishes connections with potential target BSs before breaking the existing one, so that the service disruption time can be reduced like in MDHO. Meanwhile, only one connection will be maintained at the radio-link section so as to keep low MS complexity as in hard handover. By switching between BSs fast enough, the MS can maintain its link performance and explore macro diversity gain.

In FBSS, the radio-link will not be switched to the target BS before the establishment of the new network connection to the target BS; otherwise, packets might be lost and/or become obsolete. This is especially important for real-time services. Unfortunately, the time needed for the establishment of a network connection is uncertain (a random variable) and cannot be known in advance [26]; to initiate the establishment of network connection too early will waste the network resource, but too late the radio-link performance might be degraded to an unacceptable level and that incurs packet loss.

In this section, an improved FBSS with reuse petitioning (RP) cell structure is proposed for IEEE 802.16e. By reserving some of the radio resource for use of high reuse factor, and using that radio resource to accommodate those handover users with bad radio-link performance, the packet loss rate can be substantially reduced, at the slight expense on average cell throughput.

3.1.1 Fast Base Station Switching in IEEE 802.16e

In the IEEE 802.16e system, an FBSS handover begins with a decision for an MS to transmit/receive data to/from the Anchor BS that may change within the diversity set [8]. Diversity set is a set containing a list of active BSs that are informed of the MS capabilities, security parameters, service flows and full MAC context information, and the Anchor BS is the BS in the diversity set that is designated to transmit/receive data to/from the MS at a given frame. Based on the received signal quality, the MS in FBSS handover can fast switch the Anchor BS so as to obtain the macro diversity gain. For good performance, the MS can scan the neighbor BSs and select those suitable ones to be included in the diversity set (diversity set selection/update), and the MS shall select the best BS from its current diversity set to be the Anchor BS (Anchor BS selection/update) [8].

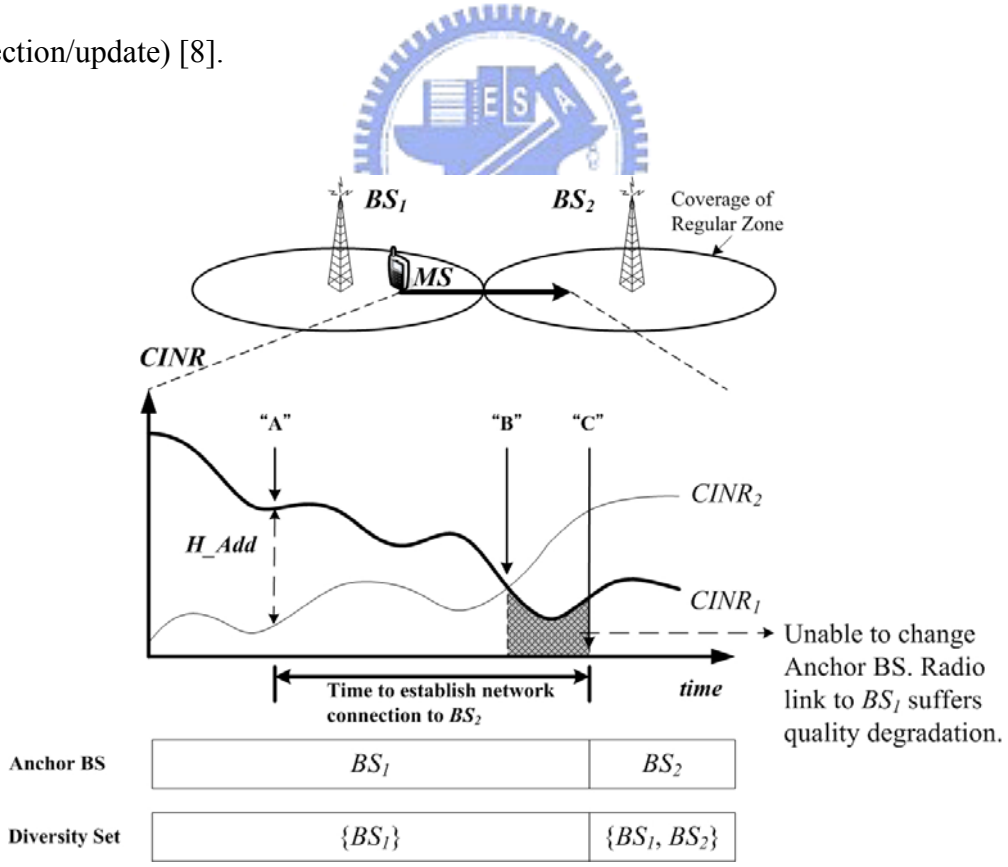

Figure 8. Cell structure, received radio-link signals, diversity set membership and Anchor BS selection of an MS involved in FBSS in IEEE 802.16e.

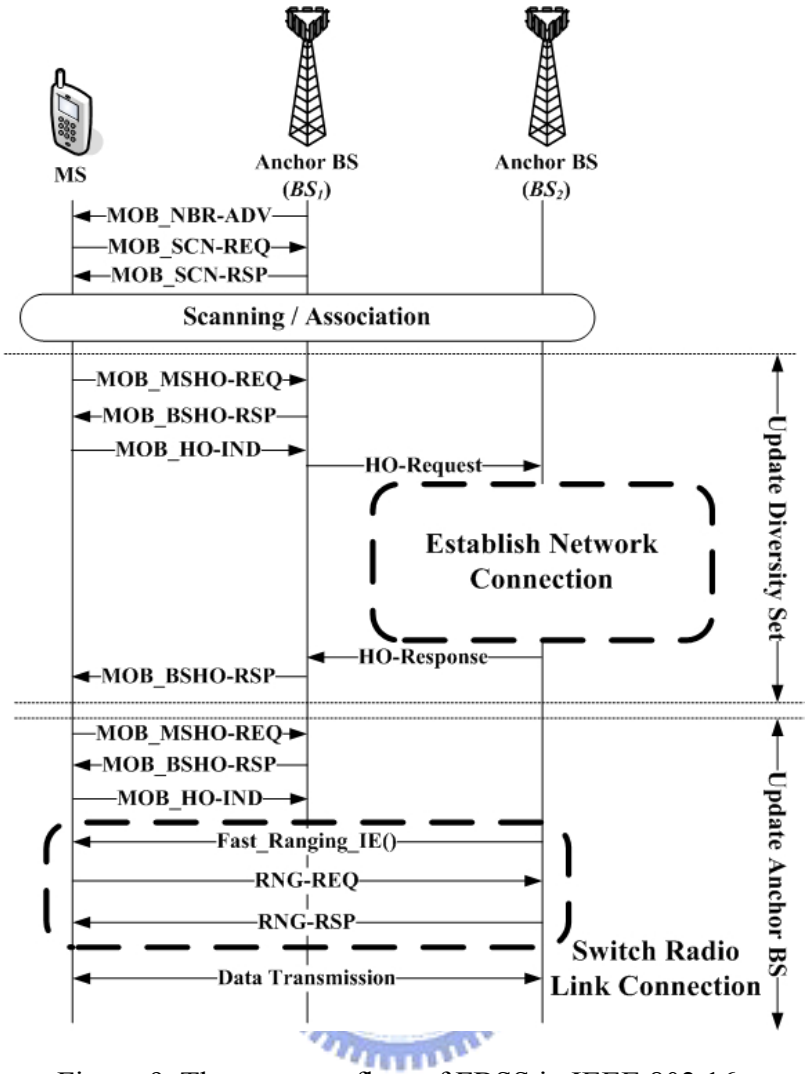

Figure 9. The message flow of FBSS in IEEE 802.16e

Figures 8 and 9 are used to explain the FBSS operation in IEEE 802.16e in details. For simplicity only two BSs are considered. Assume the MS is moving from BS_1 toward BS_2, and BS_1 is the Anchor BS at the beginning. In IEEE 802.16e, the parameter H_Add, a threshold used to trigger diversity set selection/update, is broadcasted through DCD (Downlink Channel Descriptor), and the characteristics of neighbor BSs (BS_2 in this case) including BSID, PHY Profile ID, Preamble Index, etc. through the MOB_NBR-ADV message. Base on the information, the MS may send MOB_SCN-REQ to BS_1 and get response from MOB_SCN-RSP for requesting a period of time to facilitate scanning and/or association (an optional initial ranging)

of BS_2, as shown in Figure 9. When the CINR (Carrier to Interference plus Noise Ratio) difference of BS_1 and BS_2 is less than H_Add, the MS sends MOB_MSHO-REQ with a recommended BS list including BS_2. If BS_2 is also in the recommended list in MOB_BSHO-RSP, which is replied by BS_1, then the MS sends MOB_HO-IND to request to add BS_2 to the diversity set, i.e., to initiate the diversity selection/update procedure. In Figure 8, this first happens at the time instant A. After that, BS_1 sends HO-Request to BS_2 through wire-line network to establish the network connection, and BS_2 will reply HO-Response to BS_1 if the establishment is complete. Accordingly, BS_1 can update the MS new diversity set members through MOB_BSHO-RSP.

When the MS keeps moving and if CINR_{BS_2} is higher than CINR_{BS_1}, for example at the time instant B in Figure 8, the MS may send MOB_MSHO-REQ to request to change Anchor BS from BS_1 to BS_2 (initiation of the Anchor BS selection/update procedure). The request, however, will not be granted in this example until the time instant C because the network connection to BS_2 is not yet established (for some reason) before that instant, and BS_2 will not be included in the diversity set. If the request is granted, through MOB_BSHO-RSP, the MS will send MOB_HO-IND to terminate the existing radio link connection and then perform fast ranging with BS_2, see Figure 9. Note that BS_2 needs to reserve an uplink contention-free ranging sub-channel for the MS and to place Fast_Ranging_IE in the extended UIUC (Uplink Interval Usage Code) in a UL-MAP IE (Information Element) to inform the MS this ranging opportunity. The fast ranging process can be accomplished in two frames, where the uplink ranging opportunity is indicated by the downlink MAP in the first downlink sub-frame, and then the MS sends RNG-REQ in the successive uplink sub-frame based on the radio parameters recorded in the scanning interval. Then BS_2

replies RNG-RSP along with the correction commends encoded in TLV formats in the second frame. After that, the MS begins to transmit/receive data to/from BS_2.

As is mentioned, the MS is not able to change its Anchor BS to BS_2 until the time instant C, although CINR_{BS_2} is already higher than CINR_{BS_1} at the time instant B. During the time period between B and C, the MS still talks to BS_1 but with a degraded link performance, and that may result in packet loss. One simple remedy to this problem is to use a larger H_Add; in other words, the request for diversity set update is initiated earlier. This, however, may waste network resource if BS_2 is put into the diversity set too early. In the next section, an FBSS with reuse partitioning cell structure is proposed to improve the handover performance at the expense of slight loss in average cell throughput.

3.2 An Improved Fast Base Station Switching Technique for Cellular OFDMA Systems

Reuse partitioning (RP) is a cell structure in which a regular cell is divided (ideally) into two or more concentric cell-regions, each with a different frequency reuse factor as introduced in section 2.1.1. This also implies that the radio resource of a cell has to be divided into the same number of resource-regions. A smaller reuse factor (small reuse distance) is allowed for the inner cell-regions because of the smaller transmit power, and a larger reuse factor is needed for the outer cell-regions so as to maintain the required signal quality. By allowing the inner regions to use a smaller reuse factor leads to a higher system capacity, as compared to the regular cell structure where the same reuse factor is used for the entire cell [19]. In this section, the concept of reuse partitioning is used to increase the handover performance.

3.2.1 Reuse Partitioning in IEEE 802.16e

Figure 10(a) shows a simplified TDD frame structure in IEEE 802.16e. Preamble, FCH (Frame Control Header), downlink MAP and uplink MAP are control signals of the frame. It can be treated as an example of the frame structure depicted in Figure 4(a). The cell-specific Preamble is mainly used for downlink synchronization. FCH contains DL_Frame_Prefix that indicates the length and coding scheme of the DL_MAP message. DL_MAP and UL_MAP are MAC messages that define the starting point of the downlink and uplink bursts, respectively.

In IEEE 802.16e, frequency reuse with factor K can be achieved by dividing the radio resource in a frame into K resource-regions and each one of them is allocated to different BS. In Figure 10(a), K is equal to 4 so that the radio resource (both downlink and uplink) is divided into 4 resource-regions. Note that BSs need to be

synchronized and follow the same sub-carrier permutation rule for this scheme to work.

In order to design a reuse partitioning scheme, we adopt the concept of resource zone in IEEE 802.16e [8]. As an example, in addition to the regular resource-zone for $K = 4$, a reuse partitioning (RP) zone is defined for $K = 7$, as shown in Figure 10(b). Again, within each respective zone, the radio resource is divided into K resource-regions and each one of them is allotted to different BS.

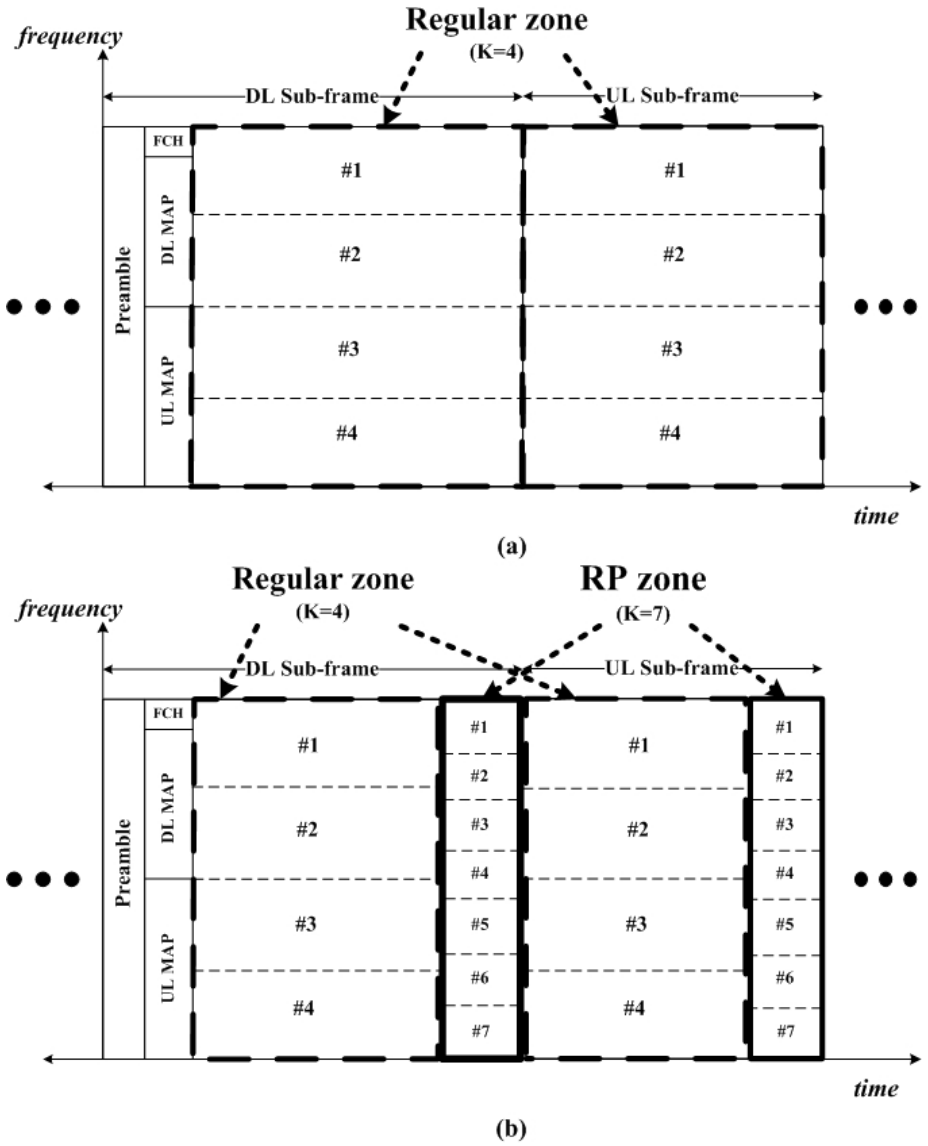

Figure 10. A simplified IEEE 802.16e TDD frame structure with (a) regular $K = 4$ resource zone, and (b) regular $K = 4$ resource zone and $K = 7$ RP zone.

3.2.2 FBSS with Reuse Partitioning

The concept of reuse partitioning is used here to increase the performance of FBSS handover. The basic idea is as follows. Under the reuse partitioning cell structure, the handover users who are in a bad channel condition are scheduled to a resource-region with a large reuse factor so that a better CINR can be maintained, and therefore the packet loss rate is reduced. This method is very effective for the handover users who are waiting for the target BS to establish the network connection, as discussed in the previous section.

Figure 11 shows the RP cell structure and the received radio-link signals, diversity set membership and Anchor BS of an MS involved in FBSS. $K = 4$ for the inner cell-region and $K = 7$ for the outer one with the resource-regions given in Figure 10(b). In the $K = 7$ resource-region, since a large reuse factor is used, the received CINR of an MS is higher as compared to the $K = 4$ resource-region. Initially, the MS talks to BS_1 by using resource in the $K = 4$ resource-region. As discussed in the previous section, during the time between B and C, although CINR_{BS_2} is higher than CINR_{BS_1}, the MS still talks to BS_1 since the network connection to BS_2 is not ready yet. In the case of using reuse partitioning, the difference from Figure 8 is that now we have $K = 7$ resource-zone, and the handover users going through this period of time can be re-scheduled to that region to improve the radio-link performance if its CINR is less than the threshold ρ_{req}. Therefore, the packet loss during this period will be mitigated and the packet loss rate can be substantially reduced.

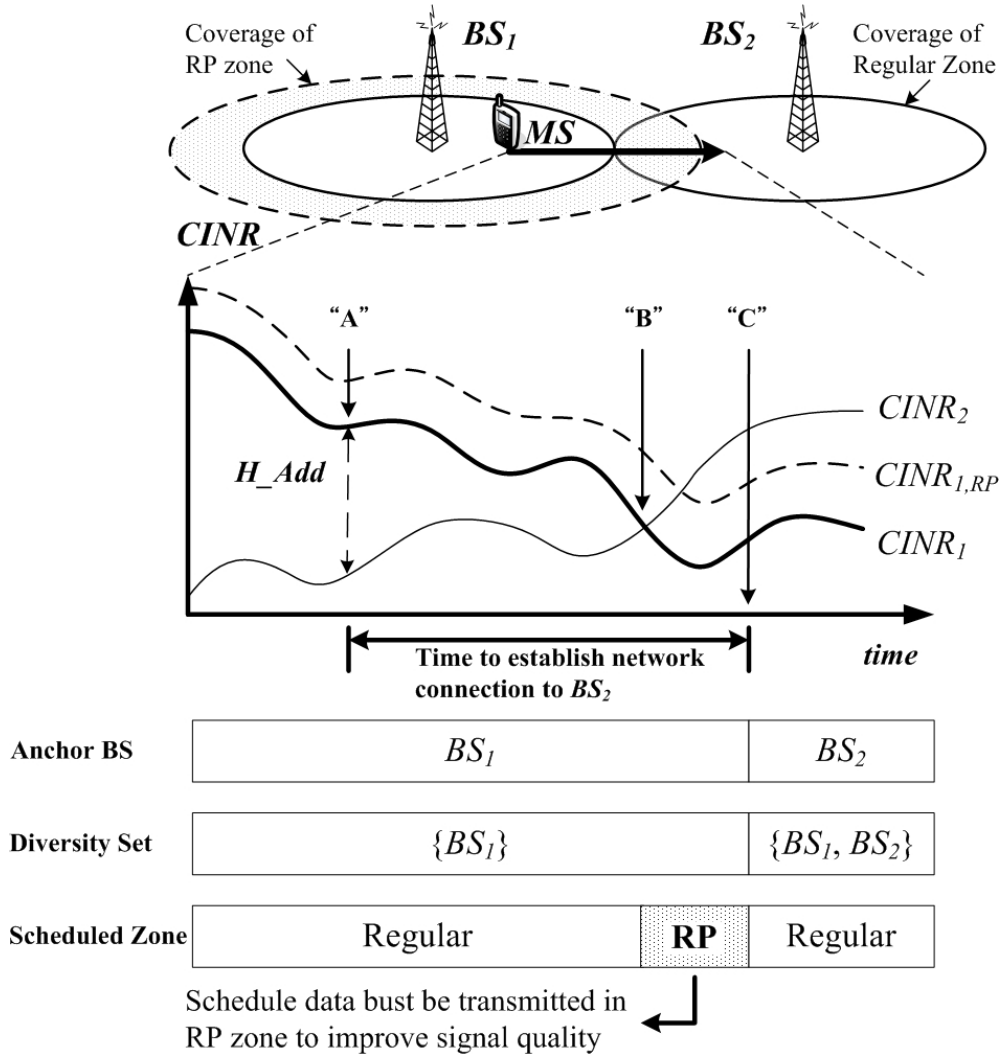

Figure 11. Reuse partitioning cell structure, received radio-link signals, diversity membership, Anchor BS selection and scheduled zones of an MS in FBSS with reuse partitioning.

3.2.3 Simulation Results

In this section, simulation results are given to illustrate the handover performance of FBSS with and without reuse partitioning.

A. Simulation Model

The IEEE 802.16e downlink OFDMA system is simulated in a multi-cell urban environment, where cells are assumed to be synchronized to each other. Total of 19 cells is simulated with 1 km cell coverage under 15 Watts transmit power. $K = 4$ for the regular resource-zone and $K = 7$ for the RP resource-zone. Each cell has three sectors. The OFDM PHY parameters are given in Table 2.

At the beginning of the simulation, MSs are generated by Poisson processes and located randomly in a cell. The path loss to every BS is calculated for each MS, and the log-normal shadow fading (with de-correlation distance of 50m) and frequency-selective fading are generated according to the models given in [27]. An MS will send a service request to the BS with the highest effective SINR, and the request will be granted if there is radio resource available. Otherwise, the MS will be blocked and removed in the simulator. The effective CINR is evaluated on the received preamble signal part by the EESM (Exponential Effective SIR Mapping) criterion [28]. The location of an MS is periodically updated based on ITU vehicular mobility model [29] with mobility of 50km/hr. According to the mechanism proposed in section 3.2.2, the diversity set of an MS may be updated according to the CINR variation. Moreover, the anchor BS is the BS in diversity set with the highest CINR, and the MS only transmits/receives the radio signal to/from the anchor BS.

The G.729 VoIP traffic model is adopted in the simulation. The VoIP packet arrives every 20 ms with a packet size of 640 bits. The packet error rate is determined by the received SINR of the data traffic part and can be obtained by looking up table given in [8].

Table 2 Parameters for system-level simulation

Parameter	Value
Channel bandwidth	6 MHz
FFT size	2048
OFDM symbol duration (including cyclic-prefix)	336μs
Cyclic-prefix	37.333μs
Sub-carrier frequency spacing	3.348 kHz
Frame duration	20ms
Downlink sub-frame duration	10ms
Sub-carrier permutation rule	Adjacent sub-carrier permutation
Number of bins	192
Number of sub-carriers in a bin	9
Number of sub-carriers for data transmission	1728
Number of sub-carriers for guard band	320 (2048-1728)
Sub-channel definition	2 adjacent bins × 3 adjacent symbols
Maximum diversity set size	3
Threshold to schedule MS into the RP zone	6 dB (ρ_{req})
Time to establish network connection	Uniform distributed between 200ms~700ms [26]

B. Simulation Results

The performances of FBSS are given in Figure 12, where P_{RP} is the percentage of radio resource allotted to the $K = 7$ resource-region. Three sets of results are given including packet loss rate, average diversity set size and cell throughput. In all of the results $P_{RP} = 0$ represents the case of traditional FBSS; that implies no RP resource-region is reserved. Figure 12(a) shows the result of packet loss rate. As can be seen, P_{RP} should be large enough, says more than 5%, in order to obtain a sizable reduction on packet loss rate. More specifically, 38.33% to 84.08% reductions are achievable by increasing P_{RP} from 7.29% to 21.88%, with respect to the

case $P_{RP} = 0$. Note that the packet loss rate reduction becomes saturated if P_{RP} is larger than around 21.88%. In addition, for a P_{RP}, a lower packet loss rate is obtained with a larger H_Add.

Figure 12(b) shows the average diversity set size, which is an indicator on the network resource usage. As expected, the diversity set size is unchanged with different P_{RP} for a specific H_Add. On the other hand, when increasing H_Add, the neighbor BSs might be added to the diversity set too early before the MS really needs to change its Anchor BS. Therefore the average diversity set size is larger and more network resource is consumed.

The cell throughput is shown in Figure 12(c). Since frequency reuse factor is larger in RP zone, the larger P_{RP}, the lower the cell throughput. The results show that less than 4.21% cell throughput will be lost even when P_{RP} is increased to 21.88%. It is because the reduction on packet loss rate can increase the effective packets received by the MS, which can increase the cell throughput.

In summary, the performance tradeoff can be investigated by Figure 13, which is translated from Figure 12(a) and Figure 12(c). By reserving some of the radio resource for high reuse factor, and using that radio resource to accommodate handover users with bad radio-link performance, Figure 13 shows that the packet loss rate of FBSS is significantly reduced at a slight expense of cell throughput.

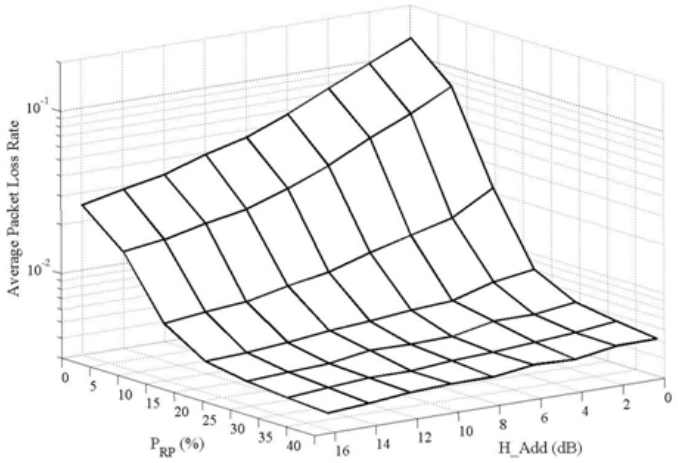

(a) Packet loss rate

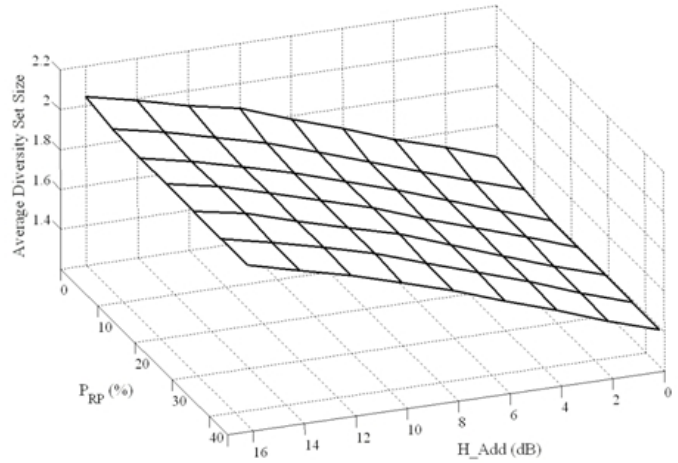

(b) Average diversity set size

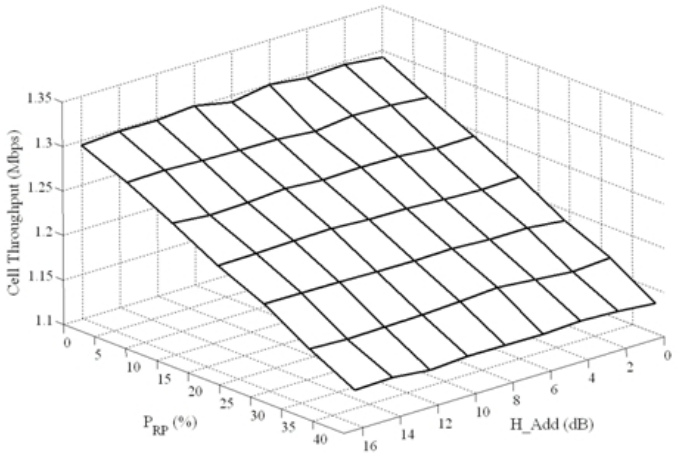

(c) Cell throughput

Figure 12. The performances of FBSS with reuse partitioning

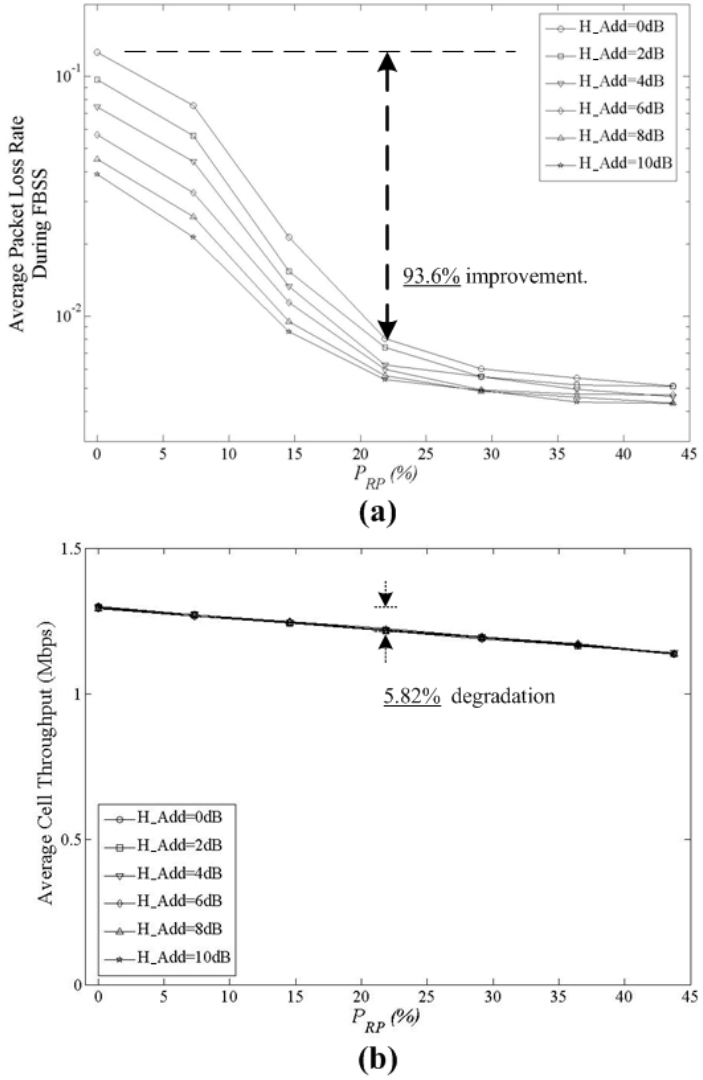

Figure 13. (a) Packet loss rate reduction and (b) cell throughput penalty

Chapter 4

Multi-hop Cellular OFDMA Systems

According to the research results shown in Section 3.1, there will be a transmit power issue when system operators try to upgrade their cellular OFDMA network to support much higher capacity and transmission rate. For example, ten times in transmission rate will result in more than ten times in transmit power in order to meet the required signal to interference plus noise ratio (SINR). Since the transmit power cannot be increased unlimitedly due to the hardware cost or battery life of a mobile station (MS), the coverage holes may exist between adjacent base stations (BS).

Traditional solution to this problem is to deploy additional BSs or repeaters to serve the coverage holes [30]. Unfortunately, the cost of BS is very high and the wire-line backhaul may not be available everywhere. Repeater, on the other hand, has the problem of amplifying interference and has no intelligence of signal control and processing [31]. Recently, relay station (RS) that receives and forwards signals from source to destination through radio has been developed as a more cost-effective solution. Since RSs do not need a wire-line backhaul, the deployment cost of RSs will be much lower than that of BSs. Meanwhile, RS can decode the signal from the source and forward it to the destination. Intelligent resource scheduling and cooperative transmission can be applied to perform better system performance.

Multi-hop relays (MR) have been proposed to enhance cell coverage and user throughput to the traditional cellular systems [32-37]. In the public deliverable of the EU WINNER project [32], multi-hop relay was introduced to increase the throughput of the boundary users and/or to relay user data to a destination that is out of BS

coverage. Within IEEE 802.16 Working Group, IEEE 802.16j Relay Task Group has been devoted to standardize an MR network with the objectives to enhance the system coverage, per-user throughput and system capacity of the IEEE 802.16 broadband wireless access standard. IEEE 802.16j is the only standard body that is currently standardizing a multi-hop relay network. In Section 4.1, the IEEE 802.16j system model will be introduced and the standardization history will be briefly reviewed.

The advantages of MR networks such as coverage extension and per-user throughput enhancement come at the expense of additional use of radio resource for multi-hop transmission. The extra radio resource needed for every transmission of user data may reduce the overall system capacity, as compared to the system with no relays [35-37]. Capacity degradation is one of the major challenges that the MR network needs to overcome before it can be widely adopted in the practical systems. Based on the coverage planning method introduced in Section 4.2, the performances of multi-hop cellular network and their tradeoffs will be investigated in Section 4.3.

4.1 IEEE 802.16j Multi-hop Relay Network

IEEE 802.16j is an amendment to the IEEE 802.16 broadband wireless access standard to enable the operation of multi-hop relay stations (RS), with the objectives to enhance the system coverage, per-user throughput and system capacity [31]. Compared with base station (BS), RS does not need a wire-line backhaul and has much lower hardware complexity and higher deployment flexibility, which can significantly reduce deployment cost of the system.

4.1.1 IEEE 802.16j Standard Activities

In response to the demand on standardization of an MR network, a mobile

multi-hop relay (MMR) study group (SG) under IEEE 802.16 Working Group was chartered in July 2005 and had the first meeting in September 2005 in Taipei, Taiwan. Over the three consecutive sessions until January 2006, MMR SG discussed the possible applications of multi-hop relay technologies and their benefits to the IEEE 802.16 broadband wireless access standard.

In March 2006, the project authorization request (PAR) of IEEE 802.16j Relay Task Group (TG) was approved by the IEEE 802 executive committee (EC), and the first Relay TG meeting was held in May 2006 in Tel Aviv, Israel. From May to September of 2006, Relay TG had spent all their time to work out the baseline documents for usage model, terminology, technical requirements and evaluation methodology.

In November 2006, IEEE 802.16j Relay TG had issued the first call for technical proposals and a large number (152) of technical contributions were submitted. This reflects the broad interests on multi-hop relay technology from the industry and academia. In January 2007, more contributions (170) were submitted to Relay TG. In this meeting, members began to achieve preliminary consensus on frame structure, network entry, bandwidth request, MAC PDU construction, power control, sleep/idle mode, handover, MBS (Multicast and Broadcast Services) and cooperative relaying issues.

According to the original schedule of IEEE 802.16j, the standard is expected to be finalized in September 2007. However, this schedule might be delayed due to many unexpected technical and backward compatibility problems, because it is very challenging to enable the relay functionalities without changing the legacy MS specification. It is widely anticipated that the standard can be approved in 2008.

4.1.2 IEEE 802.16j System Architecture

In this section, the key system features of the IEEE 802.16j MR network are overviewed. The basic system architecture considered by IEEE 802.16j is shown in Figure 14 (a), where two kinds of radio links are identified: access link and relay link. BS that is capable of supporting multi-hop relay is called MR-BS. The access link is the radio link that originates or terminates at an MS, which is either a downlink (DL) or an uplink (UL), defined in IEEE 802.16-2004. The relay link is the radio link between an MR-BS and an RS or between a pair of RSs, which can be either uplink or downlink. Following the basic architecture in Figure 14 (a), a new frame structure shown in Figure 14 (b) is designed [38], where each DL sub-frame and UL sub-frame is divided into access zone and relay zone. The DL/UL access zone is a portion of DL/UL sub-frame used for access links transmission, and the DL/UL relay zone is a portion of DL/UL sub-frame used for relay links transmission. Note that each DL/UL sub-frame may have more than one relay zone.

In order to enable RS operations without changing on the legacy MS specification, two types of RSs have been defined: Non-transparent RS and transparent RS. The non-transparent RS acts as a BS sector [8], therefore the MR-BS has to assign a preamble index to each RS, and the RS will transmit its own preamble, FCH (Frame Control Header) and MAP over the access zone. The frame structure for the non-transparent RS is shown in Figure 14 (b). Note that it is not possible for non-transparent RSs to scan and synchronize with each other by the preamble. Because they need to transmit their own preamble at the start of a frame and is not able to receive the preamble transmitted from the MR-BS or other RSs. Therefore, in Figure 14 (b) the relay amble (R-amble) located at the end of downlink sub-frame is

designed for the purpose of measurement, synchronization and neighborhood discovery over relay links [39]. Note that the R-amble may not be transmitted in each frame for overhead reduction.

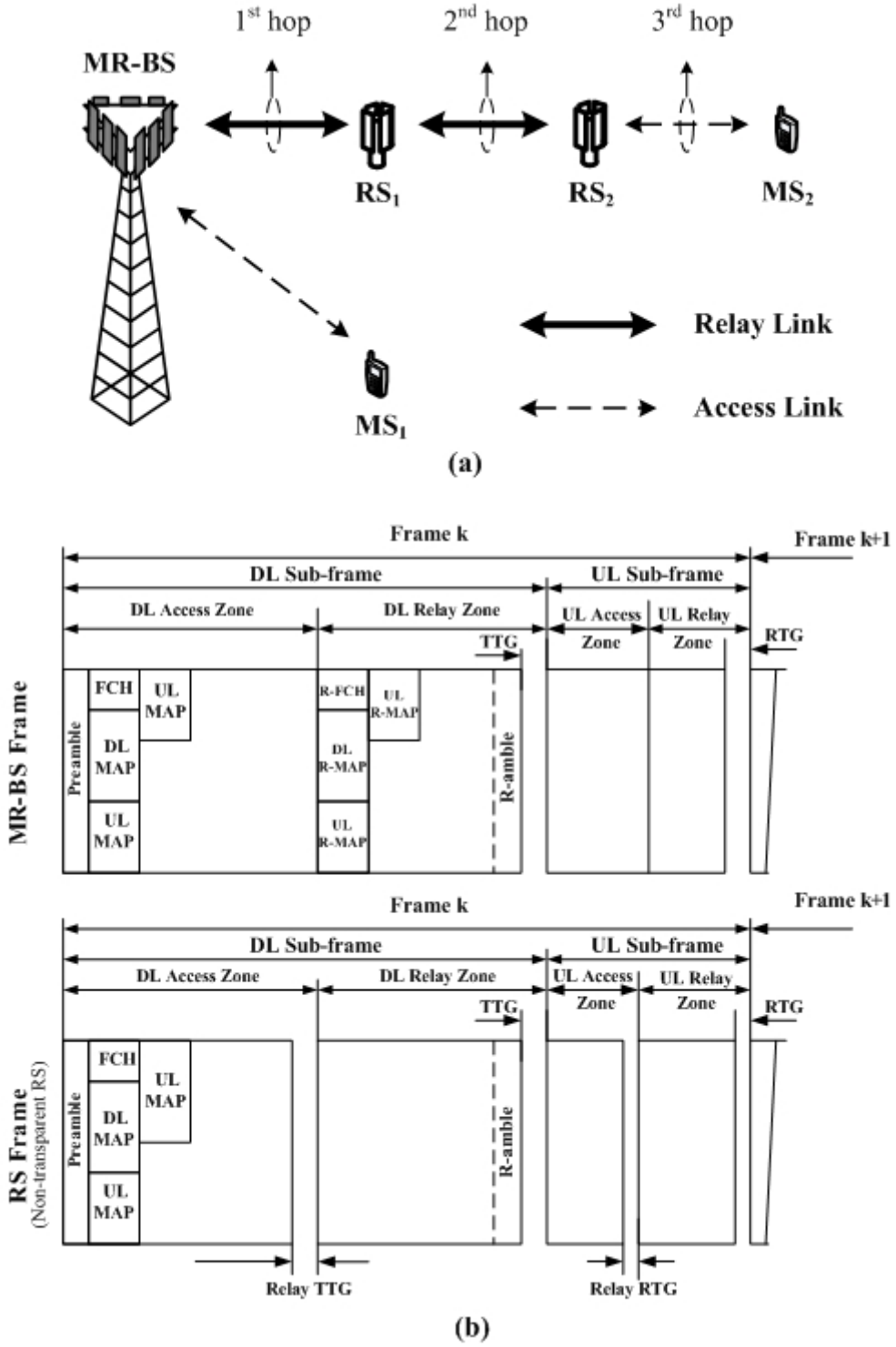

Figure 14. (a) The system architecture and (b) the frame structure for IEEE 802.16j multi-hop relay network

For the transparent RS, it does not have its own preamble, FCH and MAP. It looks transparent to MS and only relays MS's data. The frame structure for the transparent RS is similar to Figure 14(b), but the transparent RS will be in receiving mode when the MR-BS transmits its preamble, FCH and MAP.

When an MS communicates with a non-transparent RS, it will receive the preamble, FCH, MAP and data burst from the RS. On the other hand, if an MS communicates with a transparent RS, it will receive the data burst from the RS but receive the preamble, FCH and MAP from the MR-BS. Therefore, the transparent RS has to be centralized controlled by the MR-BS to transmit/receive the data burst over the designated sub-channels and symbol times. Note that the MR-BS and multiple RSs can serve a particular MS simultaneously so as to increase the received signal quality and obtain cooperative diversity gain.

As for the non-transparent RS, it generates its own FCH and MAP without the instruction from the MR-BS, so that the de-centralized control can be performed to reduce the messaging delay and the messaging overhead over relay links. Meanwhile, a group of RSs may transmit the same preamble, FCH, MAP and data burst, and these RSs will act as a single virtual station from MS's point of view [10]. In this case, the MS will not initiate the handover procedure when moving between the grouped RSs and the cooperative diversity gain will be obtained.

4.2 Coverage Planning for Multi-hop Cellular Networks

In mobile cellular system, the cell planning usually means determining the coverage and the radio parameters of each cell in advance of system deployment. A typical tool for this is link budget, which is a series of calculation on the possible gains and losses of each physical effect when transmitting the radio signal from source to destination.

A typical link budget format for downlink OFDMA system is given in Table 3 [16], and the corresponding description of each parameter is given as following [40].

Table 3 A typical format of link budget for downlink OFDMA system

Transmitter	
Transmitter Power for each Sub-carrier (dBm)	a
Transmitter Antenna Gain (dBi)	b
Back-off (dB)	c
EIRP per sub-carrier (dBm)	d=a+b-c
Receiver	
Thermal Noise Density (dBm/Hz)	e
Receiver Noise Figure (dB)	f
Receiver Noise Density (dBm/Hz)	g=e+f
Receiver Noise Power (dBm)	h
Received Interference Power (dBm)	j
Total Thermal Noise + Interference power (dBm)	k
Required SINR (dB)	l
Required Received Signal Power (dBm)	m=k+l
Maximum Allowable Propagation Loss (dB)	n=d-m
Log Normal Fading Margin (dB)	o
Allowable Path Loss for Cell Coverage (dB)	p=n-o

Transmitter Power for each Sub-carrier (dBm)

- In OFDMA systems, transmitter may apply different power control strategy to allocate the transmit power on each sub-carrier. When calculating link budget, this parameter is usually the maximum transmit power for each sub-carrier.

Transmitter Antenna Gain (dBi)

- This parameter depends on which antenna is equipped at transmitter. When the transmitter is a mobile station, this parameter is usually considered as 0dBi for omni-directional antenna. For directional antennas, this parameter will be the antenna gain over its steering direction (i.e. maximum gain).

Back-off (dB)

- In OFDM transmitters, the power amplifier needs to back-off its operation point to prevent the non-linearity effect due to PAPR (Peak to Average Power Ratio) effect [4].

EIRP per sub-carrier (dBm)

- The equivalent isotropic radiated power (EIRP) of each sub-carrier for the radio signal transmitted from the transmit antenna.

Thermal Noise Density (dBm/Hz)

- According to the physic theory, the background thermal noise will exist if the temperature is higher 0K. This density is function of the temperature of receiver: N_0=KT, where K is the Planck constant: 1.38×10^{-23} and T is

the temperature in Kelvin scale (0K=-273.15^{o}C).

Receiver Noise Figure (dB)

- Additional noise will be induced when receiving the radio signal by RF (radio frequency) components in the analog receiver. It will result in SINR degradation before decoding the signal by digital receiver.

Receiver Noise Density (dBm/Hz)

- This is the equivalent thermal noise density after considering the noise enhanced by RF components.

Receiver Noise Power (dBm)

- Before decoding the signal by digital receiver, the analog signal will be filtered to mitigate the interference and thermal noise out of the desired frequency band. Therefore, only the thermal noise within the desired frequency band will be considered, and this parameter will be the value multiplied by receiver noise density and the radio signal bandwidth.

Received Interference Power (dBm)

- This is the anticipated received interference power level when the user located at cell boundary.

Required SINR (dB)

- This is the required SINR for the user at cell boundary. If the cell planning strategy is to guarantee the coverage of the user served by QPSK, 1/2 coding rate, this value shall ensure the bit error rate (BER) be lower than

certain level. For example, 5dB SINR may ensure the BER lower than 10^{-6} when QPSK and 1/2 coding rate are considered for receiving data [8].

Required Received Signal Power (dBm)

- This is the required received signal power for the user located at cell boundary, which is calculated by the required SINR, received thermal noise power and the anticipated interference power received at cell boundary.

Maximum Allowable Propagation Loss (dB)

- This is the difference between the maximum transmit power of the transmitter and the minimum requirement on received signal power for the user located at cell boundary.

Log Normal Fading Margin (dB)

- Additional fading margin need to be reserved to combat shadow fading effect. The shadow fading due to the obstacle or buildings in propagation environment will result in the deviation of received signal strength. It is usually modeled as a log-normal random variable and independent of the propagation distance. This margin is reserved to guarantee the user located at cell boundary can have certain probability (e.g. 90%) with received SINR higher than requirement. This margin can be calculated by the standard deviation of the log-normal random variable along with the Q-function and given tail probability [15].

Allowable Path Loss for Cell Coverage (dB)

- After reserving certain margin to combat shadow fading effect, this is the

rest allowable loss to combat the path loss. The path loss is the loss only function of the distance between transmitter and receiver. By given the allowable loss for path loss, an allowable distance can be obtained by reverse calculating the path loss equation. Therefore, this distance will be the coverage of each cell.

Two cell planning examples are given by the link budgets for MR-BS and RS in downlink multi-hop cellular OFDMA systems, which are shown in Table 4 and Table 5 respectively. In these two examples, 10MHz radio bandwidth and 20^{o}C receiver temperature are considered. The required SINR is determined to guarantee the BER lower than 10^{-6} for QPSK and 1/2 coding rate.

Table 4 A link budget example for MR-BS in downlink OFDMA system

Transmitter	
Transmit Power for total Sub-carriers (W)	16.279
Transmit Power for each Sub-carrier (dBm)	18.7918
Transmitter Antenna Gain (dBi)	15
Back-off (dB)	5
EIRP per Sub-carrier (dBm)	28.7918
Receiver	
Thermal Noise Density (dBm/Hz)	-173.9325 (20°C)
Receiver Noise Figure (dB)	4
Receiver Noise Density (dBm/Hz)	-169.9325
Receiver Noise Power (dBm)	-129.5422
Received Interference Power (dBm)	-124.7995
Total Thermal Noise + Interference Power (dBm)	-123.543
Required SINR (dB)	5
Required Received Signal Power (dBm)	-116.543
Maximum Allowable Propagation Loss (dB)	147.3348
Log Normal Fading Margin (dB)	10
Allowed Path Loss for Cell Range (dB)	137.3348
Corresponding Cell Radius (km)	1.0 km

Table 5 A link budget example for RS in downlink OFDMA system

Transmitter	
Transmit Power for total Sub-carriers (W)	10
Transmit Power for each Sub-carrier (dBm)	16.6745
Transmitter Antenna Gain (dBi)	6
Back-off (dB)	5
EIRP per Sub-carrier (dBm)	17.6745
Receiver	
Thermal Noise Density (dBm/Hz)	-173.9325
Receiver Noise Figure (dB)	4
Receiver Noise Density (dBm/Hz)	-169.9325
Receiver Noise Power (dBm)	-129.5422
Received Interference Power (dBm)	-118.5827
Total Thermal Noise + Interference Power (dBm)	-118.2478
Required SINR (dB)	5
Required Received Signal Power (dBm)	-113.2478
Maximum Allowable Propagation Loss (dB)	130.9223
Log Normal Fading Margin (dB)	5
Allowed Path Loss for Cell Range (dB)	125.9223
Corresponding Cell Radius (km)	0.35

4.3 Performances Improvement by Multi-hop Relay

In addition to coverage extension and user throughput enhancement, some results have shown that the system capacity can be improved as well with appropriate deployment of RSs [32-37]. Along this line, this chapter investigates the issue of capacity enhancement for the IEEE 802.16j multi-hop relay network. In this section, an existing cellular OFDMA network in Manhattan-like urban environment is considered to deploy additional RSs for user throughput and capacity enhancement as shown in Figure 15.

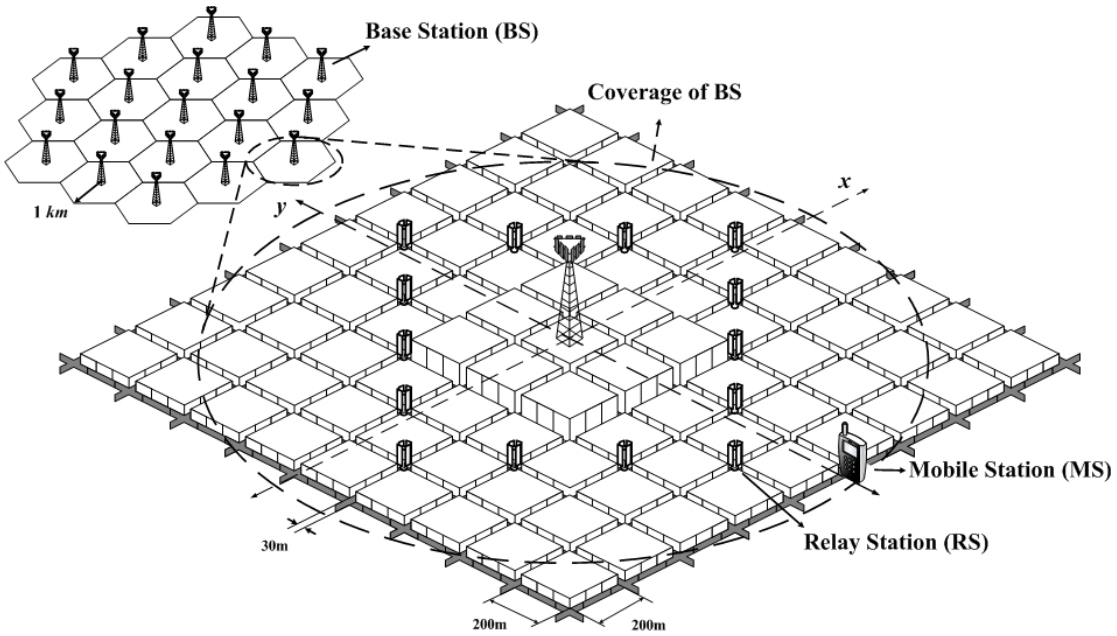

Figure 15. A multi-hop cellular network with RS deployed within the coverage of BS

4.3.1 RS Deployment Strategy in Manhattan-like Urban Environment

In the Manhattan-like environment as the one shown in Figure 15, the shadow fading due to the regulated street layout can be exploited to mitigate the multiple access interference. In the traditional cellular deployment, shadow fading is treated as a negative effect, and a margin is needed in link budget planning to ensure the service

availability at the cell boundary.

Here, firstly RS is deployed to avoid shadow fading as shown in Figure 16(a). By appropriate site selection, RS is deployed to have LOS (line of sight) with the signal source. Secondly, shadow fading is exploited to isolate the interfering signal. For example, in Figure 16(b), RS_1 has LOS with its subordinate station MS_1. Meanwhile, RS_1 has NLOS (non LOS) with MS_2. Therefore, the radio link $RS_1 \leftrightarrow MS_1$ can reuse the radio resource which is allocated the radio link $RS_2 \leftrightarrow MS_2$, and the interference from RS_1 to MS_2 is avoided largely by the shadow fading.

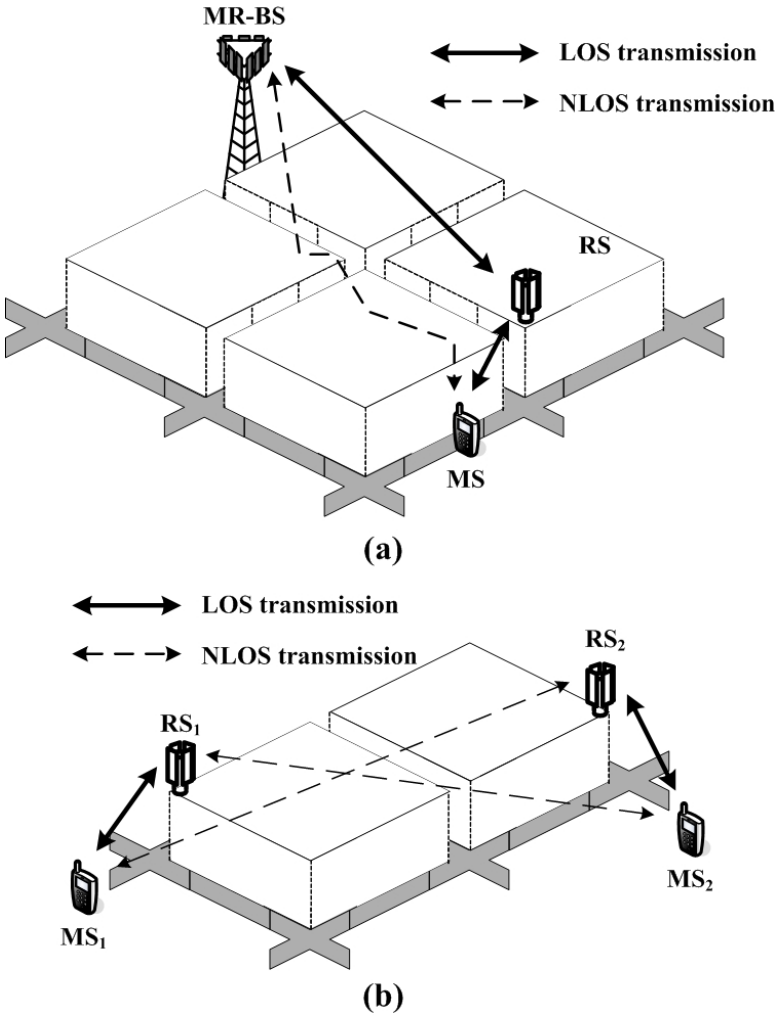

Figure 16. The proposed RS deployment method: (1) to have LOS with signal source and (2) to have NLOS with interference source

Therefore, a simple RS deployment criterion is proposed by following two steps:

1. Deploy RS at the location where it can have LOS to its signal source and to its transmission destination. If LOS is not always guaranteed, select the location where it can have highest LOS probability.
2. After initial deployment in stage 1, adjust the location of each RS to have NLOS condition to its interference sources or its interfering targets.

The first steps aims to improve the received strength of the desired signal, and the second stage aims to isolate the interference by utilizing shadow fading effect.

Following the aforementioned RS deployment criterion, the received signal quality can be substantially improved, and the shadow fading can properly utilized to isolate the interfering signals transmitted from interference sources. Therefore, within the area surrounded by objects (ex. buildings or hill), the radio resources can be reused by different relay stations without significantly interfering with each other.

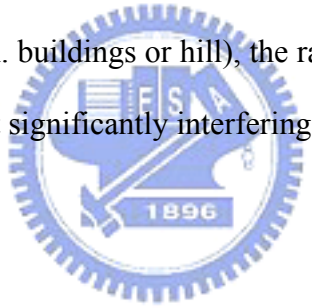

4.3.2 Simulation Results

A. Simulation Environments

A downlink two-hop cellular network is simulated in Manhattan-like environment, where 14 RSs are deployed within the coverage of an MR-BS. Total of 19 cells with three sectors per cell are considered. The RS's locations are as depicted in Figure 15, which follows the deployment method proposed in previous section. The MR-BS and RSs are deployed above rooftop, so that the relay links have line-of-sight (LOS) condition. The access links between MR-BS and MS are assumed to be non line-of-sight (NLOS). For the access links between RS and MS, LOS is assumed if they locate on the same street and the distance is less than 150m. The path-loss and shadow fading models are referenced from the multi-hop relay system evaluation

methodology in [41]. The total transmit power of the MR-BS is 45 Watts with 1 km cell coverage, and the RS/MS maximum transmit power are 5 Watts and 0.5 Watts respectively.

Two frequency reuse methods for the MR network are simulated to investigate the potential benefit of the proposed RS deployment method. The first method does not reuse the frequencies within the same MR-cell, where the orthogonal frequency channels are allocated to each relay link/access link in relay zone/access zone respectively. In this case, there is no intra-cell interference. The second method is to reuse the frequency channels within the same MR-cell, the channels for relay links are reused in each sector and the ones for access links are reused by every RSs and MR-BSs.

At the beginning of simulation, MSs are generated by Poisson process and randomly located on the street. During the simulation, the MS moves along the streets and communicates with an RS or the MR-BS based on the received signal quality. The modulation and coding scheme is adjusted on a frame-by-frame basis according to signal quality. For each frame, the number of bits successfully received in access links is recorded, and at the end of simulation, the cell throughput is calculated by dividing the number of successfully received bits in access links by the overall simulation time. The more detailed simulation parameters are given in [42].

B. Simulation Results

In Figure 17(a), the CDF (Cumulated Distributed Function) of downlink received signal quality is presented for different relay methods and different frequency reuse factors. The simulation results show that the received signal quality can be substantially improved by deploying relay stations. For frequency reuse factor $K = 1$,

a MS has 23%, 81% and 74% probability to have a received $E_b/(I_0+N_0)$ higher than 20 dB in the cases of no relay, conventional relay, and the proposed relay methods, respectively. It means that the received signal quality is improved by deploying RSs, which is mostly achieved by the lower propagation loss from serving station to MS. Therefore, per user throughput can be significantly increased by using higher order MCS in response to such a high SINR. On the other hand, if we draw a horizontal line at CDF=10% and compare the curves with $K = 1$. It shows that a mobile station has 10% probability to have signal quality lower than 4dB, 15dB and 11dB for the case with no relay, conventional resource allocation method and proposed resource allocation method, respectively. If the coverage planning criterion is to ensure mobile station has 90% probability to have signal quality better than 4dB, the conventional method and proposed method can lead to additional 11dB and 7 dB margin in link budget for coverage extension.

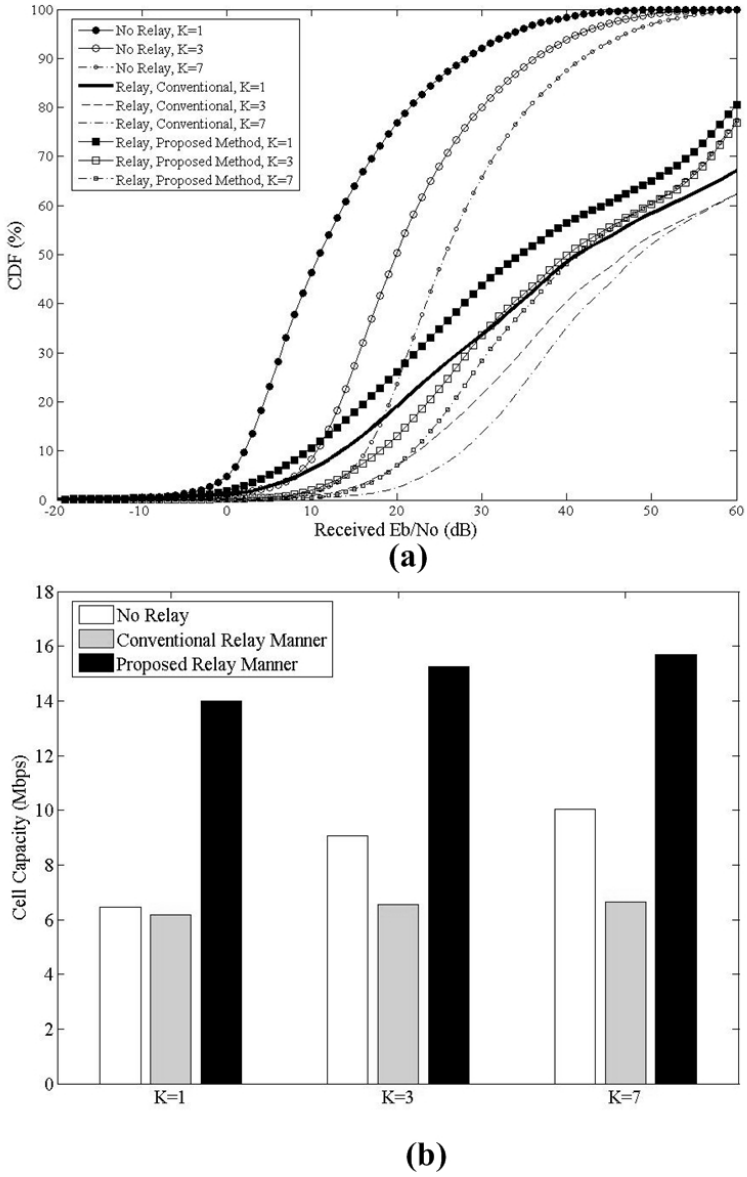

Figure 17. (a) CDF of downlink received signal quality and (b) the downlink cell capacity

The downlink cell capacity is presented in Figure 17 (b), which shows that the proposed resource allocation method and RS deployment method can lead to substantial capacity improvement than conventional method and the case with no relay. For two-hop case, a data bit is transmitted from BS to RS in 1st hop and RS to MS in 2nd hop in different time, so only one effective bit is received by MS. Therefore,

the results show that the conventional method has smaller cell capacity because all traffic in relay links shall be treated as overhead, and the improvement by higher transmission rate cannot break even with the lost on radio resources for relay links. The conventional method has -4.81%, -27.63% and -33.92 cell capacity with respect to the case with no relay for reuse factors $K = 1, 3$ and 7, respectively. On the other hand, the proposed resource reuse method along with RS deployment method can achieve 116.4%, 68.33% and 56.03% capacity gain for reuse factors $K = 1, 3$ and 7, respectively. The cell capacity is improved because radio resources are reused in different relay links and access links within each cell and the proposed RS deployment method also utilize the severe shadow fading effect to isolate the interfering signals.

In Figure 18(a), the CDF of uplink transmission power for MS is presented. Because the power control is considered in uplink transmission, therefore, the reduction on propagation loss by RS deployment will lead to lower transmit power. For $K = 1$, MSs have the probabilities 36.43%, 74.23% and 63.10% to consume the transmission power lower than 10dBm for the case of no relay, conventional method, and the proposed method, respectively. According to the better propagation condition and lower propagation loss, the uplink transmission power can be substantially reduced by RS deployment.

The uplink capacity is presented in Figure 18(b), which is defined as the effectively received bits at MSs within each cell in uplink access zone. Compared with the conventional method, it shows that 2.54%, 35.84% and 44.11% capacity gain can be achieved by the proposed resource reuse method for the cases of $K = 1$, 3 and 7, respectively. On the other hand, degradation on system capacity is observed in the MR network due to additional resource used for multi-hop transmission for the case of $K = 1$.

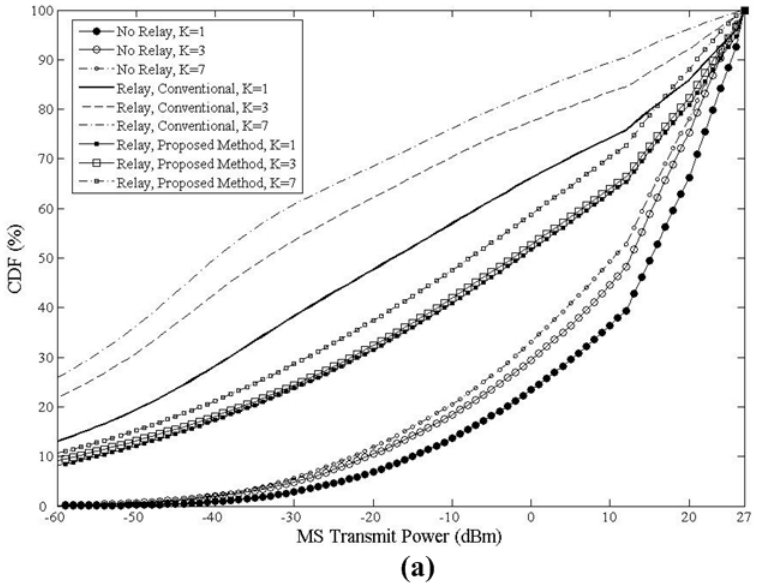

(a)

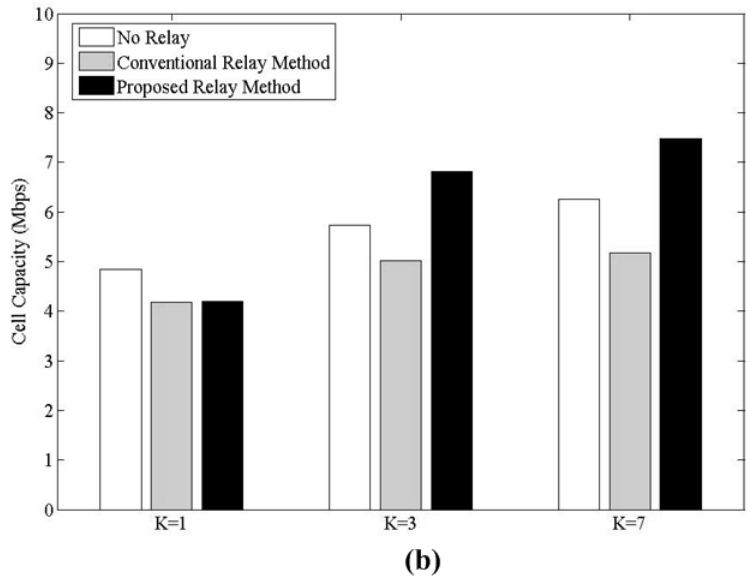

(b)

Figure 18. (a) The CDF of uplink MS transmit power and (b) uplink cell capacity

Chapter 5

New Frequency Reuse Techniques for Multi-hop Cellular OFDMA System

In this chapter, the techniques for frequency planning and reuse in multi-hop cellular OFDMA system are investigated. In Section 5.1, a new frequency planning technique is proposed for multi-hop cellular OFDMA systems. The simulation results will show that it can significantly improve the system capacity with respect to the conventional methods proposed in literatures. In Section 5.2, a new measurement and reporting mechanism based on R-amble transmission for IEEE 802.16j multi-hop relay network is proposed. Based on this new mechanism, a new frequency assignment technique based on interference measurement is also proposed for multi-hop cellular network in this section.

5.1 A New Frequency Planning Technique for Multi-hop Cellular OFDMA System

Simulation results in Section 4.3 show that frequency reuse is the key to improve the capacity in multi-hop cellular systems. In this section, the frequency planning in multi-hop relay networks will first be investigated by reviewing the existing techniques will be investigated first. Then, a simple and new frequency planning technique will be proposed to improve the capacity for multi-hop cellular OFDMA systems. For easy presentation, a reference multi-hop cellular structure shown in Figure 19 is considered in following. In Figure 19, the radius of each MR-cell is R and six RSs are deployed within each MR-cell. The MR-BS is uniformly surrounded

by the RSs which are deployed from MR-cell center with distance $2R/3$, and the coverage of each RS in access link is $R/3$ [44-49].

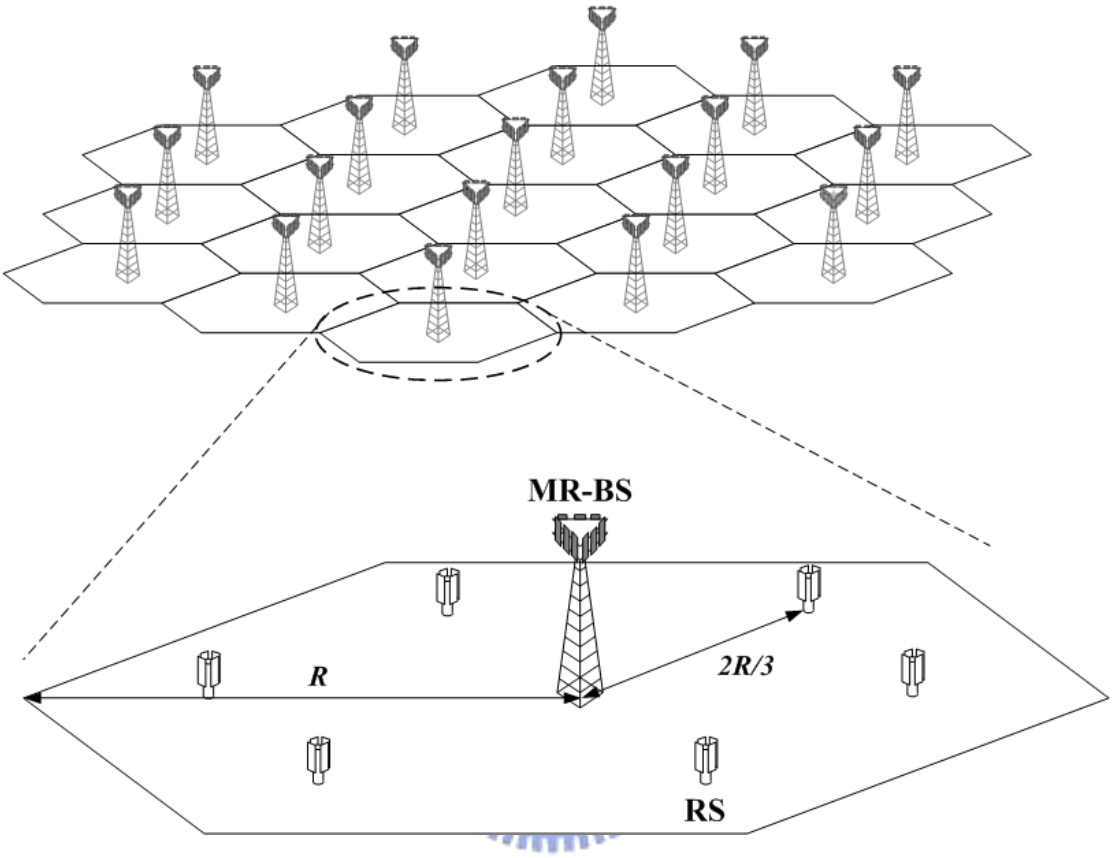

Figure 19. A reference multi-hop cellular structure

5.1.1 Frequency Planning Techniques for Multi-hop Cellular Systems

The first technique proposed in existing literature [44,45] is shown in Figure 20. Its basic idea is to allocate the frequency channels to each MR-BS first, where the channels can only be reused in the MR-BSs in different clusters [15]. Then the RSs in each MR-cell reuse part of the frequency channels allocated to the MR-BSs in adjacent cells. In Figure 20, this technique will divide the total frequency channels into K blocks, where K is the frequency reuse factor defined in Section 2.1 and $K = 4$ is considered in this example. Then the MR-BS in each cluster will be exclusively allocated by one of the blocks in the second step. In the third step, each

RS will select one of the frequency blocks which correspond to longest co-channel distance with the MR-BSs allocated by the same block. Then the RS will reuse $1/6$ of the frequency channels in that block, so as to prevent interference with the nearby RSs which select the same block.

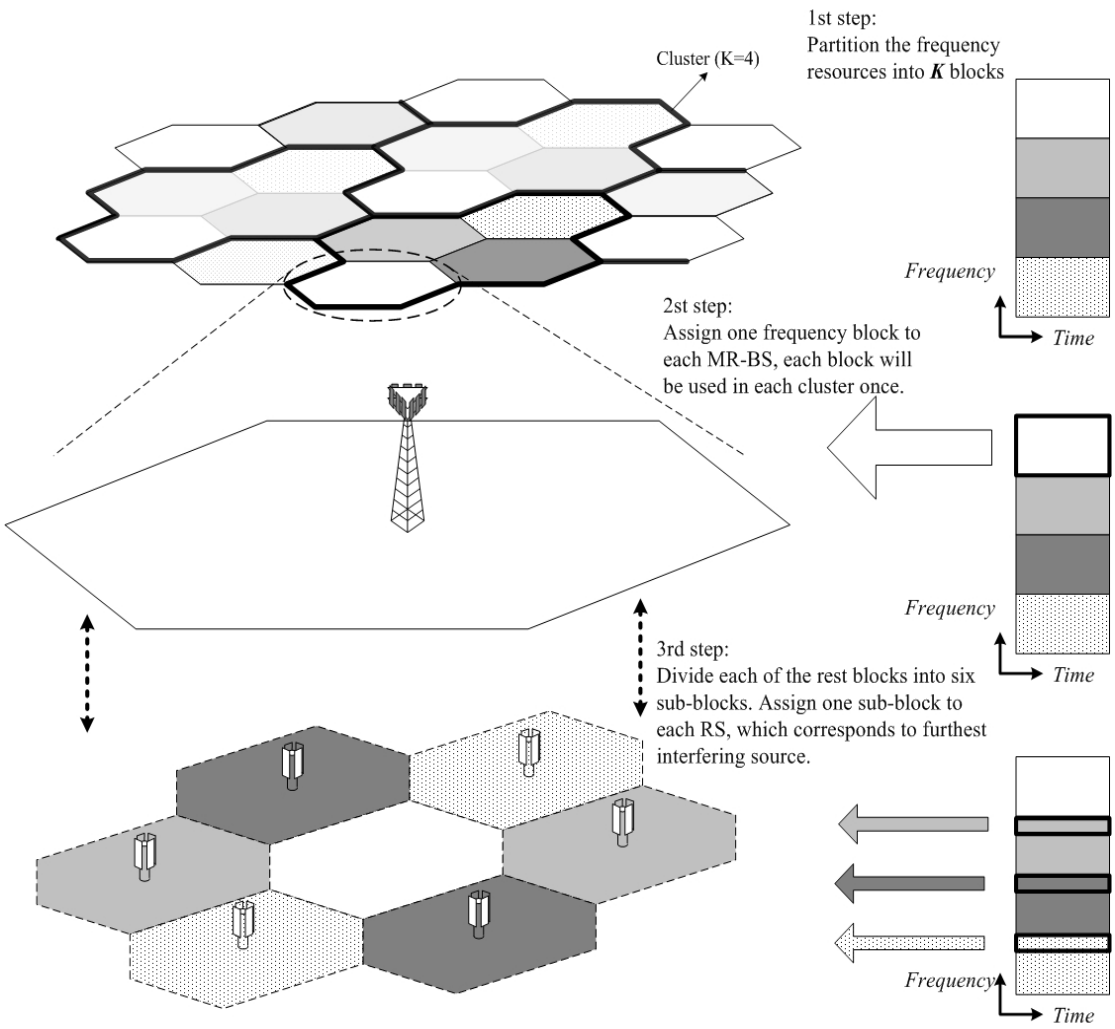

Figure 20. The frequency planning technique proposed in literatures [44,45]

The second frequency planning technique [46-49] is shown in Figure 21. Its basic idea is applying the concept of reuse partitioning to divide the MR-cell into inner cell and outer cell then perform frequency planning separately, where the inner cell is served by MR-BS and the outer cell is served by the RSs. In the first step, this technique will partition each MR-cell into inner cell and outer cell. In the second step, it will divide the access zone into two resource-zones to serve the user located in inner cell and outer cell respectively, like the example given in Section 2.1.1 with $Z = 2$. In the example shown in Figure 21, the reuse factor $K = 1$ is considered for the inner cell and $K = 4$ is considered for the outer cell. In the third step, the corresponding resource-region will be allocated to MR-BS and RSs according to the frequency reuse factor considered in each sub-zone. For the RSs in the same outer cell, the frequency channels will be exclusively allocated to each of them.

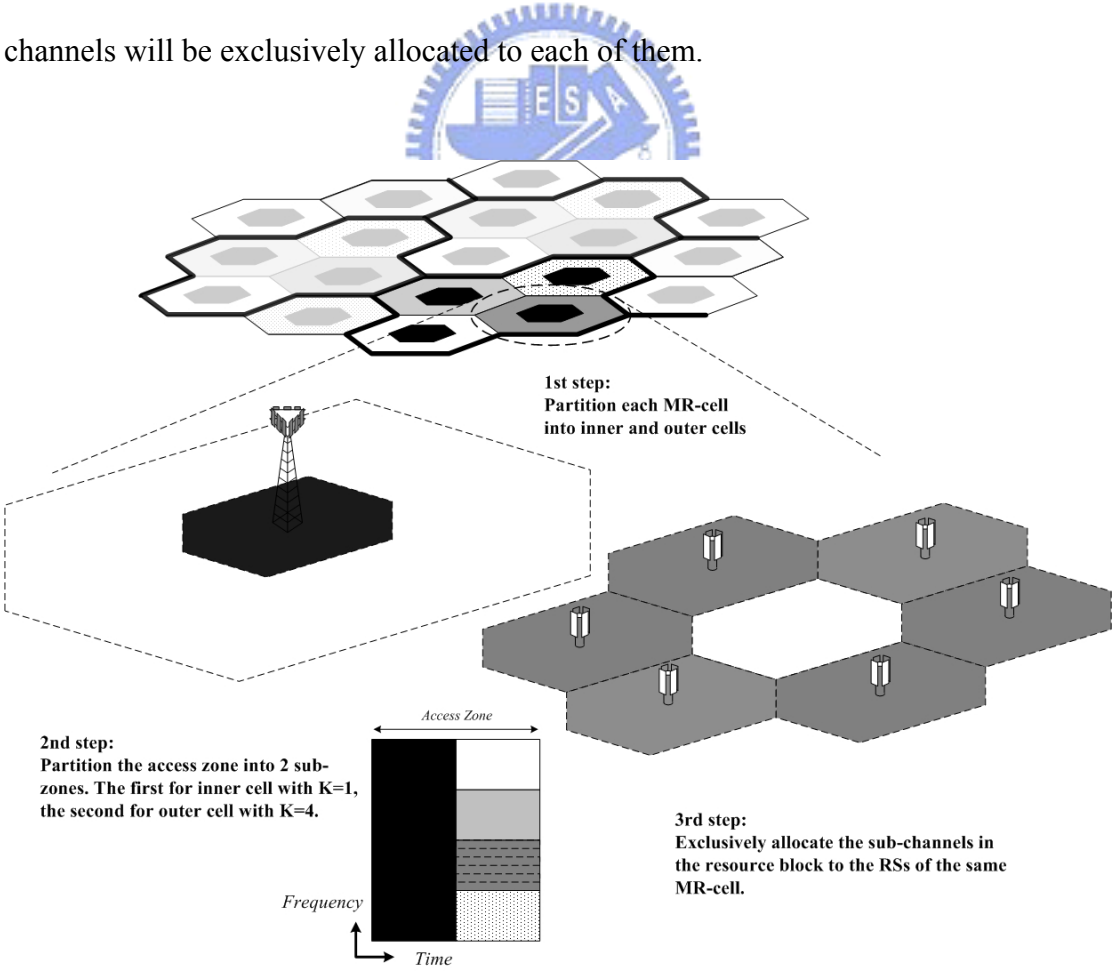

Figure 21. The frequency planning technique proposed in literatures [46-49]

In the first technique, the reuse factor considered for MR-BS frequency planning aims to guarantee the MSs located at MR-cell boundary can be served by MR-BS. However, the MSs located at cell boundary are usually served by RS in multi-hop cellular network, and the MSs directly served by MR-BS are usually located around cell center. For the MSs around cell center, the interference from adjacent cells is much lower the one received by the MS located at MR-cell boundary. Therefore, the frequency reuse factor considered by the coverage served by MR-BS can be lower for more available radio resource, i.e. this technique may result in certain overdesign and cannot fully utilize the scare resource in the system.

The second technique mitigates the aforementioned problem by applying the concept of reuse partitioning (see Section 2.1.1) to partition each MR-cell into inner and outer cells. The inner cell is directly served by MR-BS and more aggressive frequency reuse (e.g. $K=1$ in Figure 21) can be used for more resource in access links. In the outer cell served by RSs, conservative frequency reuse (e.g. $K=4$ in Figure 21) can be applied to prevent the significant interference from adjacent MR-cells. However, this technique does not allow frequency reuse among the RSs in the same MR-cell and there are still rooms to improve this technique.

In order to utilize the radio resource more efficiently, a new and simple frequency planning technique based on the "sub-cell" concept is proposed in this section. This technique aims to perform more aggressive frequency reuse in multi-hop cellular systems without the damage on coverage guaranteed.

The idea of the proposed "sub-cell" based frequency planning concept and the simple planning procedure are depicted in Figure 22. By dividing each MR-cell into multiple (i.e. 7 in this example) sub-cells served by MR-BS or RSs, the first step is to reorganize the cellular network and define the cluster from sub-cell's point of view. Then, the second step is allocating the frequency channels to each sub-cell based on

the cluster.

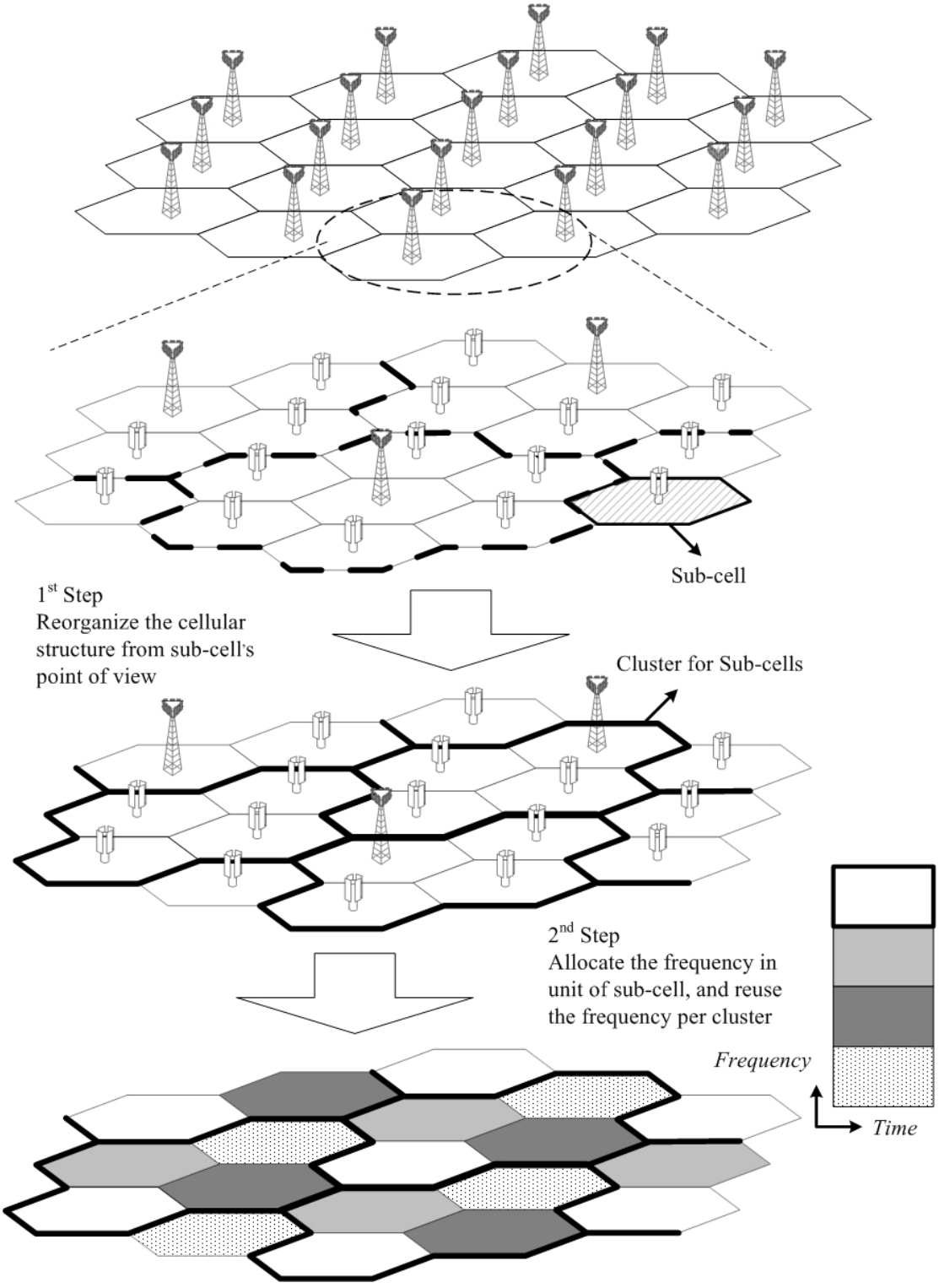

Figure 22. Proposed frequency planning technique based on “sub-cell”

5.1.2 Simulation Results

A. Simulation Environments

A downlink two-hop cellular network is simulated in Manhattan-like environment, where 6 RSs are deployed within the coverage of an MR-BS. Total of 19 cells with three sectors per cell are considered, and the location of each RS locations is as depicted in Figure 19. The MR-BS and RSs are deployed above rooftop, so that the relay links have line-of-sight (LOS) condition. The access links between MR-BS and MS are assumed to be non line-of-sight (NLOS). For the access links between RS and MS, LOS is assumed if they locate on the same street and the distance is less than 150m. The path-loss and shadow fading models are referenced from the multi-hop relay system evaluation methodology in [41,42]. The total transmit power of each RS is 10 Watts, which is derived by the link budget in Table 5. The total transmit power of each MR-BS is 4 Watts when simulating the second technique and the proposed technique, which is derived by modifying the antenna gain and fading margin of the link budget in Table 5. For the first frequency planning technique, the transmit power of each MR-BS is 16.279 Watts to cover the entire MR-cell, which is derived by the link budget in Table 4.

Two frequency reuse methods for the MR network are simulated to investigate the benefit by proposed RS deployment method. The first method does not reuse the frequencies within the same MR-cell, where the orthogonal frequency channels are allocated to each relay link/access link in relay zone/access zone respectively. In this case, there is no intra-cell interference. The second method is to reuse the frequency channels within the same MR-cell, the channels for relay links are reused in each sector and the ones for access links are reused by every RSs and MR-BSs.

At the beginning of simulation, MSs are generated by Poisson process and randomly located on the street. During the simulation, the MS moves along the streets and communicates with an RS or the MR-BS based on the received signal quality. The modulation and coding scheme is adjusted on a frame-by-frame basis according to signal quality. For each frame, the number of bits (B_A) successfully received in access links is recorded, which will be restricted by the available radio resource determined by different frequency planning technique and the access zone ratio η. The ratio η is defined as the ratio of the radio resource allotted to downlink access zone over the total radio resource available in downlink sub-frame. In addition, the number of bits able to be relayed in each frame (B_R) will be calculated based on the ratio η. Therefore, the number of bits successfully received in each frame will be $\min(B_A, B_R)$. At the end of simulation, the cell throughput is calculated by dividing the number of successfully received bits in access links by the overall simulation time.

B. Simulation Results

Figure 23 show the system capacity by given different access zone ratio and under different frequency planning technique. It shows that the proposed technique can achieve to highest capacity in each case. Compare with the first technique, the major improvement by the proposed technique is prevent the overdesign on the frequency reuse factor for the MR-BS sub-cell and use lower K to have more radio resource for access links. In addition, the proposed technique can explore more intra-cell frequency reuse opportunity with respective to the first and the second techniques. Figure 23 also shows that a tradeoff will exist by giving different η. Larger η can provide more radio resource for access link to serve MSs, but it will also result in less radio resource to forward the user traffic. The optimal tradeoff will exist when the

aggregate traffic in relay links is equal to the traffic in access line. In figure 23, the $\eta = 62.5\%$ is closest to the optimal point for the second and the proposed technique, and $\eta = 75\%$ is the best choice for the first technique.

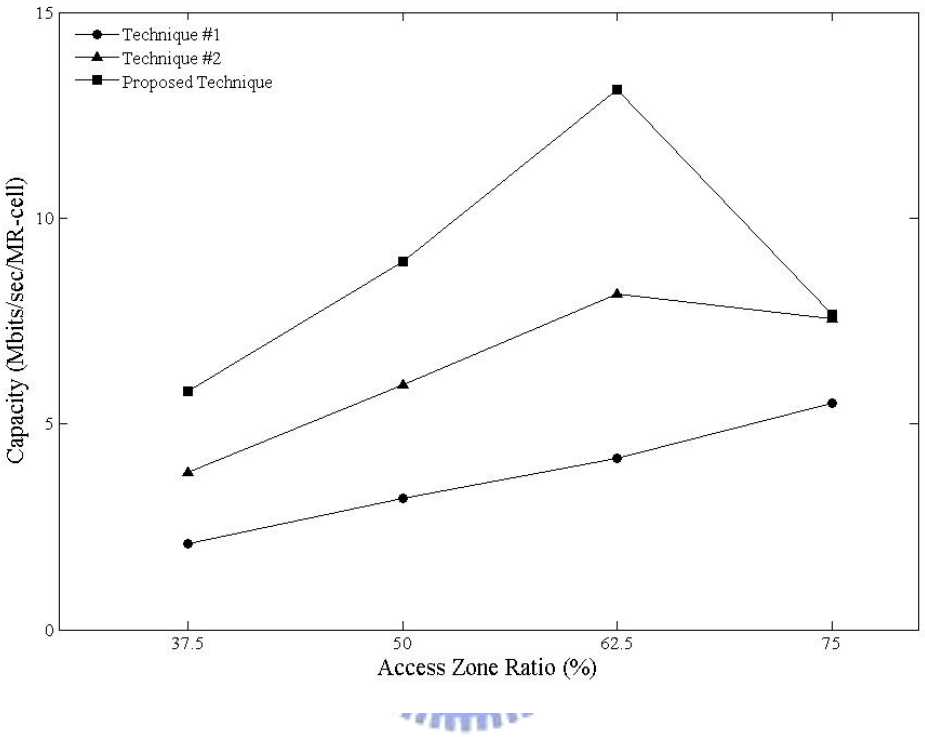

Figure 23. System capacity by given different access zone ratio (η)

Selecting the highest capacity for each technique in Figure 23, Figure 24 shows that improvement can be achieved by the proposed technique. Compare to the first one, the proposed technique performs 137.75% capacity improvement [51]. Compare with the second one, the proposed technique performs 60.87% capacity improvement. Note that such significant improvement on system capacity is achieved without losing the guarantee on coverage. The coverage guarantee defined here is

$$P\left(SINR < 5dB \,|\, \text{MS at cell boundary}\right) < 5\%$$

, and Figure 25 shows that all the techniques are compared under the guaranteed

coverage.

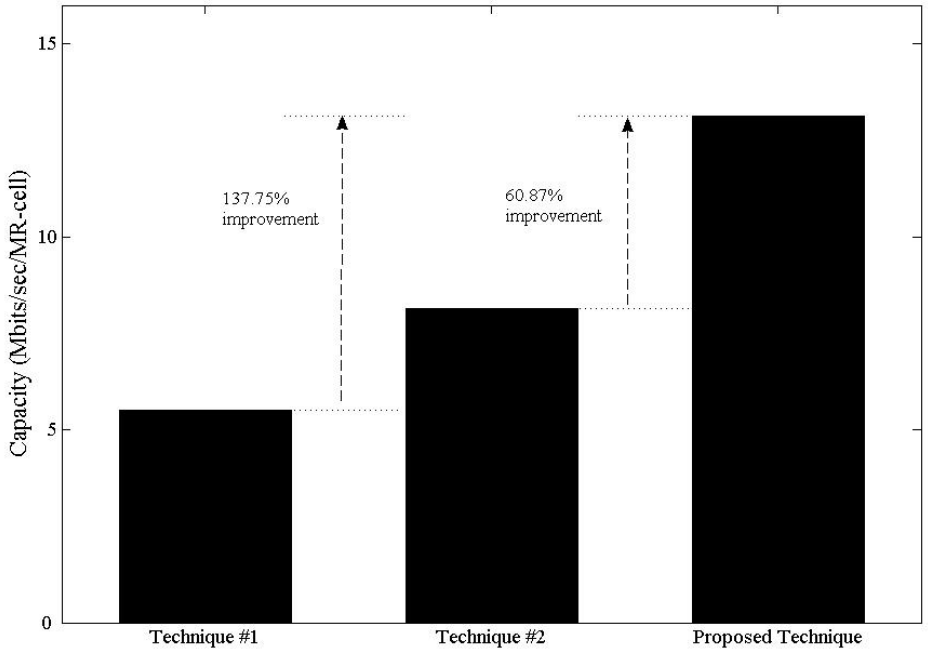

Figure 24. System capacity under different frequency planning techniques

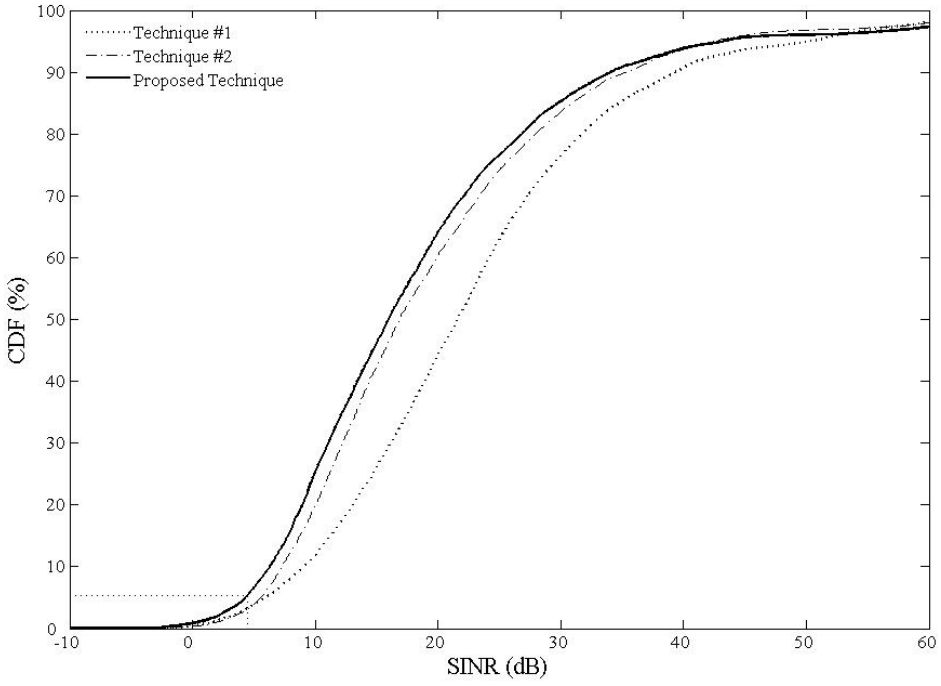

Figure 25. CDF of the received signal quality (SINR)

On the other hand, the overdesign on reuse factor by the first technique can lead to higher user throughput. In Figure 26, it shows that the first technique can lead to much higher percentage of users served by 64QAM in the MR network. However, it is achieved by the massive expense on system capacity.

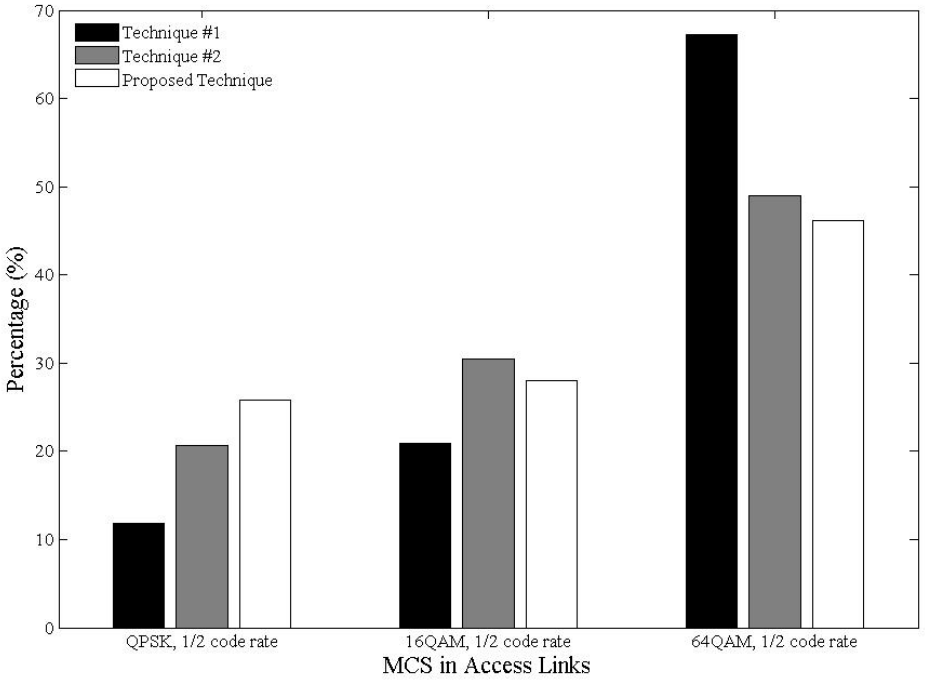

Figure 26. MCS percentage in access links

5.2 A New Measurement and Reporting Mechanism for IEEE 802.16j

In this section, a new measurement and reporting mechanism is designed for IEEE 802.16j Multi-hop Relay network. This mechanism and corresponding messaging design [52-55] have been approved by IEEE 802.16j Relay Task Group and became part of the IEEE 802.16j draft standard [10].

In IEEE 802.16j Multi-hop Relay network, MR-BS and non-transparent RS can transmit preamble for the measurement by subordinate RSs or MSs. However, this is not good enough because of following reasons:

1. Not every RS can transmit preamble (e.g. transparent RS), and other stations cannot discover this kind of RS by preamble scanning.
2. Multiple RSs may transmit the same preamble to perform cooperative diversity and act as a virtual station; therefore, those RSs cannot discover each other and other stations can distinguish the signal strength received from each of thses RSs.
3. For the RSs can transmit preamble but in the same hop, they cannot scan the preamble transmitted by each other. Because they are both in transmit mode when transmitting the preamble and unable to receive the preamble transmitted from each other.

Therefore, a new measurement mechanism is necessary for IEEE 802.16j Multi-hop Relay network for RSs and MR-BSs to discover each other.

The basic idea of the proposed mechanism is given in Figure 27, where an example with one MR-cell is provided. In Figure 27 (a), RS_2, RS_5 and RS_8 transmit the reference signal for the measurement by other stations. If the reference signal transmitted by each RS is the same, the transmission opportunity shall be separated by time or frequency as shown in Figure 27 (b). If the reference signals transmitted by

each RS can be different, the transmission opportunity can be overlapped as Figure 27 (c).

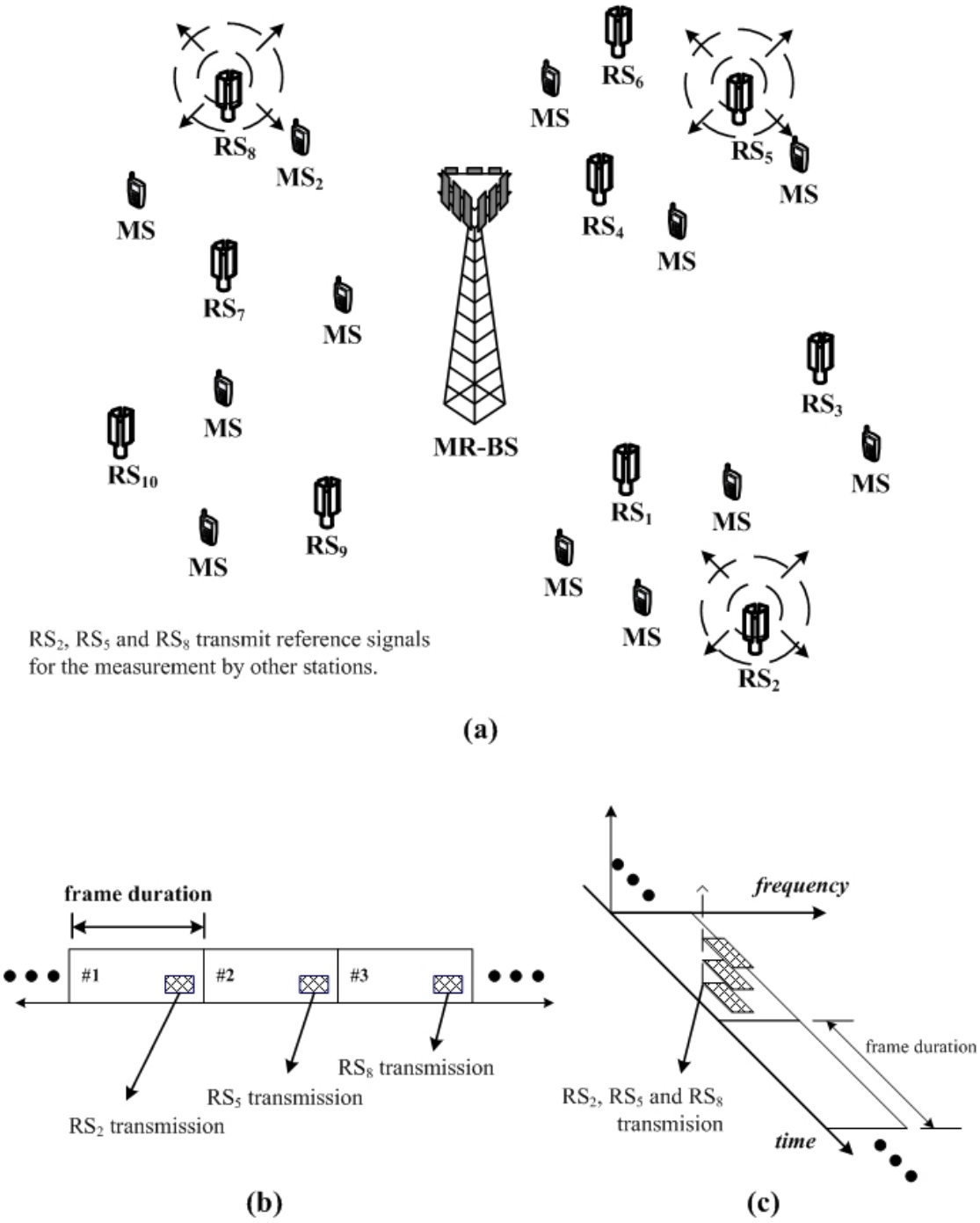

Figure 27. Examples on (a) proposed measurement mechanism, and the corresponding transmission opportunities for the RSs with the (b) same reference signal and (c) different reference signals.

In IEEE 802.16j Multi-hop Relay network, this measurement mechanism can be achieved by coordinating R-amble (i.e. Relay amble) transmission/measurement. Note that the R-amble is a PN sequence with the same format as preamble [39], but transmitted at the end of downlink relay zone as shown in Figure 14(b). Different R-ambles can be transmitted by multiple RSs or MR-BSs over the same radio resource region and decoded by other stations. Therefore, the stations which cannot discover each other due to aforementioned reasons can perform measurement and neighborhood discovery by R-amble transmission.

Since R-amble transmission is a new idea, there were no legacy messages eligible to coordinate the R-amble transmission and measurement opportunities for MR-BS or RSs. A new message and corresponding signaling procedure is designed for RS neighborhood discovery mechanism in IEEE 802.16j Multi-hop Relay network. Its basic idea is shown in Figure 28.

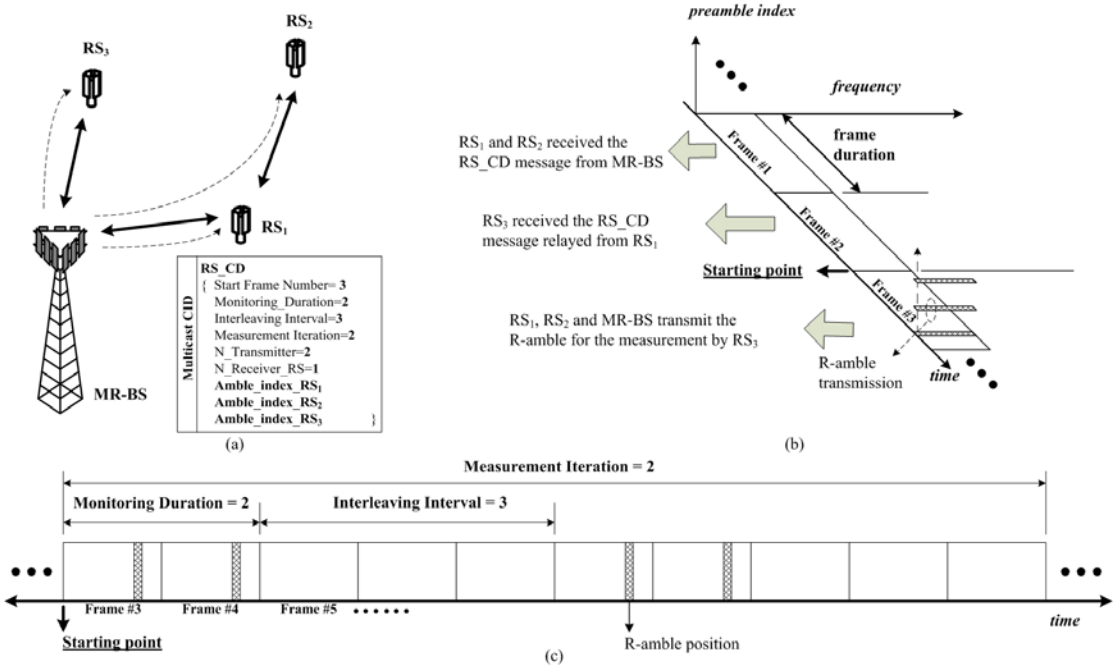

Figure 28. (a) Instructing R-amble transmission by RS-CD message, (b) the corresponding operation of the RSs and (3) the flexibility for instruction.

In Figure 28, the MR-BS multicasts the RS_CD (RS_Configuration-Description) message [53] to RS_1, RS_2 and RS_3. The parameters carried by this message are described as following: Start Frame Number in this message is the frame number index to initiate the subsequent R-amble transmission procedure. Monitoring Duration is the duration of the R-amble transmission in unit of frame. Interleaving Interval is the period which is interleaved between the consecutive R-amble transmission opportunities. Iteration is the number of requested iterating intervals. N_Transmitter is the number of RSs in this multicast group shall transmit R-amble. N_Receiver_RS is the number of RSs in this multicast group shall receive/measure the R-amble. Amble_Index is the index associated to specific R-amble sequence assigned to each RS.

In Figure 28(a), N_Transmitter=2 means the RSs (RS_1 and RS_2 in this example) associated with the first two Amble Indexes in following shall transmit the R-amble. Then, the RS (RS_3 in this example) associated with the N_Receiver_RS=1 Amble Index shall receive/measure the R-amble. In Figure 28(b), RS_1, RS_2 and MR-BS will transmit the R-amble for the measurement by RS_3 in frame#3. By defining the parameters Monitoring Duration, Interleaving Interval and Iteration, the same R-amble transmission/measurement pattern can be flexibly repeated as shown in Figure 28(c).

However, there will be a synchronization problem when different MR-BSs send their RS-CD messages individually. It is because the frame number indexes used in different MR-cell are usually different and will not be synchronized in practical systems. Therefore, the frame #m for $MR\text{-}BS_1$ and the frame #m for $MR\text{-}BS_2$ usually correspond to different time.

A method is also proposed in this dissertation by using a network coordinator to record the differences between the frame number indexes of each cell as shown in

Figure 29. In this example, the MR-BS_1 is instructing RS_1 to transmit R-amble at frame #m by RS-CD message. The proposed method is that MR-BS_1 also sends the frame index "m" and the Amble Index of RS_1 to the network coordinator. The network coordinator has a database to record the difference of the frame number indexes between each MR-cell. Therefore, the network coordinator will translate the frame index "m" to frame index "n" based on the difference between MR-BS_1 and MR-BS_2. Then it will forward the frame index "n" and the Amble Index of RS_1 to MR-BS_2, so that MR-BS_2 can inform its subordinate RSs to scan the R-amble transmitted from RS_1 at frame #n. According to this method, the R-amble transmission opportunities instructed in different MR-cells can be synchronized.

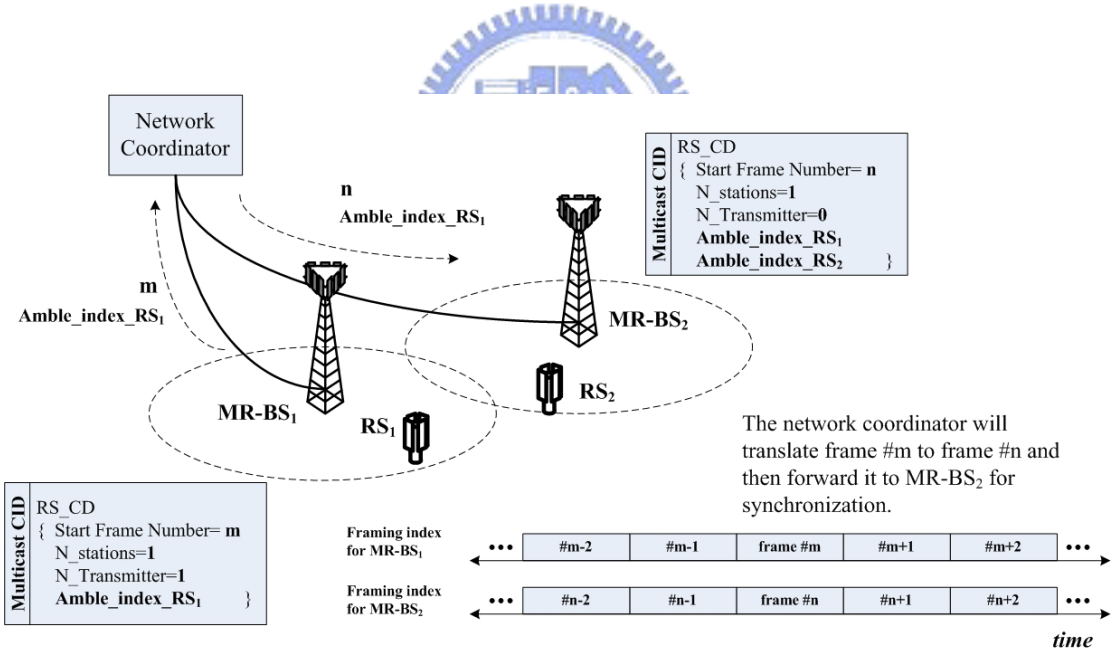

Figure 29. Proposed method to synchronize the R-amble transmission/measurement opportunities in different MR-cells

In summary, the proposed measurement and reporting mechanism can be applied for RSs and MR-BSs to discover each other in IEEE 802.16j Multi-hop Relay network. The typical procedure can be summarized as following steps [52]:

1. First, the MR-BS sends the RS-CD message to the RSs which will be involved in the neighborhood measurement mechanism, and the message is either broadcast, multicast or unicast to these RSs. The 8 LSB bits of frame number shall be set to synchronize the starting time to the RSs. If the RSs involved in this mechanism are in different MR-cell, each of the Start Frame Number sent by different MR-BSs shall synchronize to the same frame time.
2. Second, the stations follow the instruction to transmit/receive the R-amble at the designated frames in each iteration.
3. Third, the RSs report the RSSI or CINR with corresponding amble index by RS_NBR-MEAS-REP to MR-BS.

Chapter 6

A New Path Selection for Multi-hop Cellular OFDMA System based on SINR Prediction

In Section 4.3, the simulation results show that deploying RSs into cellular OFDMA network may result in performance degradation due to the overhead in relay links. In addition to the advanced frequency reuse techniques proposed in Chapter 5, this chapter proposes a novel path selection to improve the performances of multi-hop cellular systems. The proposed path selection includes a measurement mechanism, a SINR prediction mechanism and the path selection criteria. Based on proposed measurement mechanism introduced in Section 5.2, a novel SINR prediction mechanism is proposed in Section 6.1. Then, several path selection criteria are investigated in Section 6.2, and a novel selection criterion is also proposed in this section. In Section 6.3, simulation results are performed to explore the tradeoffs between these path selection criteria.

6.1 A Novel SINR Prediction Mechanism for Multi-hop Cellular OFDMA Systems

For easy presentation, the configuration in Figure 30 will be used as an example to explain the principle, where one MR-BS and three RSs are involved in the multi-hop transmission. After the RS neighborhood measurement introduced in Section 5.2, each station can measure the RSS of the R-amble transmitted from each other and report the measurement results to the MR-BS. Therefore, the following RSS matrix will be

available at the MR-BS:

$$\text{RSS matrix} = \begin{bmatrix} P_{0,0} & P_{0,1} & P_{0,2} & P_{0,3} \\ P_{1,0} & P_{1,1} & P_{1,2} & P_{1,3} \\ P_{2,0} & P_{2,1} & P_{2,2} & P_{2,3} \\ P_{3,0} & P_{3,1} & P_{3,2} & P_{3,3} \end{bmatrix},$$

where $P_{i,j}$ is the RSS of the R-amble transmitted from node #*i* and received by node #*j*, and $P_{j,j}$ is the background interference and noise at node #*j*.

In Figure 30(a), the MR-BS is transmitting data to RS_1, and the problem in this example is to determine whether RS_2 can reuse the same radio resource (e.g. sub-channel and symbol duration) to transmit data to RS_3. As shown in Figure 30(b), if RS_2 indeed reuses the radio resource, then the received SINR at RS_1 can be predicted as $P_{0,1} / \left(P_{2,1} + P_{1,1} \right)$, where $P_{0,1}$, $P_{2,1}$ and $P_{1,1}$ are made available at the R-amble measurement. This predicted value then can be compared to a threshold to determine if it is suitable to reuse the radio resource. The method of SINR prediction can be applied to every RS. For the RS that cannot transmit R-amble, the RS sounding mechanism [56] defined in IEEE 802.16j can be applied to obtain the RSS matrix. Note that R-amble may have different power boosting from data burst, and the RSS matrix shall be updated to include this difference for data burst.

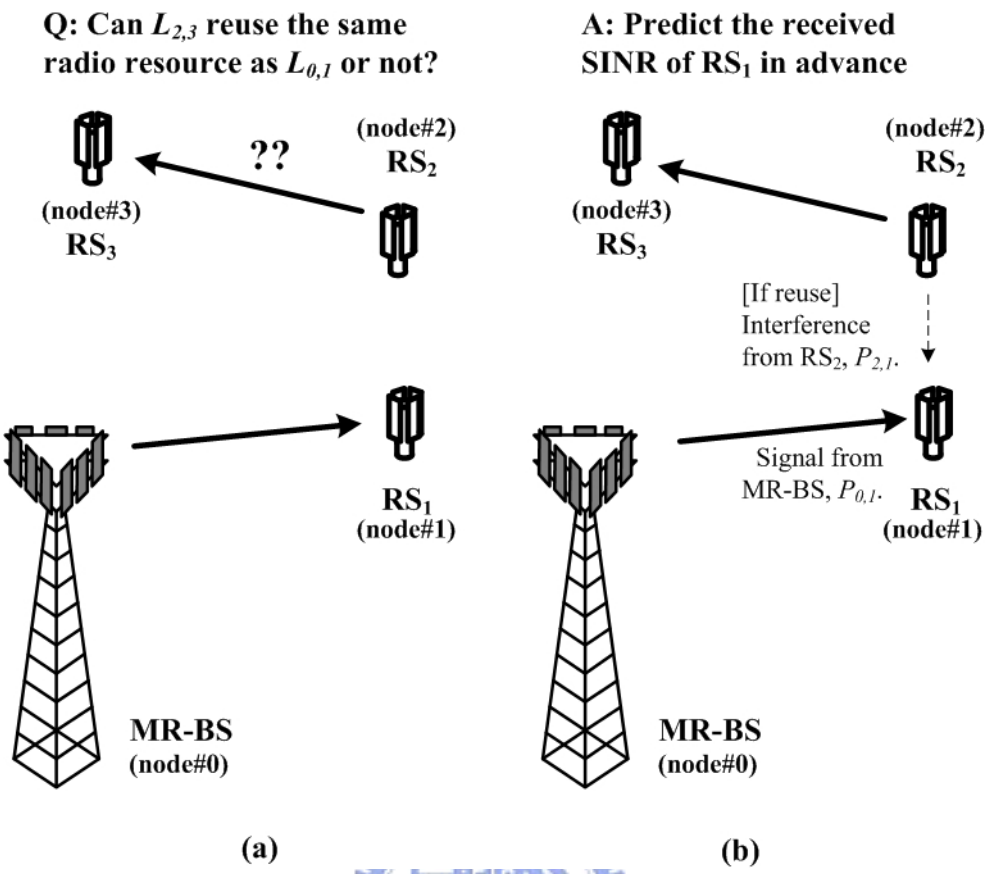

Figure 30. An example to illustrate the proposed SINR prediction method

By investigating the possible reuse patterns for the example in Figure 30, the prediction of the received SINR of each station can be summarized in Table 6. Where $L_{i,j}$ is the radio link from node #i to node #j and $\{\cdot\}$ is the set of radio links that use the same resource. For example, $\{L_{i,j}, L_{x,y}\}$ means that radio links $L_{i,j}$ and $L_{x,y}$ are allocated with the same radio resource. In this case, multiple access interference exists between $L_{i,y}$ and $L_{x,j}$. In this example, the radio resource reuse by RSs is discussed, and both the relay link and access link are applicable.

Table 6 SINR prediction results for different radio resource reuse patterns

Radio Resource Reuse Patterns		**Predicted SINR**			
		Node #0	**Node #1**	**Node #2**	**Node #3**
DL	$\{L_{0,1}\},\{L_{1,2}\},\{L_{2,3}\}$	*NA*	$\frac{P_{0,1}}{P_{1,1}}$	$\frac{P_{1,2}}{P_{2,2}}$	$\frac{P_{2,3}}{P_{3,3}}$
	$\{L_{0,1}, L_{2,3}\},\{L_{1,2}\}$	*NA*	$\frac{P_{0,1}}{P_{2,1}+P_{1,1}}$	$\frac{P_{1,2}}{P_{2,2}}$	$\frac{P_{2,3}}{P_{0,3}+P_{3,3}}$
UL	$\{L_{3,2}\},\{L_{2,1}\},\{L_{1,0}\}$	$\frac{P_{1,0}}{P_{0,0}}$	$\frac{P_{2,1}}{P_{1,1}}$	$\frac{P_{3,2}}{P_{2,2}}$	*NA*
	$\{L_{1,0}, L_{3,2}\},\{L_{2,1}\}$	$\frac{P_{1,0}}{P_{3,0}+P_{0,0}}$	$\frac{P_{2,1}}{P_{1,1}}$	$\frac{P_{3,2}}{P_{1,2}+P_{2,2}}$	*NA*

Therefore, the proposed SINR prediction method can be concluded as the following criteria [57]:

1. Prediction of the interference plus noise power received by node #i:

   The interference plus noise power can be predicted by the summation of (1) the thermal noise plus background interference power received by node #i and (2) the RSS from the station which does not intend to transmit signal to node #i but using the same radio resource.

2. Prediction of the received SINR for node #i:

   The predicted SINR received by node #i can be the ratio of "the RSS from the stations which intend to transmit signal to node #i" to "the interference plus noise power predicted by criterion (1)".

Note that this mechanism is also applicable in access link. The corresponding RSS table can be obtained by preamble scanning or the sounding mechanism [8]. However, the MS number is more the RS number and the RSS matrix need periodical update due to MS mobility. Therefore, it may result in much overhead when applying this mechanism for access links.

6.2 A New Path Selection Criterion based on SINR Prediction

In multi-hop cellular systems, deploying RS may degrade the system capacity due to the overheads in relay links. In addition to increase system capacity by advanced frequency reuse technique proposed in chapter 5, this section investigates the capacity improvement by different path selection criteria and proposes a new path selection criterion based on SINR prediction.

The basic idea on path selection problem is represented by Figure 31, where there are three possible paths available for serving the MS in downlink. In Figure 31, there are three possible paths available for serving the MS. In the path (1), the relay links between MR-BS and RS, between RSs and between RS and MS have very good quality by LOS transmission. The highest MCS (modulation and coding scheme) can be used and high transmission rate is achievable. However, it also results in most overhead to support three hops transmission. In path (2), the MR-BS directly serves the MS with worse radio link quality. But it will not result in any overhead in relay links. Path (3), compare with path (1) and (2), has medium radio link quality and overhead for two hop transmission.

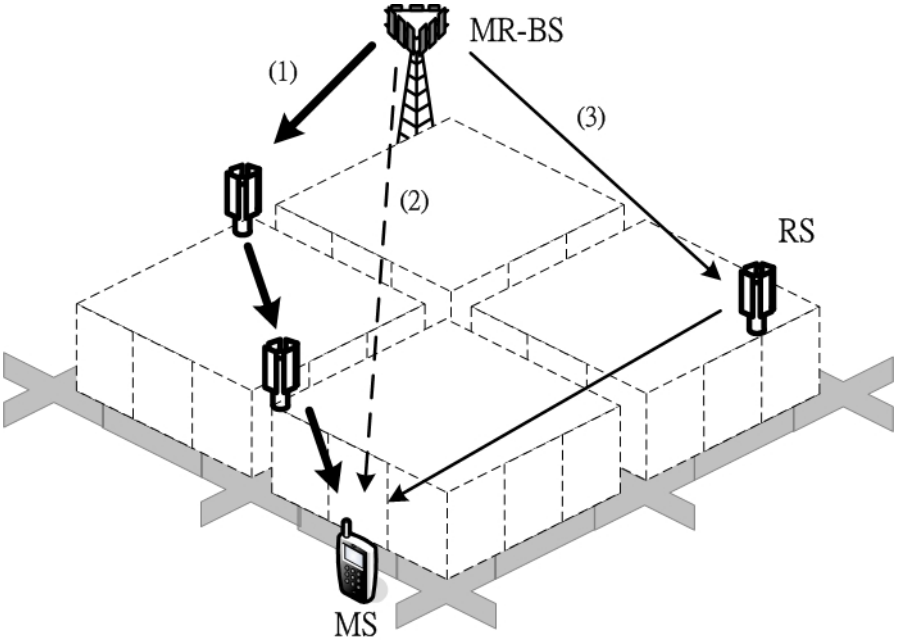

Figure 31. Path selection problem in multi-hop relay systems

Two kinds of existing path selection criteria are investigated here. The first one is selecting the path based on the received SINR by MS_i, which is called SINR-based criterion in following discussion. This criterion is very typical in traditional cellular networks [58,59]. The second criterion [60] is selecting the path for MS_i based on the utilization index

$$\beta_i(k) = \frac{N_{A,i}(k)}{M_{A,i}(k) + M_{R,i}(k)}, \tag{6.1}$$

where $N_{A,i}(k)$ is the number of bits able to be transmitted in access link of a frame for MS_i if path k is selected. $M_{A,i}(k)$ and $M_{R,i}(k)$ are the radio resource consumed by the path k for MS_i in access link and relay links respectively. The number of bits transmitted in relay links is treated as overhead and not considered in $\beta_i(k)$. It is because the data in relay links carry the same information as the one in access links. Compare with the first criterion, the second one considers the radio resource consumption by access and relay links, and will be called the load-based

criterion in following discussion.

Moreover, a new path selection criteria based on SINR prediction is proposed as the third criterion here. In equation (6.2), the new index is designed to reflect the damage by interference increment when selecting different paths.

$$\alpha_i(k) = \frac{N_{A,i}(k)}{M_{A,i}(k) + M_{R,i}(k)} - \sum_{j, j \neq i} \frac{\widetilde{N}_{A,j}(k)}{M_{A,j} + M_{R,j}} \tag{6.2}$$

The first term in Equation (6.2) is basically the same as Equation (6.1) to estimate the load on radio resource consumption. $M_{A,j}$ and $M_{R,j}$ are the radio resource consumed by MS_j in access link and relay links respectively, where $j \neq i$. $\widetilde{N}_{A,j}(k)$ is the number of bits degraded in the transmission for MS_j if the path k is selected by MS_i. This is a prediction result based on the predicted SINR, which is obtained by the following equation.

$$\widetilde{N}_{A,j}(k) = \left[\Gamma\left(SINR_j\right) - \Gamma\left(\widetilde{SINR}_j(i,k)\right) \right] \cdot M_{A,j} \tag{6.3}$$

Γ is a mapping function where its input is SINR and its output is MCS order. This function corresponds to the AMC (Adaptive Modulation & Coding) criterion considered by the system, and an example is given in Table 7 [8]. $SINR_j$ is the received SINR of MS_j before the path selection for MS_i. $\widetilde{SINR}_j(i,k)$ is the received SINR of MS_j if MS_i selects the path k, which is calculated based on the SINR prediction criteria concluded in Section 6.1.

Table 7 An example on Γ function design

SINR	$\Gamma(SINR)$	Note
$SINR \le 8dB$	1	QPSK, 1/2 coding rate
$8dB < SINR \le 10.5dB$	1.5	QPSK, 3/4 coding rate
$10.5dB < SINR \le 14dB$	2	16QAM, 1/2 coding rate
$14dB < SINR \le 16dB$	3	16QAM, 3/4 coding rate
$16dB < SINR \le 18dB$	3	64QAM, 1/2 coding rate
$18dB < SINR \le 20dB$	4	64QAM, 2/3 coding rate
$20dB < SINR$	4.5	64QAM, 3/4 coding rate

In order to explain the idea of $\widetilde{SINR}_j(i,k)$ and how to predict the damage on interference increment when selecting different paths, an example is given by Figure 32 and Figure 33.

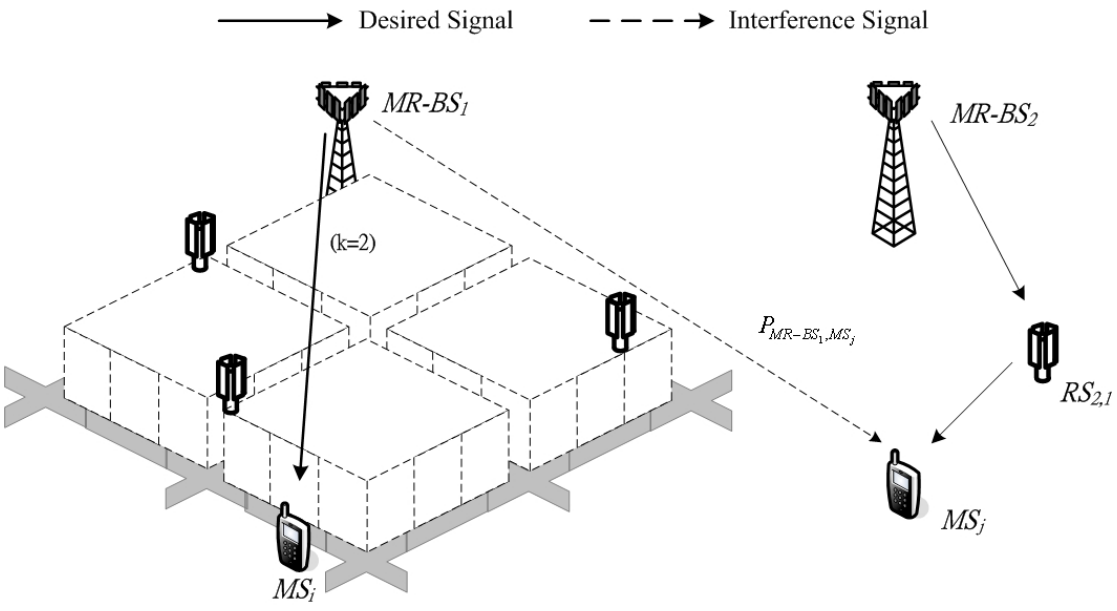

Figure 32. Interfering scenario when 2nd path is selected

In Figure 32 shows the interfering scenario if 2nd path (k=2) is selected for serving MS_i. In this case, MR-BS1 will directly serve MS_i and schedule a block of radio resource (e.g. sub-channel and time) in access link for data transmission. In this case, the MS_j served by the same radio resource (i.e. overlapped over time and frequency) will be interfered by the radio signal transmitted from MR-BS1. Therefore, the received SINR of MS_j will be degraded from $P_{RS_{2,1},j}/N$ to $P_{RS_{2,1},j}/\left(N+P_{MR-BS_1,j}\right)$ due to the interference increment. Therefore, $SINR_j$ and $\widetilde{SINR}_j(i,2)$ will be $P_{RS_{2,1},j}/N$ and $P_{RS_{2,1},j}/\left(N+P_{MR-BS_1,j}\right)$ in Equation (6.3) respectively.

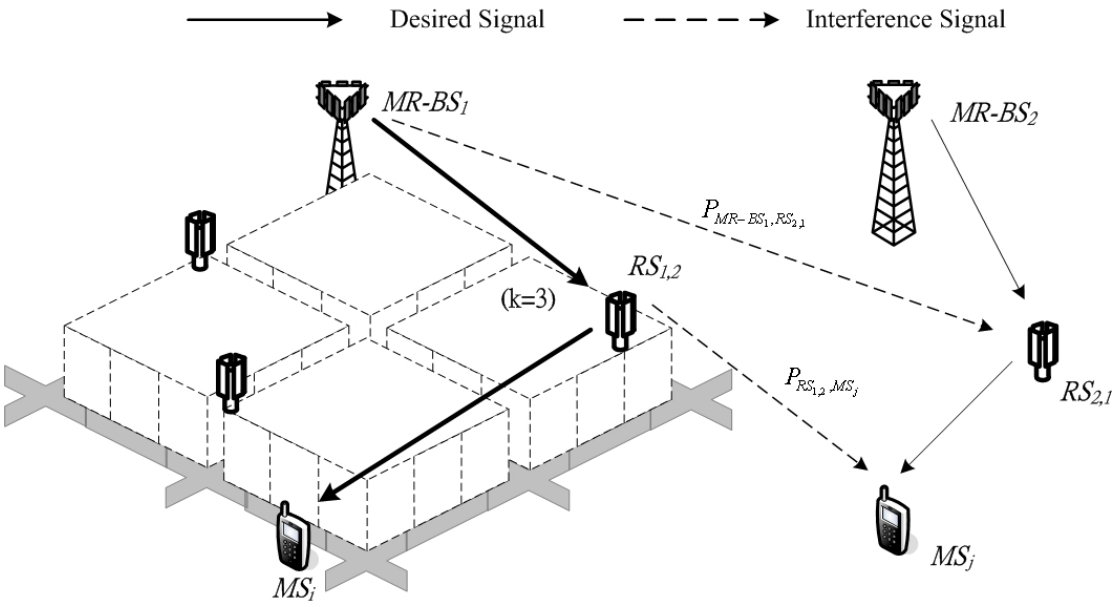

Figure 33. Interfering scenario when 3rd path is selected

Another example is given in Figure 33 to represent the interfering scenario when the 3rd path is selected for MS_i. In this case, the radio signal transmitted from MR-BS1 will interfere the received signal form RS2,1. In addition, RS1,3 will interfere the signal received by MS_j and degrade its received SINR from $P_{RS_{2,1},j}/N$ to $P_{RS_{2,1},j}/\left(N+P_{RS_{1,3},j}\right)$. Therefore, selecting different paths will not only lead to different

user throughput for desired user but also result in different level of SINR degradation for other users. The algorithm for path selection based on the proposed new criterion will be:

For each station, select the path #*k* where

$$k = \arg\left\{\max_k \left[\alpha_i(k)\right]\right\}$$
$$= \arg\left\{\max_k \left[\frac{N_{A,i}(k)}{M_{A,i}(k)+M_{R,i}(k)} - \sum_{j,j\neq i}\frac{\widetilde{N}_{A,j}(k)}{M_{A,j}+M_{R,j}}\right]\right\}. \quad (6.2.4)$$

6.2.1 Simulation Results

A. Simulation Environments

A downlink two-hop cellular network is simulated in suburban environment, where 6 RSs are deployed within the coverage of an MR-BS. Total of 19 cells with three sectors per cell are considered. The locations of six RSs in each MR-cell are as depicted in Figure 19, which follows the coverage and the sub-cell based frequency planning technique with K=7 proposed in previous section. The MR-BS and RSs are deployed above rooftop, so that the relay links have line-of-sight (LOS) condition. The access links between MR-BS and MS and between RS and MS are assumed to be non line-of-sight (NLOS). The IEEE 802.16 Type-A path-loss and shadow fading models are referenced from the multi-hop relay system evaluation methodology in [41]. The total transmit power of the MR-BS is 10 Watts with 1.5 km cell coverage, and the maximum transmit power for each RS is 1 Watts.

There are two scenarios for different level of signaling overhead considered in this simulation. The Scenario #1 assumes the measurement mechanism introduced in Section 5.2 can be applied in both relay links and access links, so that each RS or MS can report the RSS from all the stations to MR-BS. Take IEEE 802.16j multi-hop relay system as example, the R-amble measurement or RS sounding mechanisms can be used in relay links, and the preamble scanning or RS measurement mechanisms can be used in access links [8]. This scenario can lead to the most precise SINR prediction but also will result in much signaling overhead to report measurement results. In addition, the Scenario #2 assumes the measurement mechanism is only applicable in relay links, and the RSS measured by serving RS (or MR-BS) will be the

substitute when predicting the SINR for each MS. This means when predicting the received SINR for MSs, the elements in RSS matrix which corresponds to the measurement over non-serving RSs will be replaced by the results measured by serving RS (or MR-BS). The prediction results will not be very precise in this scenario, but it can save much overhead for periodic measurement instruction and reporting.

At the beginning of simulation, a large number of MSs are generated and randomly located within the system coverage. The simulation process will calculate the propagation loss from each MS to each station. Then the MSs will select the serving station based on each path selection criterion. For the SINR-based and load-based criteria, each MS will individually select the serving station based received preamble SINR and the index $\beta_i(k)$ respectively. For the prediction-based criterion, the index $\alpha_i(k)$ of MS_i will be calculated to consider the utilization degradation to all the existing MSs in the system. After the path selection for each MS, the system will calculate the received SINR according to the path selected by each MS and then determine the MCS accordingly according to the Γ function depicted in Table 7. In order to simplify the simulation complexity, the MCS of each relay link is assumed to be 64QAM and 1/2 coding rate since the RS can be properly deployed to have LOS condition to MR-BS. For each snapshot, the aggregated cell throughput obtained in access links and relay links will be calculated according to the given access zone ratio η. The ratio η is defined as the ratio of the radio resource allotted to downlink access zone over the total radio resource available in downlink sub-frame.

The access zone throughput is calculated by dividing the number of successfully

received bits in access zone over the downlink sub-frame duration, and the throughput in relay zone is by dividing the number of successfully received bits in relay zone over the downlink sub-frame duration. Then the cell throughput will be bounded by the lower one between access zone throughput and relay zone throughput. After a large number of iterations, the averaged cell throughput and other system performances are obtained and presented in following.

B. Simulation Results

Figure 34 presents the simulation results for the first scenario, where the capacities achieved by the 1st, 2nd and 3rd criteria are 13.9098Mbits/sec, 16.2772Mbits/sec and 17.7889Mbits/sec per MR-cell respectively. It shows that the 2nd criterion can lead to 17.02 capacity improvement than the first one, where the selection index considered in 2nd criterion include the possible overhead in relay links. When using the first criterion, MSs will always select the serving station with the highest received SINR. Take path (2) and path (3) in Figure 31 for example, assume the MR-BS can directly serve MS by 16QAM in path (2) and RS can serve MS by 64QAM in path (3). However, serving the MS by path (3) will consume additional resource in relay link but serving by path (2) will not. In this case, selecting the path only by SINR may result in worse capacity due to the overhead in relay link.

Moreover, Figure 34 also shows that the 3rd criterion can lead to additional 9.29% capacity improvement with respect to 2nd criterion. As depicted in Figure 32 and Figure 33, it is because the 3rd criterion can predict the capacity degradation to other links before path selection. For example, the LOS condition may exists between $RS_{1,2}$ and MS_j in Figure 33, which will result in severe interference. The 3rd criterion will prevent selecting this path but the 2nd criterion will not. Therefore, some severe interfering scenarios due to improper path selection can be prevented by the 3rd

criterion so that the capacity can be further improved by better signal quality.

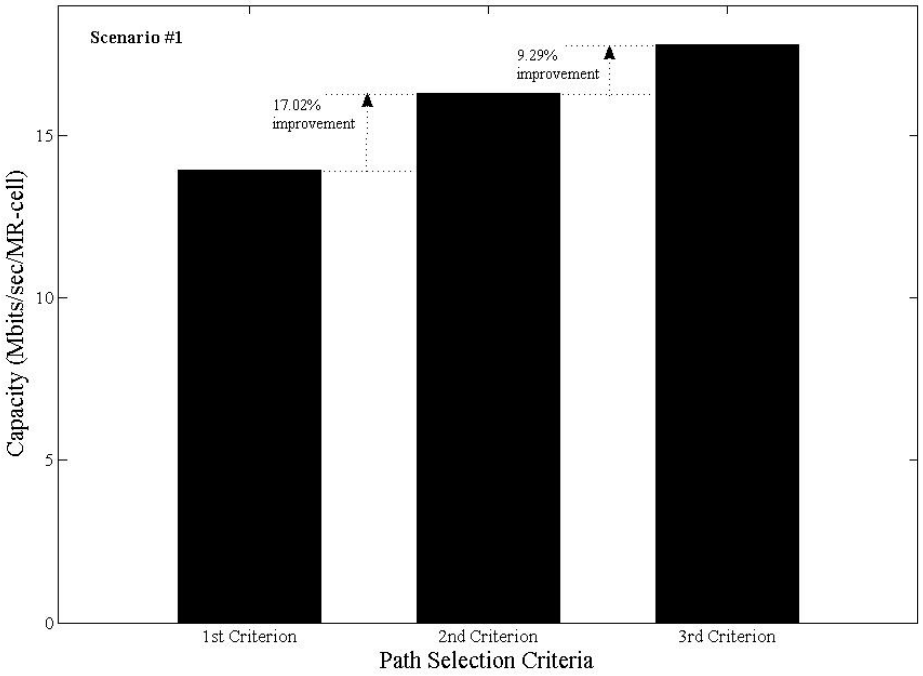

Figure 34. Capacity for each path selection criteria in Scenario #1

In Figure 35, the simulation results in second scenario are presented. Compare with the results in Figure 34, there are 6.89%, 7.01% and 12.49% capacity degradation for the 1st, 2nd and 3rd criterion respectively. It is due to the inexact SINR prediction results and improper path may be selected due to this inexact information. For 3rd criterion, the capacity degradation due to this effect is more significant than the other two criteria. It is because the 3rd criterion will select the path base on not only the receive SINR of serving station but also the SINR degradation to other MSs. The $\alpha_i(k)$ is more sensitive to inexact SINR prediction results and result in more improper path selection results.

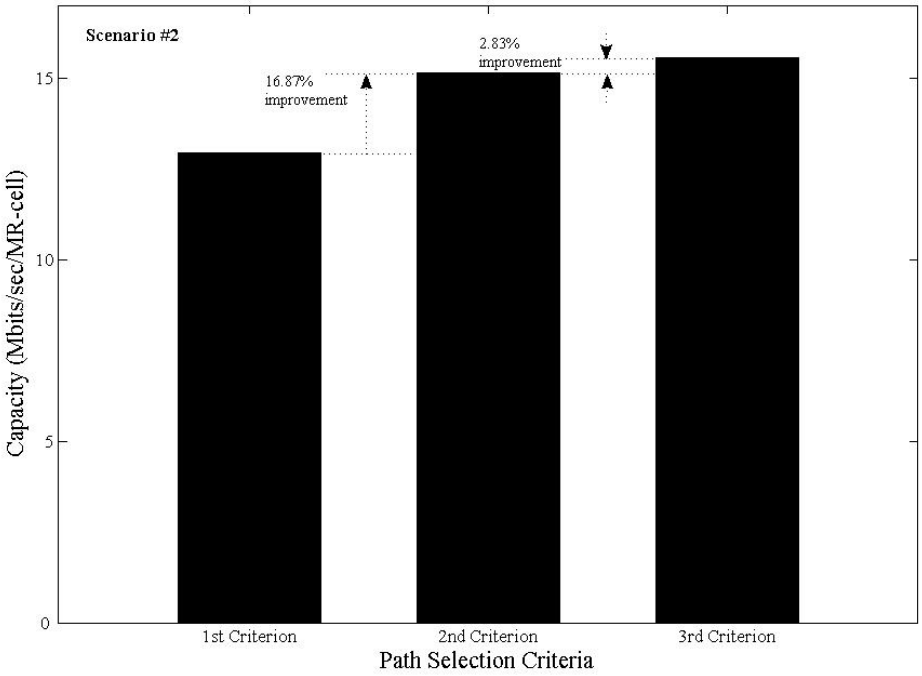

Figure 35. Capacity for each path selection criteria in Scenario #2

Chapter 7

Conclusion

In this dissertation, the performances improvement techniques for cellular OFDMA systems are proposed and discussed. The down-link capacity of multi-cell OFDMA system is investigated in Chapter 2 with diversity sub-carrier allocation which is a popular sub-carrier allocation method in practical OFDMA systems. A new mathematical analysis is proposed to efficiently evaluate the system capacity as compared to the time-consuming computer simulations. The analysis is general enough to investigate the effects of reuse partitioning, multiple MCS, different antenna configurations with and without channel reuse among sectors. It can also be used to facilitate optimal system design that gives the best tradeoff among different system parameters. Numerical results are given to show 97.1% to 300% improvements in capacity provided by employing frequency reuse among sectors (beams) along with reuse partitioning.

In Chapter 3, an FBSS with reuse partitioning cell structure is proposed to improve the packet loss rate of the traditional FBSS in IEEE 802.16e. By reserving some of the radio resource for use of high reuse factor, and using that radio resource to accommodate those handover users with bad radio-link performance, a 38.33% to 84.08% reduction in the packet loss rate of FBSS can be obtained, at the slight expense of 1.67% to 4.21% cost on cell throughput. Compared with the traditional method, using reuse partitioning cell structure can achieve more significant reduction on packet loss rate for FBSS in the IEEE 802.16e system.

In Chapter 4, an overview of the IEEE 802.16j multi-hop relay system is given first,

where IEEE 802.16j is the first international standard that standardizes the multi-hop relay technology. Then the examples on coverage planning for multi-hop cellular OFDMA systems are performed. The issues of RS deployment and radio-resource reuse in the IEEE 802.16j multi-hop relay network are investigated. By deploying RSs at locations that have LOS to the signal source and NLOS to the interference sources, radio resource is reused to improve the system capacity. Simulation results in the Manhattan-like environment are given to illustrate the attainable improvement. It also shows that per user throughput and system capacity can be significantly improved by multi-hop relay with respect to the cellular OFDMA systems with no relay.

In Chapter 5, a new frequency planning technique is proposed to reuse the frequency more efficiently in multi-hop cellular systems. By partitioning the coverage of each MR-BS and RS into a sub-cell, the proposed technique can prevent the overdesign on frequency reuse factor and explore more possibility for intra-MR-cell frequency reuse. Compared with the existing techniques, up to 137.75% capacity improvement can be achieved by the proposed technique. Meanwhile, the CDF of the received SINR shows that each technique is simulated under the guaranteed coverage.

A new path selection based on SINR prediction is proposed in Chapter 6. Based on the novel SINR prediction criterion with the input by the measurement results, the MR-BS can predict the received SINR or potential interference increment of each station in advance of path selection, radio parameter adjustment, topology configuration and etc. Then a new path selection for multi-hop cellular OFDMA systems is proposed with three kinds of selection criteria. Simulation results show that 17.02% capacity improvement can be achieved if the overhead in relay links is considered when selecting the path, and additional 9.23% capacity improvement can be achieved if the SINR can be exactly predicted all the time.

References

[1] Recommendation ITU-R M.1645, "Framework and overall objectives of the future development of IMT-2000 and systems beyond IMT-2000," International Telecommunication Union, Jun. 2003.

[2] G. L. Stuber, *Principle of Mobile Communication*, ISBN: 978-0-7923-7998-0, Kluwer Academic Publisher, 2001.

[3] 3GPP TR 25.913 V7.1.0, "3rd Generation Partnership Project; Technical specification group radio access network; Requirements for Evolved UTRA (E-UTRA) and Evolved UTRAN (E-UTRAN)," Sep. 2005.

[4] R. V. Nee and R. Prasad, *OFDM for Wireless Multimedia Communications*, ISBN: 0890065306, Artech House Publisher, 2000.

[5] H. Yang, "A road to future broadband wireless access: MIMO-OFDM-based air interface," *IEEE Communications Magazine*, pp.53-60, Vol. 43, Issue. 1, Jan. 2005.

[6] A. Jamalipour, T. Wada and T. Yamazato, "A tutorial on multiple access technologies for beyond 3G mobile networks," *IEEE Communications Magazine*, pp.110-117, Vol. 43, Issue. 2, Feb. 2005.

[7] 3GPP TS 36.201 V1.0.0, "Technical Specification Group Radio Access Network; LTE Physical Layer - General Description LTE," Mar. 2007.

[8] IEEE 802.16e-2005, "IEEE Standard for Local and Metropolitan Area Networks, Part 16: Air interface for fixed and mobile broadband wireless access systems, amendment for physical and medium access control layers for combined fixed and mobile operation in licensed bands," Feb. 2006.

[9] M. Cudak, "Draft IEEE 802.16m Requirements," IEEE 802.16m-07/002r3, Aug. 2007.

[10] IEEE P802.16j/D1, "Draft Standard for Local and Metropolitan Area Networks, Part 16: Air Interface for Fixed and Mobile Broadband Wireless Access Systems, Multi-hop Relay Specification," Aug. 2007.

[11] I. Koffman and V. Roman, "Broadband wireless access solutions based on OFDM access in IEEE 802.16," *IEEE Communications Magazine*, pp.96-103, Vol. 40, Issue. 4, April 2002.

[12] D. Kivanc, G. Li and H. Liu, "Computationally efficient bandwidth allocation and power control for OFDMA," *IEEE Transactions on Wireless Communications*, pp.1150-1158, Vol. 2, Issue.6, November 2003.

[13] R. Lee, J. Kim, J. Yu and J. Lee, "Capacity analysis considering channel resource overhead for mobile Internet access (WiBro)," *IEEE Vehicular Technology*

Conference, pp.3082-3086,Vol. 5, May 2005.

[14] S. Shin, C. K. Kang, J. C. Kim and S. H. Oh, "The performance comparison between WiBro and HSDPA," *IEEE International Symposium on Wireless Communication Systems*, pp.346-350, September 2005.

[15] T. S. Rappaport, "Wireless communications: principles & practice," ISBN: 0133755363, Prentice Hall, 1999.

[16] WiMAX White Paper, "Mobile WiMAX-Part I: A technical overview and performance evaluation, " http://www.wimaxforum.org/technology/downloads/, Feb. 2006.

[17] G. Auer, S. Sand, A. Dammann and S. Kaiser, "Analysis of cellular interference for MC-CDMA and its impact on channel estimation," *European Transaction on Telecommunications*, Vol.15, NO. 3, pp.173-184, May/Jun. 2004.

[18] G. Auer, A. Dammann, S. Sand and S. Kaiser, "On modeling cellular interference for multi-carrier based communication systems including a synchronization offset," *Proceedings of International Symposium on Wireless Personal Multimedia Communication*, Oct.2003.

[19] T-Po Chu and Stephen S. Rappaport, "Overlapping Coverage with Reuse Partitioning in Cellular Communication Systems," *IEEE Transactions on Vehicular Technology*, Vol. 46, No. 1, pp.41-54, Feb. 1997.

[20] 3GPP TR 25.996 V6.1.0, "Spatial channel model for Multiple Input Multiple Output (MIMO) simulations," Sep. 2003.

[21] B. Allen and M. Beach, "On the analysis of switched-beam antennas for the W-CDMA downlink," *IEEE Transactions on Vehicular Technology*, pp.569-578, Vol. 53, Issue. 3, May 2004.

[22] J. C. Liberti, Jr. and T. S. Rappaport, "Smart antennas for wireless communications: IS-95 and third generation CDMA applications," ISBN: 0-13-719287-8, Prentice Hall, 1999.

[23] A. Papoulis and S. U. Pillai, "Probability, random variables and stochastic process," ISBN: 0-07-366011-6, Fourth Edition, McGraw Hill, 2002.

[24] W. Choi and J. Y. Kim, "Forward-link capacity of a DS/CDMA system with mixed multirate sources," *IEEE Transactions on Vehicular Technology*, pp.737-749, Vol. 50, Issue. 3, May 2001.

[25] S. Choi, G-H Hwang, T. Kwon, A-R Lim, and D-H Cho, "Fast Handover Scheme for Real-Time Downlink Services in IEEE 802.16e BWA System," *IEEE Vehicular Technology Conference*, Vol. 3, pp.2028-2032, Jun. 2005.

[26] F. Feng and D. S. Reeves, "Explicit Proactive Handoff with Motion Prediction for Mobile IP," *IEEE Wireless Communications and Networking Conference*, Vol. 2, pp.855-860, Mar. 2004.

[27] I-K Fu, W. Wong, D. Chen, P. Wang, M. Hart and S. Vadgama, "Path-loss and Shadow Fading Models for IEEE 802.16j Relay Task Group," *IEEE C802.16j-06/045*, Jul. 2006.

[28] WiMAX Forum, "WiMAX System Evaluation Methodology V1.0," Jan. 2007.

[29] UMTS 30.03, "Universal Mobile Telecommunications System (UMTS); Selection Procedures for the Choice of Radio Transmission Technologies of the UMTS," TR 101 112 V3.2.0, Apr. 1998.

[30] R. Pabst et al, "Relay-base Deployment Concepts for Wireless and Mobile Broadband Radio," *IEEE Communication Magazine*, Vol.42, Issue 9, pp.80-89, Sep. 2004.

[31] M. Nohara et al, "IEEE 802.16 Tutorial: 802.16 Mobile Multihop Relay," *IEEE 802.16mmr-06/006*, Mar. 2006.

[32] A. Adinoyi et al, "Description of Identified new Relay Based Radio Network Deployment Concepts and First Assessment by Comparison against Benchmarks of well known Deployment Concepts using Enhanced Radio Interface Technology," *IST-2003-507581 WINNER D3.1*, Nov. 2004. https://www.ist-winner.org/

[33] N. Esseling, B. H. Walke and R. Pabst, "Performance of MAC-Frame-Based Protocols for Mobile Broadband Systems using Layer 2 Relays," Contribution of Wireless World Research Forum, Jun. 2004.

[34] H. Wu, C. Qiao, S. De and O. Tonguz, "Integrated Cellular and Ad Hoc Relaying Systems: iCAR," *IEEE Journal on Selected Area in Communications*, Vol.19, No.10, pp.2105-2115, Oct. 2001.

[35] J. Cho and Z. J. Haas, "On the Throughput Enhancement of the Downstream Channel in Cellular Radio Networks Through Multihop Relaying," *IEEE Journal on Selected Area in Communications*, Vol.22, No.7, pp.1206-1219, Sep. 2004.

[36] I. K. Fu, W. H. Sheen, C. L. Hsiao and C. C. Tseng, "System Performance of Relay-based Cellular Systems in Manhattan-like Scenario," *IEEE C80216mmr-05/041*, Nov. 2005.

[37] I. K. Fu, W. H. Sheen, C. L. Hsiao and C. C. Tseng, "Reverse Link Performance of Relay-based Cellular Systems in Manhattan-like Scenario," *IEEE C80216mmr-06/004*, Jan. 2006.

[38] C. Zhu et al, "Frame Structure to Support Relay Node Operation," *IEEE C802.16j-06/233r8*, Nov. 2006.

[39] C. Huo et al, "Relay Amble Modulation Series," *IEEE C802.16j-07/223r1*, Mar. 2007.

[40] I. K. Fu, "A Dynamic Simulation Platform for Heterogeneous Multiple Access Systems," Master Thesis, National Chung Cheng University, Jul. 2002.

[41] M. Hart et al., "Multi-hop Relay System Evaluation Methodology (Channel Model and Performance Metric)," *IEEE 802.16j-06/013r3*, Feb. 2007.

[42] I. K. Fu, W. H. Sheen and F. C. Ren, "Shadow-assisted Resource Reuse for Relay-augmented Cellular Systems in Manhattan-like Environment," *International Journal of Electrical Engineering*, pp.11-19, Vol. 14, No. 1, Feb.2007.

[43] I. K. Fu, W. H. Sheen and F. C. Ren, "Deployment and Radio Resource Reuse in IEEE 802.16j Multi-hop Relay Network in Manhattan-like Environment," to be published in the proceeding of *International Conference on Information, Communications and Signal Processing*, Dec. 2007.

[44] H. Hu, H. Yanikomeroglu, D. D. Falconer and S. Periyalwar, "Range Extension without Capacity Penalty in Cellular Networks with Digital Fixed Relays", *IEEE Global Telecommunications Conference*, pp.3053-3057, Vol. 5, Nov. 2004

[45] L. Huang, M. Rong and H. Shi, "Comparison of Two Frequency Reuse Schemes in Fixed Relay System", *International Conference on Wireless Communications, Networking and Mobile Computing*, pp.432-436, Vol. 1, Sep. 2005

[46] T. Liu, M. Rong and P. Li, "Radio Resource Allocation in Two-hop Cellular Relaying Network", *IEEE Vehicular Communications Conference*, pp.91-95, Vol. 1, May 2006

[47] T. Liu, M. Rong, D. Yu, Y. Xue, and E. Schulz, "Reuse Partitioning in Fixed Two-hop Cellular Relaying Network", *IEEE Wireless Communications and Networking Conference*, pp. 177-182, Vol. 1, Apr. 2006

[48] P. Li, M. Rong, and T. Liu, "Reuse Partitioning Based Frequency Planning for Cellular Network with Two-hop Fixed Relay Nodes", *IEEE International Symposium on Personal, Indoor and Mobile Radio Communications*, pp.1-5, Sep. 2006

[49] P. Li, M. Rong, and T. Liu, "Reuse Partitioning Based Frequency Planning for Relay Enhanced Cellular System with NLOS BS-Relay Links", *IEEE Vehicular Technology Conference*, pp.1-5, Sep. 2006

[50] 3GPP TR 25.996 V6.1.0, "Spatial channel model for Multiple Input Multiple Output (MIMO) simulations," Sep. 2003.

[51] Y. L. Tseng, "Novel Frequency Planning Techniques for IEEE 802.16j Multi-hop Relay System," Master Thesis, National Chiao Tung University, Sep. 2007.

[52] I. K Fu et al, "Neighborhood Discovery and Measurement for Fixed/Nomadic RS in IEEE 802.16j Multi-hop Relay Network," *IEEE C802.16j-07/171r2*, Mar. 2007.

[53] H. Zhang et al, "Relay Configuration Description Message," *IEEE C802.16j-07/217r5*, May 2007.

[54] I. K. Fu et al, "Editorial Comments to P802.16j Baseline Document: 6.3.26 RS

Neighborhood Discovery," *IEEE C802.16j-07/399r1*, Jul. 2007.

[55] I. K. Fu et al, "Editorial Comments to P802.16j Baseline Document: 6.3.2.3.75 RS Configuration Description Message," *IEEE C802.16j-07/400r1*, Jul. 2007.

[56] W. P. Chen et al, "Interference Detection and Measurement in OFDMA Relay Networks," *IEEE C802.16j-07/229r6*, Apr. 2007.

[57] I. K. Fu et al, "Interference and SINR Prediction for IEEE 802.16j Multi-hop Relay Network," *IEEE C802.16j-07/172r3*, Apr. 2007.

[58] X. Shen, M. Tang, Y. Wang, B. Liu and P. Zhang, "Joint Routing and Re-routing Control in Two-hop Cellular Relaying System," *IEEE Asia-Pacific Conference on Communications*, pp.1-5, Aug. 2006.

[59] L. Tao, R. Mengtian, P. Li, D. Yu; Y. Xue and E. Schulz, "Radio Resource Allocation in Two-hop Cellular Relaying Network," *IEEE Vehicular Technology Conference*, pp.91-95, Vol. 1, May 2006.

[60] Y. Liu, R. Hoshyar, X. Yang and R. Tafazolli, "Integrated Radio Resource Allocation for Multihop Cellular Networks With Fixed Relay Stations," *IEEE Journal on Selected Areas in Communications*, pp.2137-2146, Vol. 24, Issue 11, Nov. 2006.